December 2014

Mechanical Properties of Glass Fiber Reinforced Polymer Bars After Exposure to Elevated Temperatures

Mohammed Abdulqader Jalil Alsalihi
University of Wisconsin-Milwaukee

MECHANICAL PROPERTIES OF GLASS FIBER REINFORCED POLYMER BARS AFTER EXPOSURE TO ELEVATED TEMPERATURES

by

Mohammed A. J. Alsalihi

A Thesis Submitted in

Partial Fulfillment of the

Requirements for the Degree of

Master of Science

in Engineering

at

The University of Wisconsin – Milwaukee

December 2014

ABSTRACT

MECHANICAL PROPERTIES OF GLASS FIBER REINFORCED POLYMER BARS AFTER EXPOSURE TO ELEVATED TEMPERATURES

by

Mohammed A. J. Alsalihi

The University of Wisconsin-Milwaukee, 2014
Under the Supervision of Professor Habib Tabatabai

In the past few decades, the use of composite materials has become more widespread in different fields and industries**.** Part of this increase comes as an answer to the corrosion issues that ordinary steel faces. Fiber Reinforced Polymers (FRP)s offer a number of advantages that make them an adequate solution to challenges in the rapidly developing construction industry. However, the behaviors of these materials at elevated temperatures and their post-exposure properties are not sufficiently investigated and understood.

In this work the mechanical properties of glass fiber reinforced polymer (GFRP) bars are studied after exposure to elevated temperatures at different durations. The variation of the modulus of elasticity, tensile failure strain, and tensile strength are investigated. The study included tests of 64 dog-bone-shaped GFRP test specimens,

as well as 10 full-size GFRP bars, where the specimens were subjected to elevated temperatures of up to 350^{o}C at different exposure durations of up to 30 minutes.

In most cases, the post-heat tensile strength of GFRP dog-bone specimens was reduced with longer durations of heating exposure. However these reductions were less than 10%. Little variation was observed in the post-heat modulus of elasticity of GFRP samples heated to elevated temperatures in the range of 250^{o}C to 350^{o}C, and for durations of heating not longer than 30 minutes. Some of the samples heated to 350^{o}C exhibited pseudo-ductile failure patterns.

TABLE OF CONTENTS

LIST OF FIGURES

LIST OF TABLES

ACKNOWLEDGEMENTS

All praise to Allah, the beneficent, the most merciful. And peace and blessings be upon his messenger, beloved Mohammed.

I would like to extend my deep appreciation to my advisor, Professor Habib Tabatabai for his continuous support, patience, and guidance throughout this work.

I would like to also thank Mr. Rahim Reshadi for his dedication and assistance in the experimental program.

My sincere gratitude to my mother and father for their limitless love and support. Finally, my heartfelt appreciation to my brothers and sisters for always encouraging me and being there for me.

CHAPTER 1: INTRODUCTION

1.1 Background:

In the past few decades, the use of composite materials has become more widespread in different fields and industries. It is expected that by the year 2015, well over 10 million tons of composite materials will be manufactured [12, 14]. Part of this increase comes as an answer to corrosion issues that ordinary steel faces. Corrosion of steel in marine structures, bridges, and other structures has been a significant problem, causing deterioration of steel reinforced concrete members, and requiring expensive maintenances and repairs. Despite efforts to reduce and prevent this detrimental phenomenon, the issue of corrosion is still of significant negative factor in structures exposed to harsh environmental conditions.

Factors contributing to the increase in the use of Fiber Reinforced Polymer (FRP) are related to the following advantages of FRP:

1- Unlike steel, FRPs are not susceptible to corrosion due to direct exposure to the elements, carbonation of surrounding concrete, or exposure to chlorides from de-icing salts.
2- The unit weight of FRP is three (Glass Fiber Reinforced Polymer) to six (Aramid Fiber Reinforced Polymer) times less than steel [27].
3- FRP materials have a relatively “high stiffness/weight ratio” [18].
4- FRP materials are relatively easy to manufacture, handle, and cut [18].

5- FRP materials are electrically non-conductive [1].

6- FRPs are unaffected by magnetic fields [1].

7- FRPs can be manufactured with a variety of properties, based on the chemical configuration of the constituent fibers and resin used, and the method of production [19].

FRP materials have been used in a variety of applications including: parking garages and bridge decks (to address corrosion), high voltage substations and subways (because they are non-conductive) [1, 7], and MRI rooms in hospitals (because of their non-magnetic nature) [1].

The disadvantages of FRPs can be summarized as follows:

1- FRP materials are brittle. The stress-strain behavior is linear up to failure without a yield plateau [1]. This can lead to failures without any warning. Also bars cannot be bent as done in steel bars [1, 5].

2- They have lower modulus of elasticity compared with steel (GFRP and AFRP) [3, 5]. This can result in larger deflections and wider crack widths [3, 5].

3- FRPs are relatively weak in shear and compression [1].

4- FRPs are unsuitable for use at high temperatures. This is due to the degradation of the resin material, which affects mechanical properties. Furthermore, flammability and toxic gases emitted due to fires are significant drawbacks.

5- FRPs have a relatively higher cost compared to steel.

6- Most FRPs are not recyclable [12].

The problem of the brittle fracture is a major impediment in the widespread use of FRP materials. A number of researchers including Nanni et al. [17] (1993), Bakis et al. [10] (1996), Harris et al. [8] (1998), You et al. [9] (2007), and by Cui & Tao [11] (2009) have examined the possibility of producing hybrid FRP composites, containing two or more types of FRP materials, to produce pseudo-ductility (bilinear stress- strain behavior) and overcome the issue of brittle failure.

There are a limited number of studies conducted on the physical and mechanical properties of FRP materials at elevated temperatures, including post-fire exposure properties [1, 16]. Changes in FRP composites due to exposure to high temperatures needs to be better studied and understood, to be able to effectively assess the overall post-fire residual strength of members [19].

1.2 Objectives:

The overall goal of this study is to better understand the behavior of FRP materials following exposure to elevated temperatures. The specific objectives are as follows:

1- To investigate the variations in the mechanical properties of glass fiber reinforced polymer (GFRP) bars caused by prior exposure to high temperatures up to 350^{o}C, at varying durations of up to 30 minutes.

2- To study the possibility of producing GFRP bars that exhibit a pseudo-ductile failure behavior through prior heat treatment.

1.3 Scope:

Two types of test specimens were used in this work:

1- Small 9-in-long dog-bone-shaped specimens machined from 3/4-in-diameter GFRP bars. These specimens were heated to temperatures of 250^{o}C, 300^{o}C, and 350^{o}C, for durations up to 30 minutes.

2- Large 3/4-in-diameter GFRP bars (43.5 in long) heated to 350^{o}C.

Samples were left to cool down to room temperature, and then tested for residual tensile strength and ultimate strains. . Modulus of elasticity and energy densities were also calculated.

1.4 Organization of Thesis:

The body of this thesis is comprised of the following sections:

Chapter 2: this chapter provides a review of a part of the literature available on the subject of fiber-reinforced polymer composites, their constituent components, behavior at elevated temperature, and their post heat treatment residual mechanical properties. In addition, this chapter reviews some of the attempts made by researchers to develop ductile FRP composites.

Chapter 3: describes the types of specimens used in the experimental program, their shapes and dimensions, the heat treatment procedure, the preparation of the

samples for the tensile strength test, and the apparatus used for the heating process and the testing procedure.

Chapter 4: provides a description of the results obtained from the experimental program.

Chapter 5: in this chapter, the results are examined, discussed and reviewed.

Chapter 6: contains a summary of the conclusions made from the work, as well as recommendations for future studies.

CHAPTER 2: LITERATURE REVIEW

In this chapter, a brief description of fiber reinforced polymers, and their constituent components is presented. Also, a review of the available literature on the changes in mechanical properties of fibers, resins, and fiber reinforced polymers at elevated temperatures (or after heat treatment) is provided. Finally, a discussion of works of some researchers to produce hybrid fiber reinforced polymers is presented.

2.1 Fiber Reinforced Polymers FRP:

Fiber Reinforced Polymers (FRP) are composite materials made from fibers, such as glass, carbon, vinylon and aramid fibers, embedded in a resin matrix, such as epoxy, vinyl ester, polyester, or phenolic [20]. The word “polymer” has two components; “poly” and “mer”, which mean “many” and “parts”, respectively [27]. The resin serves as the binder that holds the fibers together, keeping them straight, and facilitating transfer of loads and distribution of stresses between the fibers [3, 17, and 30]. Resins also play the role of a protective layer from environmental influences [17]. Perhaps the most widely used type of FRP is glass fiber reinforced polymer (GFRP) [12]. It is estimated that over 90% of the fiber reinforced composites manufactured have glass fibers used as their reinforcement [12]. One of the reasons for this widespread usage is, as Yang et al. [13] put it, its “high specific performance to cost ratio”.

FRP bars are anisotropic [24], and are typically made through pultrusion, in which bundles of long parallel fibers are made into the desired bar diameters by running them through a bath of liquid resin, after which they pass through a die that compresses the fibers and the shapes them into different size bars [3, 26]. The bars then go through surface treatment by making indentations, treating with sand particles, or wrapping with helical fibers around the bar to improve bond properties of the final product [3]. The combination of fibers and resin allows for the creation of properties that neither material has on its own, with the preservation of the individual chemical features of these constituent components [26].

FRPs of all shapes and forms are used in civil engineering applications in three forms: 1) externally wrapped reinforcement, such as those used to strengthen damaged columns and beams, 2) internal reinforcement as longitudinal bars or stirrups, or 3) full-scale structural members, where the entire member is made of FRP [27].

In general, tensile strength is more dependent on the fiber properties, while some other properties, such as shear strength, are more affected by the properties of the resin matrix. The mechanical and physical properties of FRP materials are dependent on a number of factors, the most influential of which are the type of fiber, the type of resin, and the percentage of each component, as well as the fiber arrangement (braided, straight…etc.) [20]. The effect of the relative properties of the fibers and the resin, is usually described through the following "rule of mixtures" [3] :

$$P_{FRP} = P_f \upsilon_f + P_m \upsilon_m$$

Where P_{FRP}: is the mechanical property of the FRP,

P_f: is the mechanical property of the fibers,

υ_f: volume fraction of fibers,

P_m: is the mechanical property of the matrix,

υ_m: volume fraction of the matrix.

When using the rule of mixtures in calculations regarding properties of composite materials, the influence of the matrix in FRP composites is sometime neglected, due to its small effect on that property. For instance, the total modulus of elasticity of the FRP bar is said to be a function of the moduli of the constituting fiber types, while neglecting the contribution of the matrix material [11]. This is due to the supposition that the resin's only role is to convey the load among the different fibers of the bar [11]. However, that is not to say that the type of matrix and its properties do not have any influence on the elastic modulus.

Bakis et al. [10], used the rule of mixtures to predict the modulus of elasticity of a number of different hybrid FRP rods, and their predictions were very close to the experimental values. But when the rule of mixtures was used to calculate tensile strengths of the hybrid rods, the authors [10] were getting lower values than the experimental values for most types of rods. It should be noted that the modulus of elasticity of FRP bars has wide range of variation in comparison with steel bars,

because different companies make their products using different types of resin and fibers with a variety of proportions [3].

Unlike steel, FRPs are highly resistant to corrosion. This is particularly true in environments where there is exposure to sea water, deicing salts, or freeze-and-thaw cycles [27]. In spite of the efforts made to protect the steel in members exposed to harsh conditions through epoxy coating, galvanization, cathodic protection, or other measures, steel corrosion remains a source of concern and economic loss [27].

Apart from the advantage of the corrosion resistance, FRP materials offer a number of other appealing qualities, including light weight, ease of handling, high strength in the direction of the fibers, non-conductivity, and transparency to magnetic fields [1, 27]. Nevertheless, FRPs are not perfect materials, and they have their shortcomings. Examples include their brittle failure behavior, their relatively higher cost in comparison with steel (where steel reinforcing bars are 2-3 times less expensive than GFRP bars [27]), lower modulus of elasticity (compared to steel, and relative weakness in shear and compression [1]. Furthermore, FRPs are not suitable for use at high temperatures, due to the degradation of the resin and combustion.

2.2 Resins

Resins are used in composite materials for the purposes of binding the fibers together, and to allow for the transfer of loads between fibers. There are two main

families of resins: thermoset resins (e.g. vinyl ester, epoxy, polyester), and thermoplastic resins (e.g. polycarbonate, polystyrene, polyetheretherketon, polymethylmethacrylate) [17, 19]. Thermosetting resins, which are more commonly utilized for structural applications, are produced using a liquid resin with a curing agent, fillers, and small proportions of other materials [17, 19]. As their name implies, thermoset resins experience permanent chemical alteration when cured, and cannot be returned back to their original liquid state by the use of heat [26, 27]. Thermoset resins have better strength and modulus than thermoplastic resins [26]. Thermoplastic resins soften when heated to elevated temperatures, and solidify again when cooled down [27]. Considering that there are many different types of resins with a variety of different components, it is very difficult to frame the mechanical and thermo-mechanical properties of these materials in an overall form [19]. Rather, the properties of these materials need close study of each type of resin [19].

One of the problems regarding the use of some common types of resins in structural applications is their somewhat poor behavior when subjected to elevated temperatures. These resins, especially those that are styrene-based, exhibit low fire endurance, characterized by their rather quick ignition times, release of poisonous fumes, and heat, as well as the consequent reduction in the mechanical properties of the residual material [21]. An exception is the phenolic resin that display better resistance to fires, emit less amounts of harmful gases, and more of which is left as a carbonaceous char [21].

Gibson et al. [21, 22] investigated the mechanical properties of 12-mm-thick composite laminates, using three different types of resins (vinyl ester, polyester, and phenolic). The laminates were subjected to fire and then cooled to room temperature [21, 22]. For the post-exposure case, the authors reported that the laminates were divided into three distinct zones: a fully charred zone, an intermediate zone of delamination and decomposed resin, and a third zone of intact material [22]. A notable difference reported between the polyester and vinyl ester laminates on one hand and the phenolic laminate on the other, was that the charred zone was mainly washed-out of the polyester resin material, and the fibers were clearly visible, as opposed to the phenolic laminate's damaged zone that retained considerable amounts of fractured char [21, 22]. The authors developed a model that classified the fire-exposed laminate to two main zones: a fully degraded zone of no residual mechanical capabilities and an intact zone of full mechanical properties, where the two zones are separated based on a line representing residual resin content (RRC) of 80% [21]. The adoption of the 80% RRC was based on the experimental results suggesting that, once 20% of the resin is lost, the rest is of little influence in carrying any mechanical loads [21, 22]. For the samples that were loaded in compression while being heated, a temperature limit of 170^{o}C was utilized, as opposed to the RRC limit, due to the shortness of the duration before failure commenced, thus preventing the formation of a tangible decomposed area [22].

Sorathia et al. [24] examined the strength of composite materials during fire, as well as residual strength after exposure to fire, in an investigation on the

practicality of utilizing composite material on ships. For the post fire exposure properties, 3 in x 3 in x 0.25 in specimens were subjected to elevated temperatures ($25kW/m^2$) for 20 minutes, after which each sample was divided into 5 coupons, and tested for residual strength [24]. The authors [24] reported that samples made of epoxy and glass were separated into layers during exposure, because of decomposition of the epoxy [24]. Samples made with phenolic and graphite retained an average of 53% of their strength, while PEEK (polyether ether ketone) and graphite samples retained an average of 75% of their strength [24].

The authors also explored the influence of having a "barrier" material for reducing the intensity of damage caused by fire exposure on composites, where they studied the effectiveness of 11 different types of solutions [24]. The best results in protecting the composite material were achieved through the use of ablative and intumescent barriers [24].

Dodds et al [25] studied the performance of composite laminates of different thicknesses, between 5 and 22 mm, exposed to fire in a furnace. Laminates of glass fibers (chopped strand mat or woven roving) and different resin types (phenolic, isophthalic polyester, or epoxy) were used in the investigation [25]. Unlike the laminates made with epoxy or polyester, the phenolic specimens exhibited layer separations, crackling sounds and rise of smoke early into the fire tests [25]. The authors suggested that the layer separation might be caused by larger amounts of

water being retained in these samples [25]. However, the best endurance under elevated temperatures was observed in the phenolic laminates [25].

2.3 Fibers

Fibers are generally made by pushing the liquefied raw material through tight holes of a spout, after which the fibers are allowed to solidify [27]. After solidifying, they are pulled to allow for the molecules to be arranged in the direction of the fiber [27]. There are many types of fibers, but the most commonly used ones in civil engineering applications are carbon, aramid, and glass fibers.

2.3.1 Glass Fibers

There are several types of glass fibers used in composites, the most widely used of which maybe E-glass or electrical glass [28]. It has comparably low cost, and good strength and stiffness, but it is somewhat weak in impact endurance [28]. S-glass (also called R-glass or T-glass) is another type of glass fiber that possesses high strength and high modulus, as well as a higher price in comparison to the E-glass [28]. Other types are A-glass (alkali resistant glass fibers) and C-glass (chemical resistance glass fibers) [27, 28]. One of the disadvantages of glass fibers is their relatively low modulus compared with carbon or aramid fibers [26]. Other than their use in the structural field and in the aerospace industry, glass fibers are used in the making of "thermal insulators, boat hulls, lightweight parts of automobiles, and rubber tires" [27].

2.3.2 Carbon Fibers

Carbon fibers are produced from three types of precursors: Pitch, Rayon, and Polyacrylonitrile PAN sources [27]. The latter is the source for most manufactured carbon fibers [27]. The production of carbon fibers includes heating the raw material to very high temperatures [27], where the temperature reaches around 3000^{o}C for the manufacturing of high modulus carbon fibers, and approximately 2600^{o}C for high strength fibers [30].

Carbon fibers possess the highest strength and modulus compared to other common types of fibers, and are unaffected by ultra-violet rays, or alkaline materials [26]. However their impact endurance is less than that of aramid and glass fibers [30]. The cost for carbon fibers was very high when it was first marketed [27, 30]. However, as the consumption of this material has increased greatly and the quality has improved, the cost has lessened significantly [27, 30].

2.3.3 Aramid Fibers

Aramid fibers are another type of fiber used in civil engineering composites. All aramid fibers exhibit low unit weight and high strength [29]. These fibers are stronger that glass fibers and weaker than carbon fibers [26]. The most broadly used aramid fibers are Kevlar-49 and Twaron 1055 [27]. Aramid fibers possess good endurance for abrasion, chemical decomposition, and thermal disintegration [29]. Aramid fibers are weak in compression and are vulnerable to ultra-violet rays,

making them prone to damage when unprotected in sunlight. However, they display good performance under impact [26, 27, 29].

2.4 Thermal Properties of Glass Fibers

Thomason et al. [12], conducted a broad investigation on the post-heat strength and modulus of single E-glass fibers heated for 15 minutes at temperatures up to 600^{o} C. in their work, the mechanical properties of silane (APS) sized (or γ-aminopropyltriethoxysilane sized), and unsized (uncoated) fibers were studied after specimens cooled down to room temperature [12]. About 75 sample fibers were tested for each temperature studied [12]. Their tests showed that the fibers lost tensile strength and experienced reduction in maximum strain as the target temperature increased [12]. The loss in tensile strength surpassed 70 % of the room temperature strength value when fibers were heated to 600^{o}C [12]. The decline in strength was not that significant for temperatures below 250^{o}C [12]. Most of the reduction occurred at temperatures between 250^{o}C and 450^{o}C [12]. Similar behavior was reported for the failure strain of the fibers, as shown in Figure (2-1) and Figure (2-2):

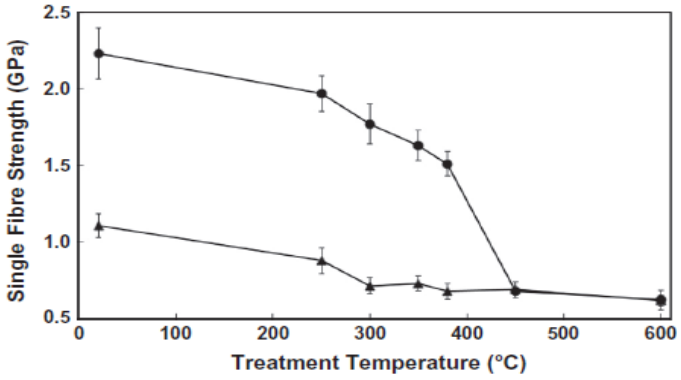

Figure 2-1 Strength vs. temperature for glass fibers [12](triangle: water sized, circles: silane sized)

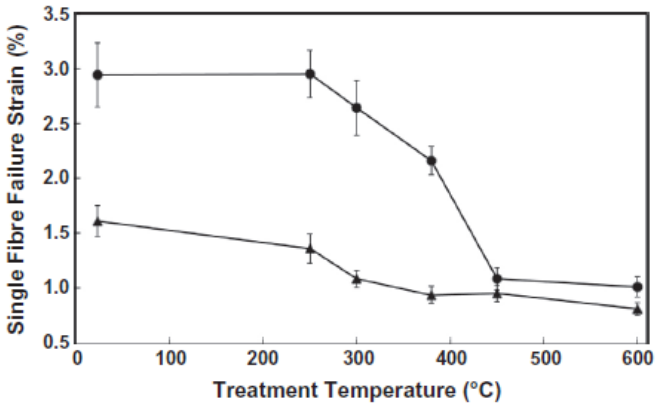

Figure 2-2 Peak strain vs. temperature for glass fibers [12] (triangle: water sized, circles: silane sized)

When the mechanical properties of heated FRP composites are discussed, most of the post-high-temperature changes are often attributed to degradation in the matrix material [12]. However, as Thomason et al. [12] point out, the fact that unsized fibers show loss of strength starting from relatively low temperatures, suggests that the degradation occurs in the fibers of glass in addition to the matrix material.

Thomason et al. [12] reported that APS sized and unsized fibers showed an increase in their tensile modulus with an increase in temperature. The samples were heated at the target temperatures for a duration of 15 minutes. Fig. (2-3) shows the change in tensile modulus with temperatures [12]:

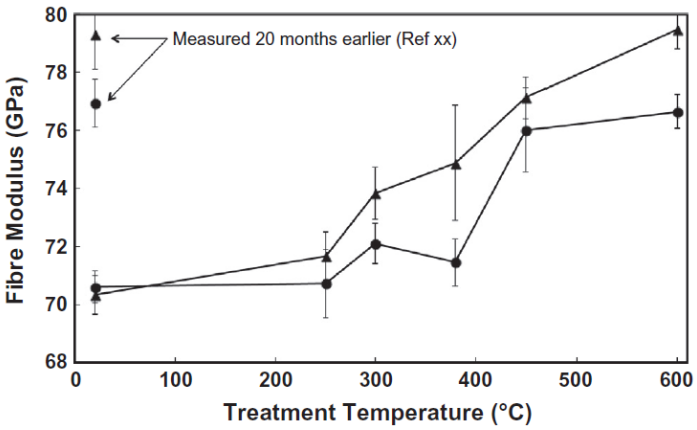

Figure 2-3 Modulus vs. temperature for glass fibers [12]

Yang et al. [13], came up with a thermo-mechanical analysis technique to determine the coefficient of thermal expansion, the glass transition temperature (Tg), and the influences of thermal compaction on APS coated, single glass fibers that were heated to temperatures of up to 900^{o}C.

Two processes are mentioned by researchers to explain the changes that take place when glass fibers are heat treated. One is referred to as "thermal expansion", and the other as "structural relaxation" or "thermal compaction" [13,15] . Otto [15] defines thermal compaction or (compaction) as the phenomenon where the fibers experience densification and their mechanical and physical properties revert to those of the bulk glass from which they were manufactured [15].

Yang et al. [13] reported that single fibers showed an initial linear expansion with temperature, followed by nonlinear expansion at higher temperatures, with sudden and rapid increase in the rate of expansion occurring at the Tg temperature. In other words, the coefficient of thermal expansion has a certain value at temperatures less than 300^{o}C, above which it starts to decline as the temperature increases, and ultimately rapidly increases again at temperatures near Tg [13]. An average value of 6.1 μm/(m ^{o}C) was reported for the coefficient of linear thermal expansion (less than 300^{o}C).

A Tg of 760 ^{o}C was obtained for the heating rate of 5 ^{o}C/min. The authors also noticed that fibers tend to shrink while heated, and their shrinkage follows a logarithmic curve with respect to the duration of the heat treatment [13]. The authors attributed this phenomenon to the reduction in viscosity with heating, until it is lowered to a point where internal forces lead to a reorganization and readjustment in the structure of the material, which in turn causes a rise in the viscosity and a lessening of the internal stresses [13].

Yang et al. [13] studied the effect of heat treatment on the elastic modulus of glass fibers, both while being heated, and after cool-down to room temperature. In the first case, they monitored the modulus of elasticity at temperatures from (20-700) ^{o}C, and observed a linear stress-strain response for temperatures under 400^{o}C [13]. However, a gradual change to a nonlinear curve was detected for higher temperatures up to 500^{o}C, where the modulus measurement was imprecise due to

the unstable nature of the slope of the curve [13]. In general, while being heated, fibers showed a reduction in the modulus of elasticity with increasing temperatures until about 550^{o}C, after which the modulus declined at a much higher rate [13]. This reduction is attributed to the thermal expansion of the fibers [13].

The post-heat treatment elastic modulus of the fibers (heated for 30 minutes at temperatures from (50-650) ^{o}C) exhibited a rise with increasingly higher temperatures [13]. This increase is in agreement with the contraction that the fibers experience when heated [13]. Both phenomena are attributed to the thermal compaction or structural relaxation of heated glass fibers [13]. Another contributing factor suggested by the authors (related to post-heat elastic modulus) is the dissipation of water from the fibers that is thought to result in an increase in the stiffness of the fibers [13].

Feith et al. [14] investigated the influence of heat treatment (temperatures between 150^{o}C and 650^{o}C), the duration of treatment (up to two hours), and the type of atmosphere inside the heating device on the strength and elastic modulus of silane sized E-glass fibers. The elastic modulus of the fibers as well as their residual strength was determined after allowing them to cool down to room temperature [14]. The testing was done for single fibers, fiber bundles, and dog bone shaped composite specimens made from the heated fibers after cool down with vinyl ester resin [14].

Feith et al. [14] reported that changes in the elastic modulus of the heated fibers were not noted regardless of heat treatment, or the type of samples used (i.e. single fibers, bundles or composite laminates). Feith et al. [14] reported a reduction in strength with increasing temperatures. The largest reduction occurs in the beginning of the heating process, after which the strength becomes stable. The higher the temperature, the faster the strength reaches its stable value. For the single fiber tests, after reaching the stable value, the decrease in strength was less than 10% at 250^{o}C, and approximately 70% at 650^{o}C [14]. As for the fiber bundles, the reductions at 250^{o}C and 650^{o}C were roughly 10% and more than 95 %, respectively [14].

Feith et al. [14] credit the variation between the bundles and single fibers to the friction inside the fiber bundles. The authors also note that "*decomposition of polymer resins (epoxy, polyester, vinyl ester, phenolic) doesn't begin until the temperature exceeds 300-400 C. This suggests that glass fibers begin to lose strength during thermal recycling before matrix pyrolysis has commenced*" [14].

In terms of the effect of the atmosphere of heating on the strength reduction, Feith et al. [14], reported less strength reduction when fibers were heated in nitrogen, versus being heated in dry air or ambient air. Yet, this effect was reported to disappear for temperatures higher than 450 ^{o}C, and for durations longer than 30 minutes [14].

Feith et al. [14] also conducted thermogravimetric analysis (TGA) on the glass fibers, and reported that the mass loss for fiber heated up to 650^{o}C (at a rate of 10 ^{o}C/min) was about 0.5%. Glass fibers do not experience a noticeable mass loss, except for some loss in water retained in the fiber [14].

In an examination of the fracture surface of the fibers, the researchers [14] reported that degradation due to heating affects the surface of the fibers alone, and not the core. This idea was supported by the fact that in all cases, failure initiated from the circumference of the fibers [14].

Otto [15], describes the mechanism of compaction and the reasons behind some of the changes in properties that occur when glass fibers are heat treated. In light of the glass fiber manufacturing in which the glass is quenched from 2000^{o}F in about one tenth of a second, glass fibers tend to show properties similar to those of bulk glass at high temperatures, such as a lower density and a lower modulus compared to annealed glass at ambient temperatures [15]. The elastic modulus of non-heat-treated glass fibers is nearly 15 % less than the modulus of the bulk glass from which it was produced [15]. However, heat treating glass fibers allows the viscosity to be reduced to a level that allows for a relief of high internal stresses and rearrangement of the microscopic structure of the glass fiber [15]. This leads to a more compact configuration, an increased elastic modulus, and a denser formation, which is more similar to bulk glass [15].

One of the indications of the existence of the compaction phenomenon, as Otto [15] cites, is the shrinkage that takes place in the length of glass fibers. The fiber experiences an initial expansion when heat treated, but as the heating temperature is increased (at about 400^{o}C), the fiber begins to contract due to the compaction that takes place in its structure [15]. The highest levels of compaction are achieved at treatment temperatures of around 600^{o}C to 650^{o}C [15]. Based on his tests, Otto [15] suggested that the thermal contraction for any certain temperature is uniform in all directions of the fiber structure, and follows a logarithmic curve with time.

Otto [15] further discusses the possibility of contribution of thermal compaction to relief of stresses applied to glass fibers. More stresses can be relieved with higher heat treatment temperatures [15]. Relieving stresses from an already densified and compacted fiber requires heating the fiber such that the viscosity is sufficiently lowered for the stress relief to occur [15].

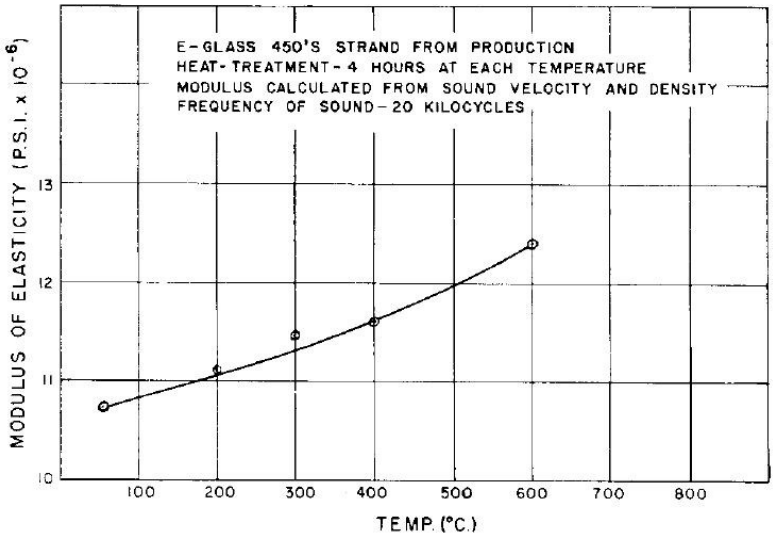

Figure 2-4 Change in elastic modulus of glass fibers with temperature [15].

2.5 FRP Properties (Tested at High Temperatures)

At elevated temperatures, composites generally "exhibit anisotropic heat transfer – they burn, give off smoke and release heat, char, and delaminate" [24]. When dealing with fiber reinforced polymers at elevated temperatures, it is necessary to be familiar with behavior of the constituent components of the composite material at these temperatures, and the extent to which their mechanical and physical properties are influenced.

One of the key factors that is of great importance is the glass transition temperature of the matrix material. The T_g of the matrix is of more interest (compared to the fibers), because the fibers' glass transition temperature is usually much higher. For instance, the T_g of glass fibers was an average of 760^{o}C as measured by Yang et al. [13]. At this temperature, polymers tend to soften and their molecular arrangement changes, which causes a considerable reduction in some of their mechanical properties [18]. Before reaching Tg, fibers are still capable of carrying some load [18]. However, glass transition temperatures for polymers in general, such as polyester and vinyl ester, are much lower (60^{o} C for polyester to 130^{o} C for vinyl ester) [18]. This hinders the composite material form effectively carrying loads at much lower temperatures due to the degradation of bonds between the fibers and the resin [18]. Therefore, when carbon-based FRP materials are subjected to temperatures equal to or higher than the glass transition temperature of the resin, they show reduction in their mechanical properties [18].

Part of this reduction is recoverable once the material cools down to room temperature, while the remaining loss is permanent [18].

Other points of great importance for resins may be the flow temperature and decomposition temperature, for thermoplastics and thermosets, respectively [19]. The decomposition temperature is the temperature at which thermoset resins start to decompose and decay [19]. The amount of decay and loss in mechanical properties is a function of how tight the meshing of the polymer sequences is, where the tighter the web is, the less reduction in the mechanical properties the resin will experience [19]. On the other hand, the flow temperature, which is a characteristic of thermoplastic resins, is the temperature at which the material becomes completely fluid [19].

When tests are run on FRP composites at high temperatures, an inconsistency maybe noticed when results from different types of tests are compared with each other, as Katz et al. [6] points out. The reason may be due to the anisotropic quality of FRP composites, where the properties of the FRP material in the transverse direction are different from its properties in the longitudinal direction [6]. When heated, the matrix in the composite FRP material tends to lose its ability to transfer load at a lower temperature than the fibers [6]. So if the test type depends more on the matrix performance at high temperatures, as is the case for shear tests or bond tests, more susceptibility to elevated temperatures can be

noticed as opposed to the case where the fibers are mainly being loaded such the test of the tensile strength of FRP sample [6].

Katz et al. [6] performed bond tests (in concrete) using four types of FRP bars with different types of resins used for each of the bar types. The bars were heated from room temperature to 250°C and their bond strengths were compared, across a few points between 20°C and 250°C [6]. A steel specimen was also tested under the same condition [6]. Since the behavior of FRP bars (in terms of bond strength) depends mostly on the resin, Katz et al [6] reported a significant reduction in the bond strength of the bars (from 11-13 MPa) at room temperature for three out of the four bars to (1.1-1.7) MPa as the temperatures reached 250°C.

Katz et al [6], also noted that at temperatures lower than the glass transition T_g , traces of concrete were seen on the bars' surfaces after pullout tests. But at temperatures higher than the T_g , traces of the surface polymer were observed on the inside of the concrete cylinder, indicating the softening and separation of the polymer [6].

Wang et al. [2] studied the strength and modulus of elasticity of GFRP and CFRP bar in comparison with steel bars at high temperatures up to 600° C. Specimens were heated in a kiln up to a certain target temperature and then loaded to failure while maintaining the elevated temperature [2]. The authors noted mostly linear stress - strain curves for both GFRP and CFRP bars [2]. They reported high variations between the strengths of specimens of each group at high temperatures

[2]. Also, at temperatures up to 400°C, the GFRP bars preserved about 90% of their room temperature modulus of elasticity, but started showing large reduction at temperatures higher than 400°C (less than 30% at 500° C) [2]. Figure (2-5) shows the normalized moduli as a function of temperature [2]. A rise and subsequent fall can be seen for the moduli FRP specimens [2].

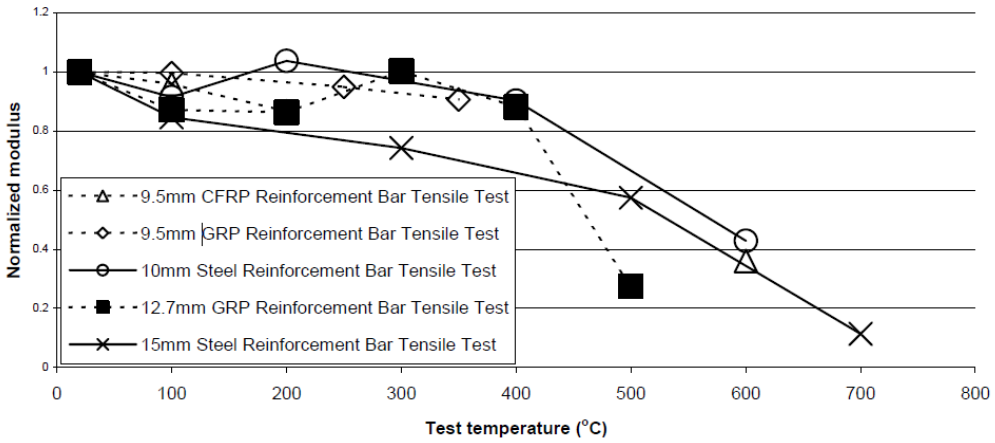

Figure 2-5 Normalized moduli vs. temperature for GFRP and steel bars under tension [2].

Robert et al. [18] examined changes in the mechanical properties of GFRP bars when exposed to extreme temperatures. They ran tensile, shear, and flexural strength tests on GFRP bars at high temperatures (up to 315°C) and subzero temperatures (down to -100°C) [18]. The importance of the exploration of low temperatures properties is due to the detrimental effects of extreme temperatures on the microstructure of the FRP material and the micro-cracks that could develop [18]. Such micro-cracks allow water to penetrate into the material and cause deterioration through the freeze and thaw cycles [18]. In the tensile strength tests

that were conducted at high temperatures, the GFRP bars showed a gradual decrease in tensile strength with increasingly higher temperature [18]. The largest drop in the tensile strength occurred at around the Tg of the polymer material, with an approximate 50 % loss in strength when the temperature reached 300^{o}C [18].

On the other hand, an increase in the tensile strength was noticed when specimens were cooled to subzero temperatures, with a 20% increase in strength at -100^{o}C [18]. Shear and flexural strengths showed pronounced reductions and increases when specimens were heated and cooled, respectively [18]. This variance in the extent to which the different strengths were affected, according to the authors, was due to the fact the tensile strength is more dependent on the fibers' strengths, which are not highly affected by these temperatures [18]. The shear and flexural strengths are more influenced by the resin material that is damaged at these temperatures [18]. As expected, the flexural modulus of the bars showed a drop around the Tg temperature of the matrix [18]. Micrographs of specimens heated to 350^{o}C, exhibited micro-cracks in the structure of the bar, proving the damage sustained by the resin material at such high temperatures [18].

Kumahara et al. [20] examined the mechanical properties of a variety of different types of FRP bars at elevated temperatures [20]. The bars were heated for an hour before testing for tensile strength [20]. The authors reported a large variation among the different types of bars used in the experiment (table (2-1)) [20]. For example the CaR and GT bars maintained their room temperature tensile

strength up to 250^{o}C, but the strength of CaR dropped to 60% of original strength at 350^{o}C [20]. The AB and AR samples showed an approximately linear reduction to about 30% and 10% of original strength at 250^{o}C and 350^{o}C, respectively [20]. GR specimens went through an initial drop of tensile strength (to 80%) at 60^{o}C, and retained this value until about 140^{o}C after which it decreased gradually to 40% at 350^{o}C [20]. Kumahara et al. [20] also measured the elastic modulus of the specimens at the different heating temperatures, as shown in Figure (2-6) from their report.

Table 2-1 Type and notation for test specimens used by Kumahara et al [20].

<table>
<tr><th>Symbol</th><th>Surface Configuration</th><th>Fiber Type</th><th>Binder</th></tr>
<tr><td>Ca7</td><td>Twisted String</td><td rowspan="2">PAN-Carbon</td><td rowspan="4">Epoxy</td></tr>
<tr><td>CaB</td><td rowspan="2">Braided</td></tr>
<tr><td>CiB</td><td>Pitch-Carbon</td></tr>
<tr><td>CaR</td><td>Spiral</td><td>PAN-Carbon</td></tr>
<tr><td>CiTC</td><td rowspan="2">Straight</td><td rowspan="2">Pitch-Carbon</td><td>Cement Paste</td></tr>
<tr><td>CiTE</td><td rowspan="2">Epoxy</td></tr>
<tr><td>AB</td><td>Braided</td><td rowspan="2">Aramid</td></tr>
<tr><td>AR</td><td>Spiral</td><td>Vinyl Ester</td></tr>
<tr><td>GT</td><td>Straight</td><td rowspan="2">Glass</td><td>PPS</td></tr>
<tr><td>GR</td><td>Spiral</td><td>Vinyl Ester</td></tr>
</table>

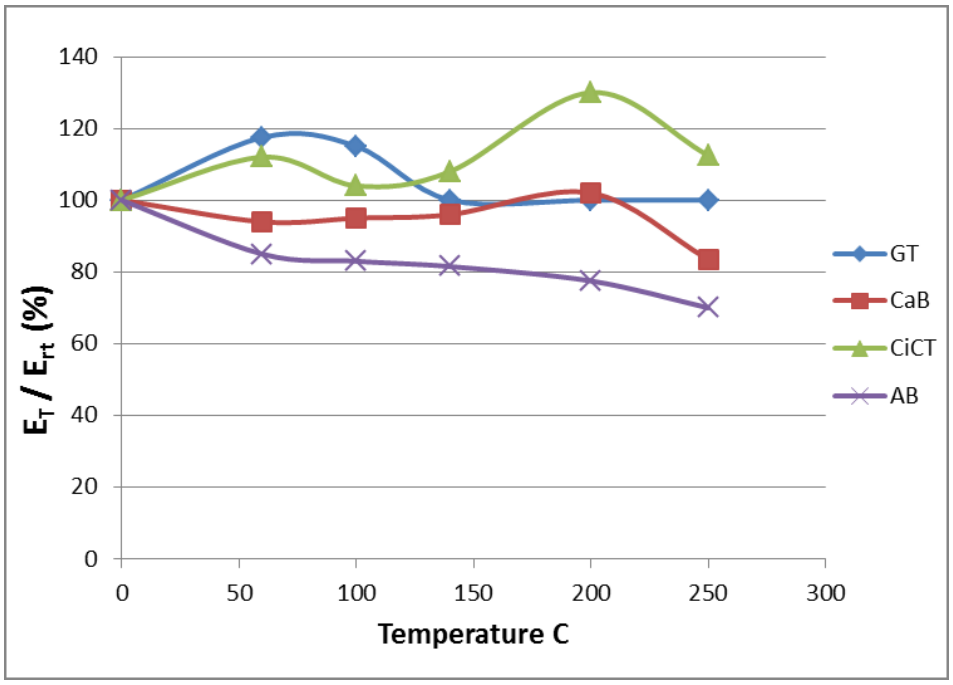

Figure 2-6 Normalized elastic modulus of specimens tested under elevated temperature relative to room temperature modulus [20].

2.6 Post Heat Treatment Properties of FRP Bars

Ellis [1] conducted a study on the residual mechanical properties, the post heating bond strength to concrete, and the post-heating flexural strength (in concrete) of 3/4-in-diameter GFRP bars previously exposed to elevated temperatures of up to 400°C.

The bars prepared for tensile strength tests, were heated to 100°C, 200°C, and 400°C with the use of heating tapes while simultaneously being loaded to about 42% of their room temperature strength (representing imposed dead load) [1]. The specimens were then cooled down and tested for tensile strength [1]. The specimens were reported to exhibit reduced tensile strength and elastic modulus as

the target temperature was increased [1]. The ratio of the elastic modulus of pre-heated bars to control bars was 98%, 97%, and 83% for 100^{o}C, 200^{o}C, and 400^{o}C respectively [1]. Also, the ratio of the tensile strength of pre-heated bars to that of control bars was 87%, 98%, and 83% for 100^{o}C, 200^{o}C, and 400^{o}C respectively [1].

As for the stress-strain curves, linear elastic behavior (all the way to failure) was observed in most pre-heated bars [1]. However, some bars that were pre-heated to 200^{o}C and 400^{o}C exhibited a bilinear stress-strain curve, with the post "yield" part constituting up to 25% and 34% of the total strain curve, respectively [1]. This was explained by Ellis [1] to be possibly caused by the layering of the bar due to exposure to high temperatures.

In the bond tests, nine samples were pre-heated (without being loaded during the heating process) to 100^{o}C, 200^{o}C, and 400^{o}C [1]. One end of each bar was embedded in a concrete cylinder [1]. The bars were subsequently pulled out of the concrete during bond tests [1]. Ellis [1] reported reductions in the bond strength with higher pre-heat temperatures. The percentage of the bond strength in relation to the bond strength at room temperature was 96%, 76%, and 27% at 100^{o}C, 200^{o}C, and 400^{o}C, respectively [1]. It was also noticed that the resin was separated from the bar at lower pre-heating temperatures to being completely removed (no residue) for the bar with higher temperatures [1].

For the flexural tests, nine GFRP-reinforced concrete beams were heated to the target temperatures while simultaneously subjected to a load corresponding to

42% the nominal flexural capacity of the control samples [1]. The beams were tested to failure in flexure after cooling down to room temperature [1]. The heat-treated beams, in several tests, showed an ability to carry higher loads than the control samples [1]. Ellis suggested that this might be caused by the reduction in bond and stiffness of the rebars in the heat-treated beams [1]. In his work, Ellis [1], also provides an analytical procedure for the approximate calculation of the residual flexural capacity of flexural members after being exposed to high temperatures followed by a cool down to room temperature.

Alsayed et al. [16] conducted an investigation on the post heat treatment properties of a number of Φ 12 mm E-glass and vinyl ester GFRP bars, with a fiber content of 83%. They heated the bare bars as well as embedded-in-concrete bars to temperatures ranging from 100^{o}C to 300^{o}C for durations of 1, 2, and 3 hours [16]. Alsayed et al. [16] reported a reduction in the strength of both bare bars and concrete encased bars, with higher temperatures and longer durations of heating. They recorded reductions in strength for the bare bars from 9.7% for one hour of heating at 100^{o}C and 21.8% reduction for three hours at the same temperature [16]. For the 300^{o}C condition, they report 21.3% reduction at 1 hour to 41.9% reduction at 3 hours of exposure [16]. Meanwhile, the reduction in the strength of the concrete-covered bars was reported to be in the range of 3.1% for 1 hr of heating at 100^{o}C to 35.1% for 3 hours at 300^{o}C [16]. A similar trend was reported for the failure strains of the bars [16]. Strains of 2.44%, 2.25%, and 2.2% were obtained for exposure temperature of 100^{o}C with durations of 1, 2, and 3 hours, respectively [16]. While

the corresponding strains for 200°C were 2.11%, 1.92%, and 1.82% [16]. For exposure temperature of 300°C, the maximum strains of 2.01%, 1.67%, and 1.50% were reported for the same exposure durations [16]. It is worth noting that a larger reduction in failure strain was reported between 1 and 2 hours of heating, and less reduction occurred for the extra hour of treatment [16]. All samples showed a linear stress-strain curve for all conditions of treatment, and the form of failure was brittle for all samples [16]. The authors also reported that very little reduction in the elastic modulus of the samples was observed, where the greatest loss in modulus did not exceed 5% [16]. Figure (2-7) shows the moduli recorded in their tests [16]:

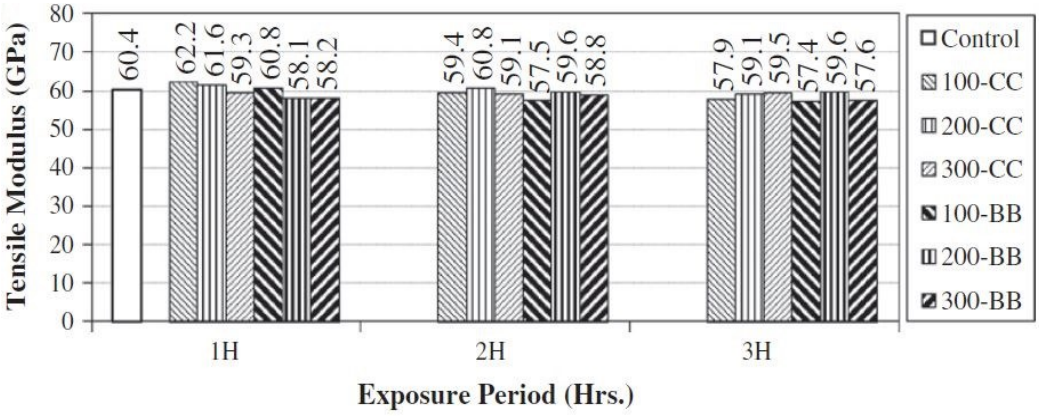

Figure 2-7 Modulus versus temperature and duration; BB: Bare Bars, CC: Concrete Covered Bars [16].

Alsayed et al. [16], suggested that the reason for the relatively unchanged moduli might be related to the way these bars are degraded with heat, where most of the damage is done to the matrix material. Scanning electronic microscopy showed the texture of the resin to be rough and the resin covering the fibers in the unheated control samples [16]. But as the bars were heated to higher temperatures,

the smoother the resin was and the more visible the fibers became, until the resin was nearly gone and the glass fibers were mostly bare in the bars heated for 3 hours at a temperature of 300^{o}C.

The concrete cover's contribution was obvious in reducing the losses in strength of the bars, but the protective quality was diminished with higher temperatures [16].

Kumahara et al. [20] also studied the post-heat properties of the specimens indicated in table (2-1), where specimens were left to cool down before testing their tensile strength. They reported loss of less than 20% in the tensile strength for most samples with exposure temperatures below 250^{o}C, exhibiting reduction at some temperatures, and relative increase in tensile strength at other temperatures [20]. However, some specimens (AB and GR) exhibited a drop at 140^{o}C and 200^{o}C, respectively, reaching about 40% of the preheating strength at 400^{o}C [20]. In general, when subjected to temperatures of 400^{o}C, composite bars that had an organic resin material, preserved 40% - 60% of their pre-heat strength, while those that had inorganic binder, maintained at least 80% of their pre-treatment strength [20].

As for the elastic modulus of the specimens, the CiTE, CiB, CaB, GT, and AB maintained approximately 100% of their room temperature elastic modulus, after being heated for one hour at temperatures up to 250^{o}C [20]. Figure (2-8) shows

variation of elastic modulus for some of the specimens from the work of Kumahara et al [20]:

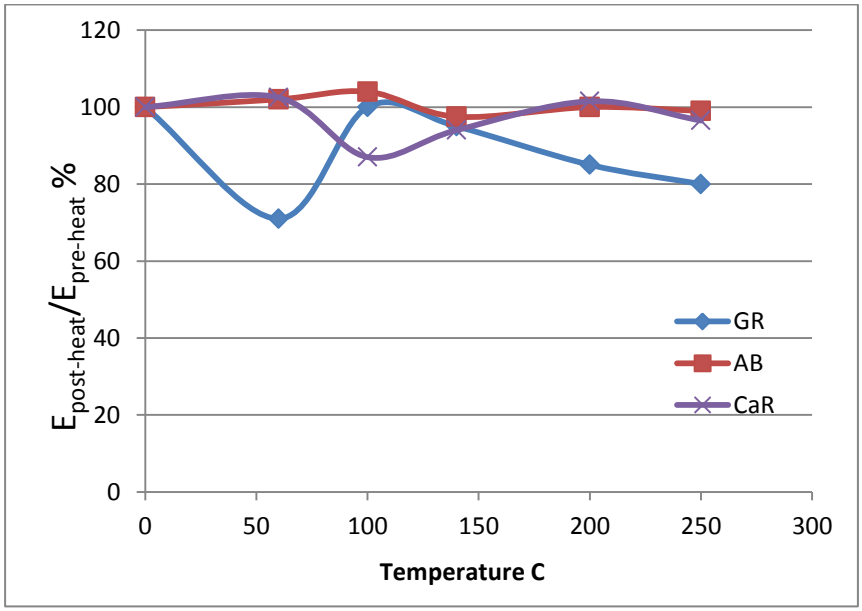

Figure 2-8 Changes with temperature in the ratio of post-heating elastic modulus to the pre-heating modulus [20].

Sayed-Ahmed et al [26], investigated the mechanical properties of CFRP tendons after exposure to temperatures of 100, 200, 300, 400, and 500^{o}C for a duration of 24 hours [26]. The tensile strength tests were performed on the samples after they had cooled down to room temperature. The authors also examined the effect of cold temperatures (-60^{o}C) on the tensile strength of the tendons. The researchers reported that as the exposure temperatures increases, the color of the tendons became darker [26]. For exposure temperatures of 400^{o}C and higher, the specimens were starting to smell, due to the fact that the resin was starting to decompose [26]. At a temperature of 500^{o}C, all the epoxy had vaporized, leaving the

loose carbon fibers behind [26]. Due to the damage caused to the resin material in the specimens heated to 400^{o}C, the anchorage of the bars became weak, causing them to slip when tested for tensile strength [26].

As for the levels of the residual tensile strength of the specimens, Sayed-Ahmed et al [26], reported strengths of 2427.3 MPa, 2383.9 MPa, 2328.3 MPa, 2160.5 MPa, 1496.7 MPa, and 613.9 MPa for temperatures of -60^{o}C, 20^{o}C, 100^{o}C, 200^{o}C, 300^{o}C, and 400^{o}C respectively. There was evident reduction in strength caused by the heat treatment of the tendons [26]. The authors also investigated the coefficient of thermal expansion of the CFRP tendons, and calculated it to be -0.86±0.0.9 x 10^{-6} /^{o}C [26].

2.7 Hybrid Composite Bars:

In the past few decades, there have been a number of attempts to solve the problem of the brittle failure behavior of FRP composites. A number of researchers worked on producing hybrid FRP composites that show some degree of apparent ductility – mostly bilinear stress-strain curves. One method to achieve this is by Braiding, where two or three or more types of FRP fibers are combined together in the form of strands

The cross-section of the hybrid bar maybe divided into a core and a sleeve area [8]. The core can be made of one type of fiber, and the sleeve maybe another type or types [8].Alternatively, the hybridization maybe done through random mixing of the different fiber types [8].

The braided hybrid structure of the bar cross-section causes the bar to behave in a pseudo-ductile manner, where the fibers with higher modulus of elasticity carry a larger share of the initial load imposed on the bar. The axial stress in the entire bar up to apparent "yield" point is dominated by these fibers. After the "yield" point, when partial failure of the high modulus fibers occurs, the lower modulus fibers take the lead up to complete rupture of the entire bar. In general, the overall properties of the hybrid bar depend on types of fibers used, their percentage, and their position within the diameter of the hybrid bar [17].

Bakis et al. [10] worked on producing hybrid FRP bars with two to three different types of fibers. The types of fibers incorporated were chosen to give a good range of maximum strain capacities, and to develop hybrid bars with distinct gradual failure [10]. They provide a detailed description of the manufacturing process for hybrid bars [10]. Bakis et al. [1] reported that the hybrid rods exhibited a pseudo-ductile behavior, in which the carbon fibers would fail first at lower strain values, followed by the failure of other fiber types.

Nanni et al. [17] studied the mechanical properties of two types of 1 meter long hybrid bars, made of a FRP skin and a steel core. In the first type, aramid and epoxy were used for the composite skin, and in the second, vinylon and epoxy were used [17]. Two types of steel cores were utilized, mild steel and high strength steel [17]. Nanni et al. [17] reported a bilinear stress-strain behavior, with a definite yielding point. In specimens with high strength steel core, failure of the sleeve was

trailed by failure of the core [17]. A maximum strain of 2.78% to 2.95% was reached in the samples with aramid skin, which was higher than that achieved in regular aramid bars [17]. However, the specimens that had vinylon as their sleeve did not reach a significantly higher failure strain compared to ordinary vinylon bars [17]. The authors also reported a noticeable increase in the ultimate strength of the steel core in the specimens with aramid skin [17]. Nanni et al. [17] suggested the use of the "rule of mixtures" to estimate the properties of the hybrid bars. The use of larger percentage of FRP in the sleeve had a positive effect on the strength and rigidness of the hybrid bar [17].

Harris et al. [8] (1998), manufactured 5-mm-diameter braided hybrid FRP bar with a core of carbon fibers and a sleeve of aramid fibers, both with an epoxy resin as the matrix. A bilinear stress-strain curve was achieved, with an obvious yielding point [8]. Higher modulus of elasticity was attained for the first part of the bilinear curve (78.6 GPa) [8]. Relatively high level of strain at maximum stress (2.5 %) was attained [8]. The moment-curvature responses of beams reinforced with the hybrid FRP bars were fairly similar to responses from beams reinforced with steel bars of the same size [8]. Also, satisfactory bond strengths (to concrete) were accomplished through the incorporation of ribs at the surface of the bars [8].

You et al. [9] studied the hybrid effect in bars consisting of (carbon and glass) fibers in vinyl ester or polyester. The arrangements were based on how the fibers were spread in the cross-section of the bar [9]. The carbon fibers were placed either

in the core, placed around a glass-fiber core, or dispersed randomly with glass fibers [9]. The authors were able to achieve a (9% to 33%) improvement in ultimate strain compared to all-carbon-fiber rods [9]. The highest strain effect was achieved in the specimens where carbon and glass fibers were spread over the entire cross-section in a vinyl ester resin [9]. The best tensile strength increase was observed in the samples with the carbon fiber in the core [9]. The lowest results were obtained for the samples that had the carbon fibers around a glass fiber core [9]. You et al. [9] did not report any pseudo-ductile behavior.

2.8 Effect of Bar Surface:

One of the key factors regarding the use of fiber reinforced polymer bars in concrete members is the achievement of sufficient bond between FRP bars and concrete. Therefore, surface texture and roughness is introduced on the surface of FRP bars. This may include indentations, protruding deformations, or other types of surface treatments, such as incorporation of sand particles.

Malvar [4] tested four types of 3/4-in-diameter GFRP bars with greater than 45% fiber content in a vinyl ester or polyester matrix and varying surface conditions. Malvar [4] concluded that "deep indentations in the longitudinal fibers will reduce bar strength". Malvar [4] also noted that the utilization of surface deformations, in the form of fibers being helically wrapped around the bar, causing indentations or protruding deformations, are satisfactory with regard to the development of adequate bond strength. However, use of deformations that are glued to the surface

of the FRP bar is not recommended, due to the probability of it being peeled off the surface under stresses [4].

CHAPTER 3: EXPERIMENTAL SETUP

3.1 Introduction:

In this chapter, a description of the test specimens, heating procedures, sample preparation and testing methodology is provided. The main focus of the experiments was on tensile testing of GFRP reinforcing bars. The bars used for the tensile strength test were - ASLAN 100 - #6 GFRP bars (0.75 inch diameter) produced by Hughes Brothers [7]. Two types of sample sizes and shapes were used in the tension tests:

1- Dog-bone shaped specimens of 9 in length, with a 0.3 in middle diameter (DB-specimens) machined from 3/4-in-diameter GFRP bars.
2- Full size (FS) samples of 3/4-in-diameter and 43.5 in length, without any changes made to its shape (FS-specimens).

3.2 Dog-Bone (DB) Specimens

3.2.1 Sample Description

These specimens are shaped from the #6 GFRP bars used for the experiments. The gripping area of these samples is (2.64) in long and have a diameter of (0.73) in. The middle - free length – part of the dog bone samples is (2.73) in in length and 0.3 inch in diameter, as shown in the figure (3-1) and figure (3-2):

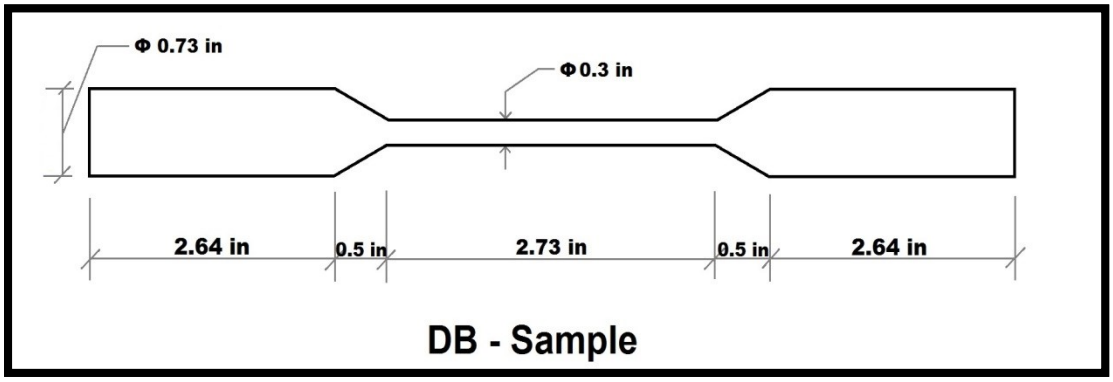

Figure 3-1 DB-Sample dimensions.

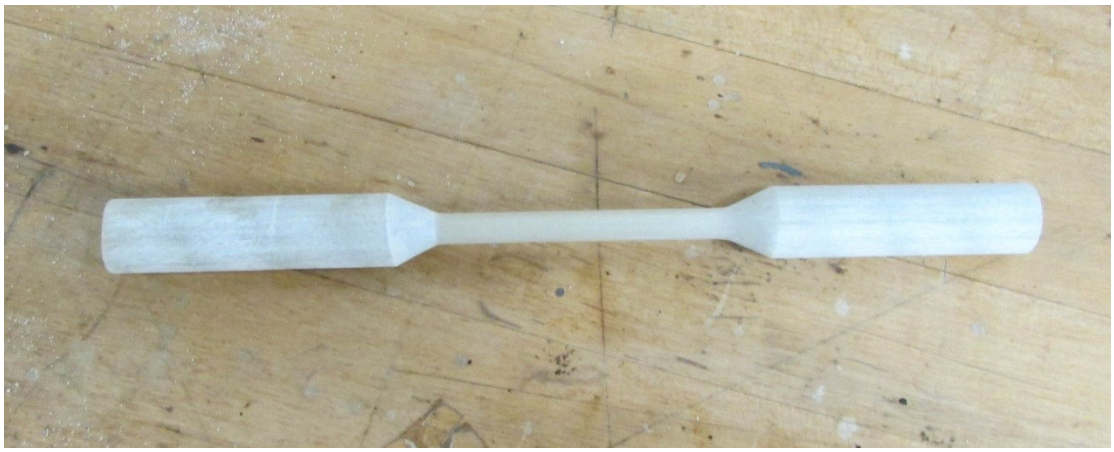

Figure 3-2 A Dog-done tension test specimen.

A total of 64 dog-bone specimens were used in this study. Four of these samples were control samples, while all other specimens were divided into groups, and each group was heat treated in an oven for a certain duration at a target temperature. Table (3-1) shows different test groups and description of the specimen heating process

Table 3-1 Description of specimens heating program, temperatures, and durations.

Group Name	No. of Samples	Max. Heating Temperature °C	Duration (min)	Description
DB-C	4	N A	N A	Control samples-tested without heating.
DB 250-0	5	250	0	Samples heated from ambient temperature to 250°C and subsequently removed from oven.
DB 250-5	5		5	Samples heated to 250°C and kept for an additional 5 min. at 250°C before removal.
DB 250-10	5		10	Samples heated to 250°C and kept for an additional 10 min. in the oven.
DB 250-30	5		30	Samples heated to 250°C and kept for an additional 30 min. in the oven.
DB 300-0	5	300	0	Samples heated from ambient temperature to 300°C and subsequently removed from oven.
DB 300-5	5		5	Samples heated to 300°C and kept for an additional 5 min. in the oven.
DB 300-10	5		10	Samples heated to 300°C and kept for an additional 10 min. in the oven.
DB 350-30	5		30	Samples heated to 300°C and kept for an additional 30 min. in the oven.
DB 350-0	5	350	0	Samples heated from ambient temperature to 350°C and subsequently removed from oven.
DB 350-5	5		5	Samples heated to 350°C and kept for an additional 5 min. in the oven.
DB 350-10	5		10	Samples heated to 350°C and kept for an additional 10 min. in the oven.
DB 350-30	5		30	Samples heated to 350°C and kept for an additional 30 min. in the oven.

3.2.2 Heating of Dog Bone Specimens

The samples were prepared for the heating process by first wrapping them tightly with two layers of heavy duty aluminum foil in the middle part (figure (3-3)). This was done to help achieve a more uniform distribution of heat to all parts of the test specimen, and to restrict oxygen on the surface of the samples. Test sample heated in air could catch fire at high temperatures, and thus damage the sample. A layer of fiberglass insulation material was applied over the gripping area, and the insulation was wrapped with a layer of the same type of aluminum foil (figure (3-4)). Insulating the gripping ends of the specimens was done to reduce the chance of weakening the end area due to heat, and to prevent the initiation of failure there. Narrow strips of high temperature tape were used to hold the aluminum foil against the surface of the specimens.

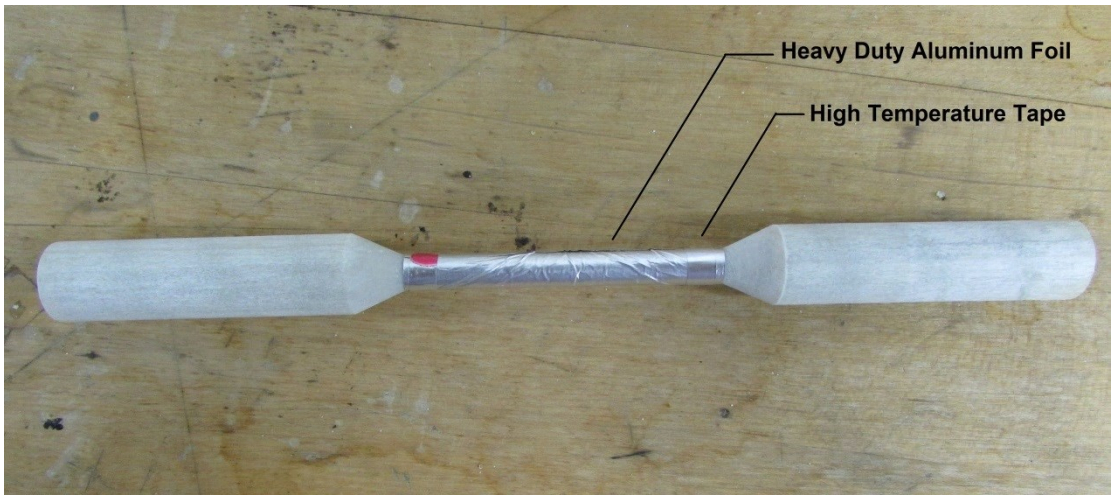

Figure 3-3 Middle part of dog-bone specimen wrapped with aluminum foil.

Figure 3-4 DB-specimen in preparation for heat treatment.

After preparation of specimens, they were heat treated in a Lindberg/Blue M Thermo Scientific 1100^{o}C box furnace (figure (3-5)) to the target temperatures and durations described in table (3-1). They were placed in the oven at ambient temperature, and the oven was then heated to the target temperature.

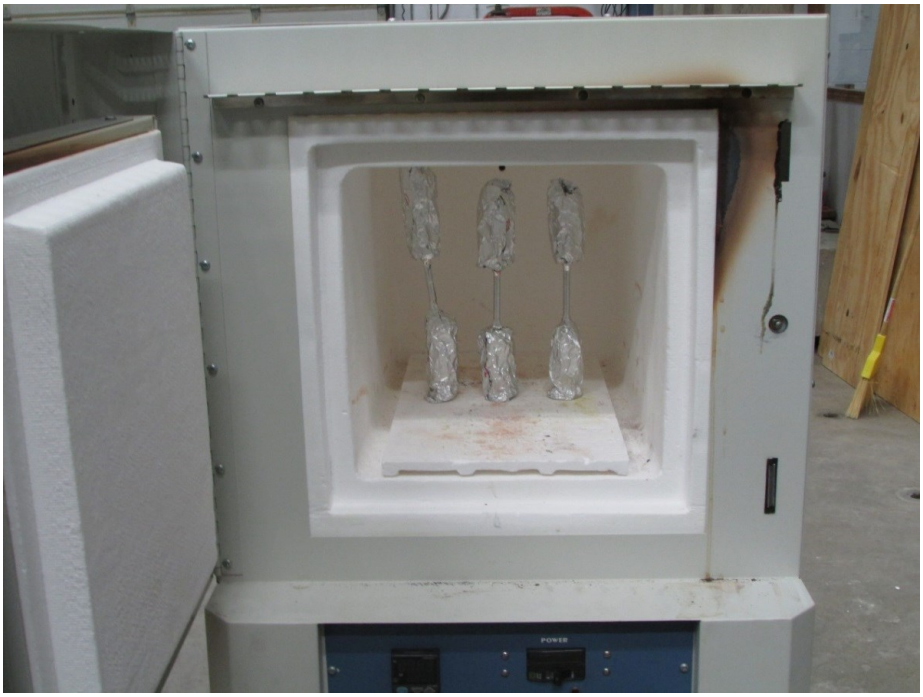

Figure 3-5 Dog-bone samples placed inside the furnace.

After samples reached their target temperature, they were additionally kept in the oven (at their target temperature) for the defined durations. The specimens were then taken out of the furnace and left to cool down at room temperature for at least 24 hours, before preparing them for the tensile strength test.

A number of preliminary tests were made to study the heating rate and behavior of the box heater, and to ensure compatibility in heating behavior for the different target temperatures of interest. The heater was operated empty to 250, 300, and 350^{o} C for 30 minutes in each case to obtain temperature-time data.

Figure (3-6) shows the temperature-time behavior as the oven is heated from ambient temperature to the target temperature. It took about 12 min, 15.5 min, and 24 min to reach 250^{o}C, 300^{o}C, and 350^{o}C, respectively. The temperature was then held constant for 30 minutes at each target temperature.

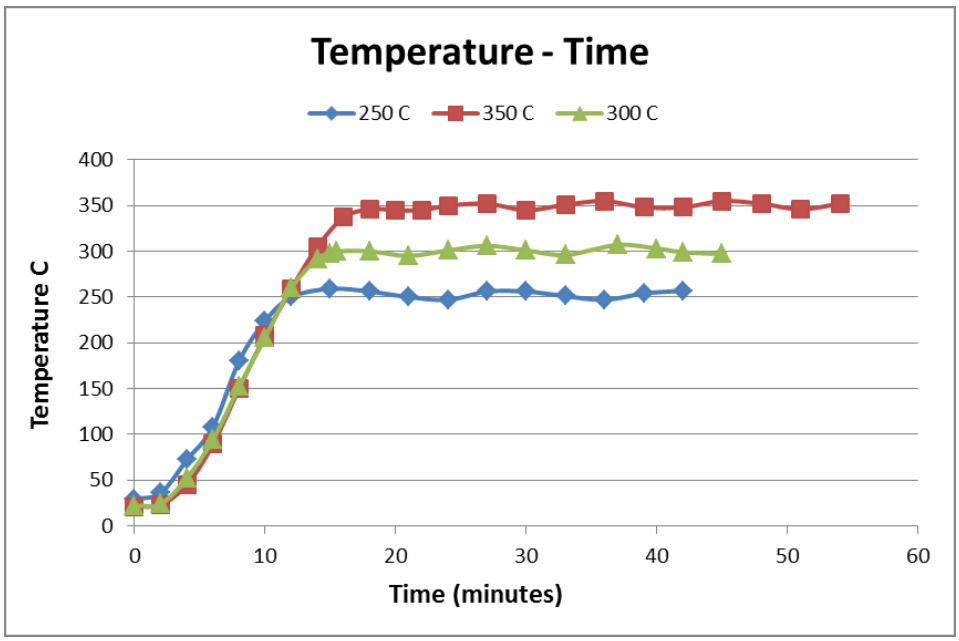

Figure 3-6 Temperature-time behavior of the box heater.

3.2.3 Testing of Dog-Bone Specimens:

Specimens were taken out of their aluminum foil casing, and prepared for the test. Two linear variable differential transducers (LVDT)s were attached to a fixture that was in turn, fastened to the specimens (figure (3-9)). The two LVDTs took measurements of the specimen's elongation during the tests. A data acquisition system was used to collect the LVDT data. The fixture was designed to attach the LVDTs to the specimen over a precise gage length. This was done by allowing contact points (that were 0.1 in wide only) between the fixture and the specimen's surface. A preliminary test was conducted using a strain gage directly mounted on the surface of one specimen, to relate measured strain gage readings to LVDT displacements (i.e. to verify the accuracy of the gage length).

Prior to the tests, the diameter of the middle part of the specimens was measured at three different places using a micrometer. The average of those three measurements was used for stress calculations.

Specimens were tested in a 110-Kip MTS Universal testing machine, with hydraulic grips and hydraulic control system. The machine was setup to a displacement-controlled testing mode. A number of preliminary tests were conducted based on suggested values of displacement rate from ASTM D3039 [23], to come up with the most adequate displacement rate to be applied in the actual tests. The ASTM D3039 [23] recommends a test duration of 1 to 10 minutes. The rate

used was 0.038 in/min, leading to an average duration of tests (to failure) of about 220 seconds (3.6 minutes).

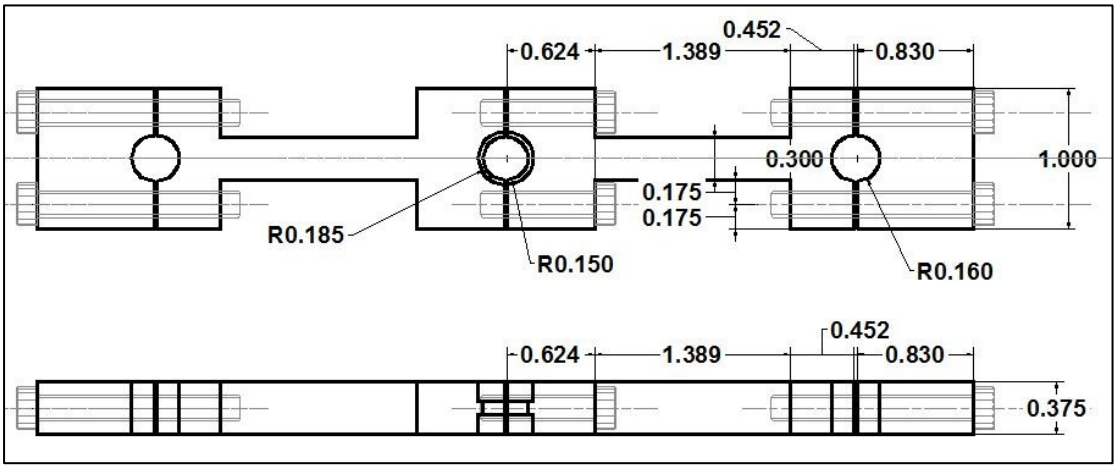

Figure 3-7 Upper aluminum fixture used to attach the LVDTs to the DB-specimen

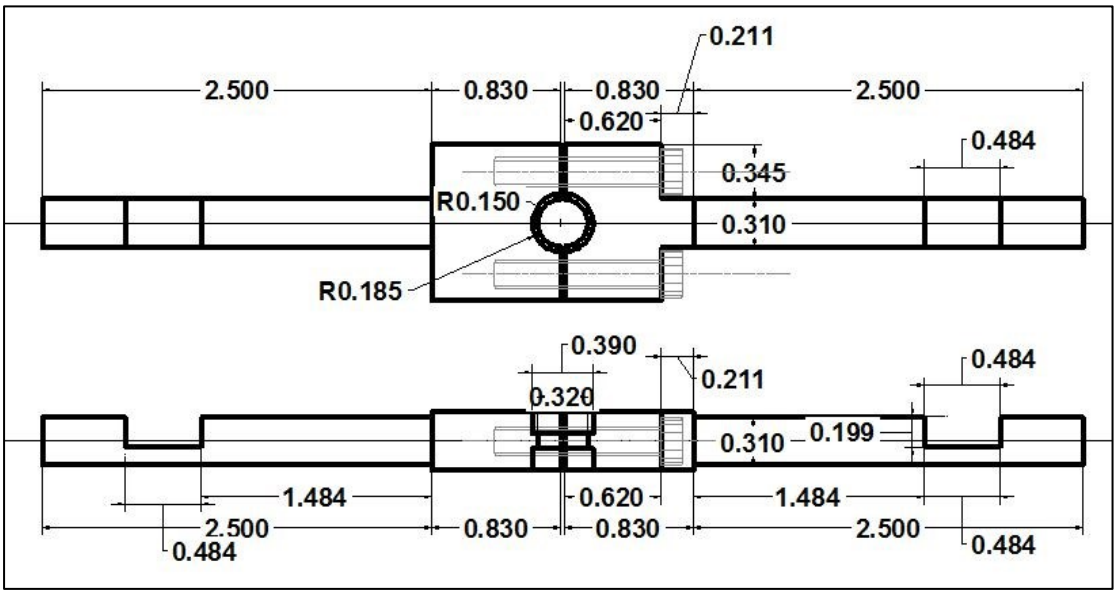

Figure 3-8 Lower aluminum fixture used to attach the LVDTs to the DB-specimen

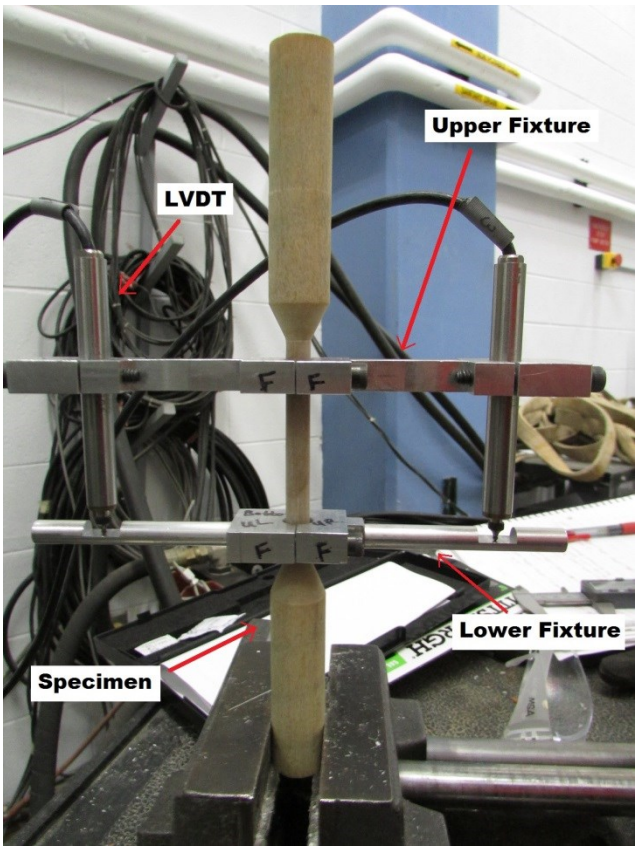

Figure 3-9 Dog-bone specimen prepared for tensile strength test

3.3 Full Size (FS) Specimens

3.3.1 Sample Description

The size, length, and preparation method for the full size tension tests were based on those utilized by Ellis [1]. The specimens were 43.5 inch long, and had a diameter of 0.75 inch (19 mm). No machining was involved in the preparation of these specimens. Instead, steel pipes were used to form anchorage areas at both ends of the specimens, to prevent them from slipping during the tension tests, and to resist transverse grip forces.

A total of nine FS-specimens were used in the experiments, and they were divided into two groups. The first group was not pre-heated (control specimens) while the other group was pre-heated to 350^{o}C in a custom-made oven. The specimens were placed in the oven at ambient temperature, and the oven was then heated to the target temperature. Unlike the DB-specimens, all FS-specimens were removed from the oven immediately after reaching target temperature and were not exposed to high temperatures for any additional duration.

Table (3-2) shows the FS-sample groups, and heating temperatures:

Table 3-2 Pre-heating program description for FS-specimens.

Group Name	**No. of Specimens**	**Heating Temperature ^{o}C**	**Description**
FS-C	**4**	**N A**	**Control samples - tested without heating.**
FS-AFR-350	**6**	**350**	**Samples heated to 350^{o}C, immediately removed from oven, and tested after they cooled down to room temperature.**

3.3.2 Pre-Heating of FS-Specimens

The specimens were pre-heated in a cylindrical oven specifically designed for this experiment. The body of the oven was made of two layers of metal (a double-wall furnace vent pipe), and was equipped with a longitudinal heating element fixed along the center of the cylinder (Fig.(3-13)). Two aluminum bar-holders were located near each end of the cylinder (see Fig.(3-10)) to hold the bars at a certain distance

from the heating element, and prevent them from contacting the heating element or the metal sides of the oven. A layer of fiberglass insulation was wrapped around the body of the oven (see figure (3-11)).

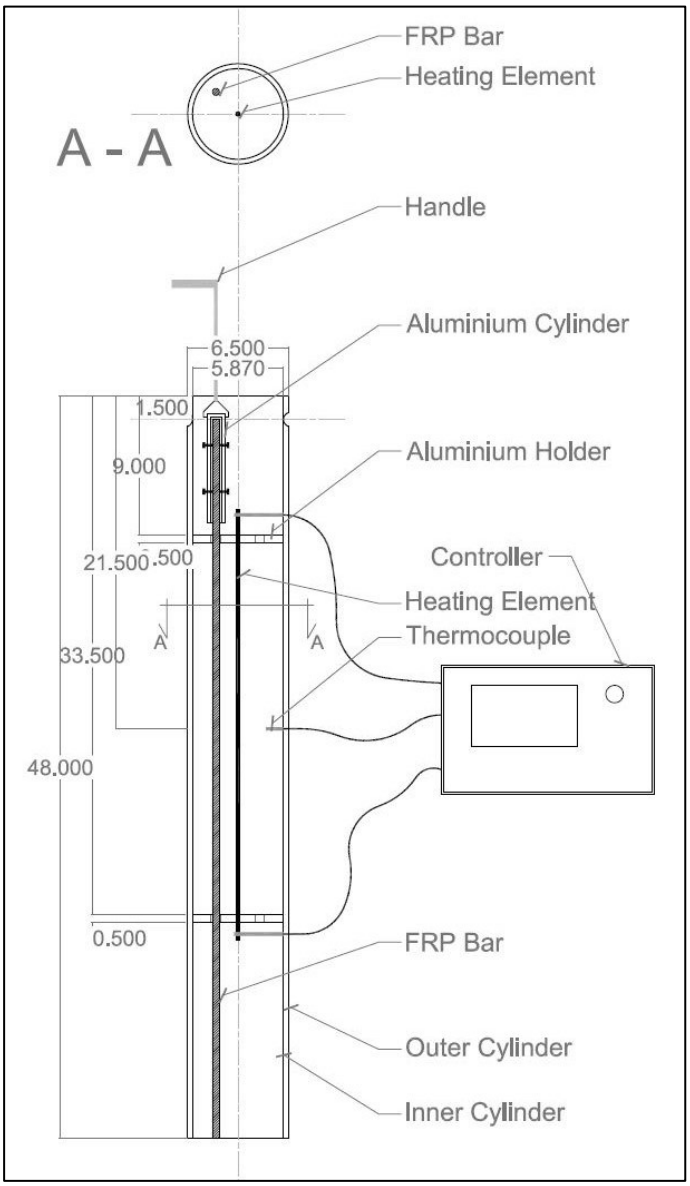

Figure 3-10 Description of the custom-made cylindrical oven used to heat FS-specimens (All dimensions are in inches)

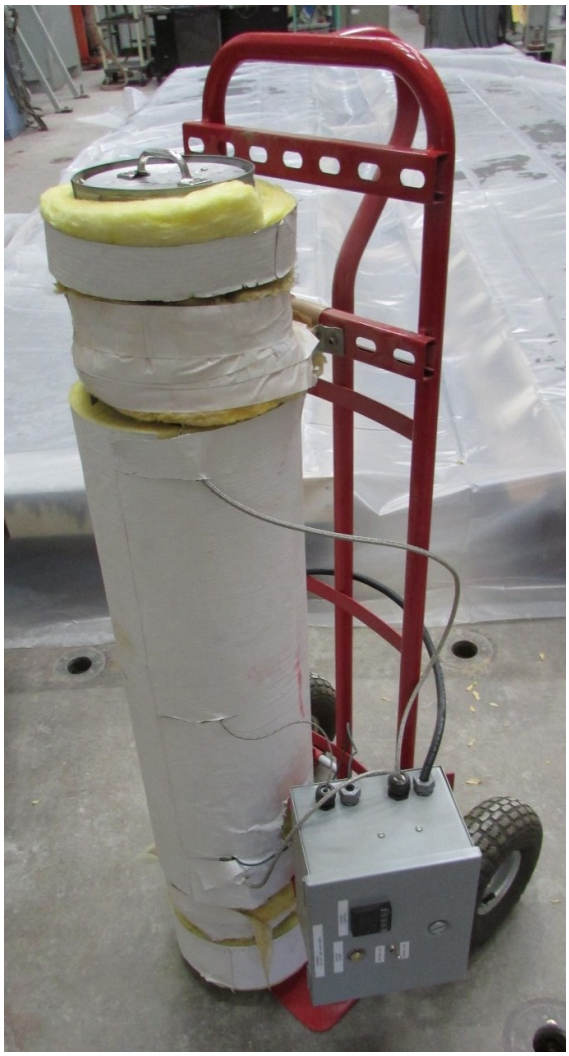

Figure 3-11 Heater used for the FS-samples heating

In preparation for the heating process, the specimens were wrapped with two layers of a heavy-duty aluminum foil (Fig. (3-12)) that was used to serve as a barrier to restrict oxygen from reaching the surface of the bars. Test samples heated in air could catch fire at elevated temperatures. Also, the aluminum foil serves as a facilitator for the uniform distribution of the heat to all sides of the bar surface. The

aluminum foil was secured around the bars using thin strips of high temperature tape.

Figure 3-12 Wrapped bar in preparation for heating.

Figure 3-13 Specimen in place through aluminum holder.

An aluminum cylinder with bolts drilled into its sides was used to hold the test bars and assist in rotating the bar while being heated. The grip, as shown in figure (3-14) is held from a handle, through which the bar is rotated manually a quarter of a turn every minute throughout the duration of the heating process. This

insures the uniform exposure to the heat, as opposed to having one side continuously exposed to the heating element. A small hole was drilled into the cap of the heater to pass the handle of the aluminum grip.

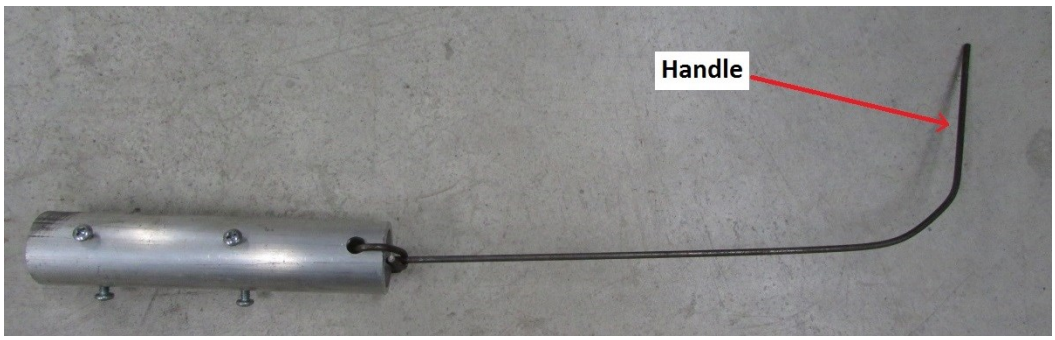

Figure 3-14 Aluminum grip.

Figure 3-15 Specimen prepared for heating.

After pre-heating the bar, and placing it in one of the rings of the aluminum holder, the lid of the heater was secured in place, and the oven was turned on. The temperature was monitored and controlled through a temperature controller. After target temperature was reached, the bars were taken out of oven, and the aluminum foil was removed. The bar was then left to cool down to room temperature (for at least 24 hours) (Fig. (3-16)). No more than one specimen was heated in the oven at any one time.

Figure 3-16 FS-Specimen after heating and removing aluminum foil.

Preliminary heating cycles were run using the cylindrical oven, to study the temperature-time behavior of the oven. Figure (3-17) shows the temperature-time response in three tests. The target temperature was reached in approximately 36.7 minutes.

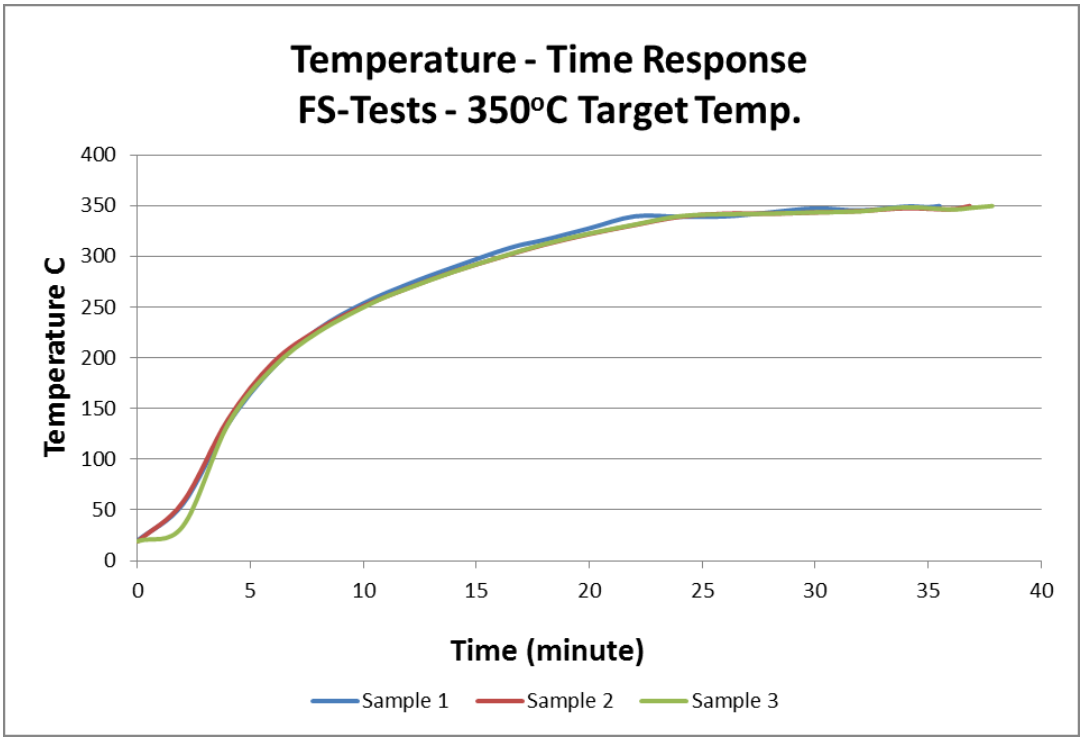

Figure 3-17 Oven heating rate for FS samples heated to 350^{o}C

3.3.3 Preparation of FS-Specimens for Tensile Strength Test

The preparation of the GFRP bars for the tensile strength test requires providing a gripping system for the bar, to be able to perform the test without

anchorage slippage and premature failure problems. Castro et al. [3], reviewed a number of gripping systems adopted by researchers in the past, including potted grips, parabolic grips, externally-threaded metal pipes, and split steel tubes. In the first three methods, the work of the gripping systems depends on bearing and shear mechanisms in conveying the forces. In the fourth method (adopted by Castro et al [3], Ellis [1], Wang et al. [2], and used in this research), A transverse compressive forces is applied on steel pipes filled with a grout surrounding the ends of each test bar. Other researchers such as Nanni et al [17], employed reusable cones made of FRP, filled with epoxy and silica sand.

In this work, two 1-foot long circular steel pipes of 1.25 inch inner diameter and 1.68 outer diameter ($1\frac{1}{4}$ in, X-Strong pipe) are used for the gripping system (as shown in Fig. (3-18)). The GFRP bar is embedded 11.5 inch into the steel pipe at each end of the bar, leaving 20.5 inches as free length of the bar. In this type of gripping system, providing a suitable embedment length and sufficient pipe size are key factors [2]. Castro et al. [3] recommend using an embedment length not less than 15d to prevent the bar from slipping out of the steel pipe.

The use of the grips is critical for overcoming the problem of the weakness of GFRP bars in shear. This would cause crushing of the anchorage area of the bars if the test is performed without some sort of a grip system that alleviates and redistributes the high stress in the anchorage area.

The material used to fill the space between the bar and the steel pipe is a high strength non-shrink Portland cement-based grout, with expansive additives. When pressure is exerted by the machine on the steel pipes, the grout conveys that pressure to the GFRP bar surface.

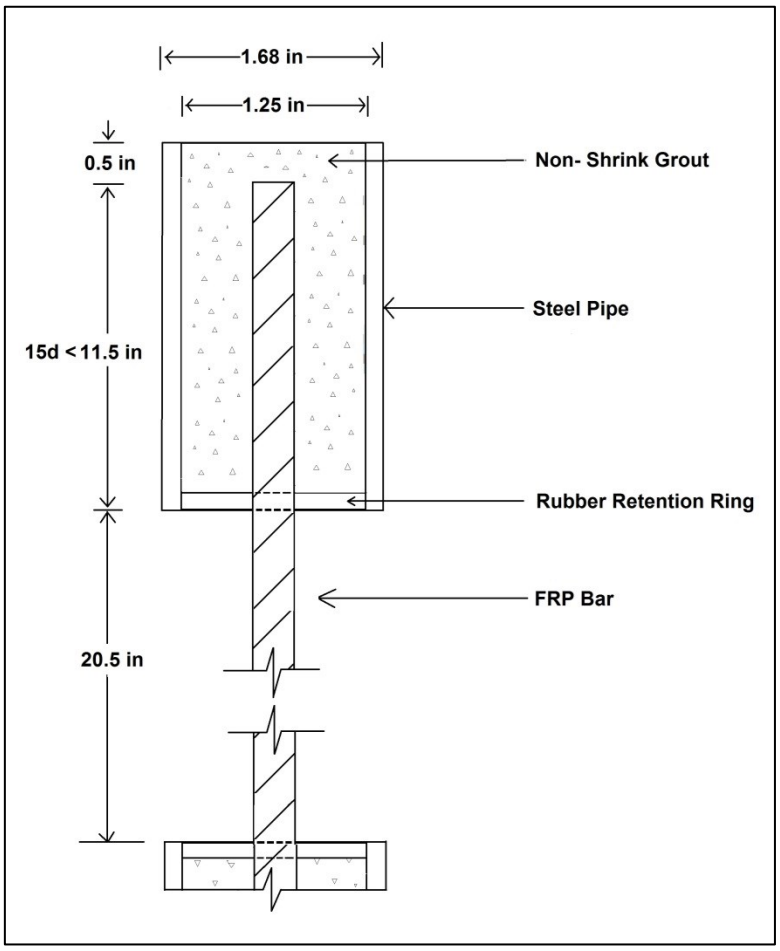

Figure 3-18 FS-specimen gripping system

A setup made with steel angles and wood was used to hold the specimens vertically in place, for casting of the grout inside the pipes (figure (3-19)). This setup was used to ensure that the specimens were perfectly straight, and the steel grips were concentric and parallel with respect to the axis of the bar [10]. A rubber ring of

0.25 in thickness was installed between the bar and each steel grip, to help in keeping the bar centered in the middle of the grips. Another function of the rubber rings was to prevent the grout from leaking out when it was being poured into the pipes [3]. In addition to the rubber rings, duct tape was used at the lower ends of the steel grips to further insure sealing of the grips against grout leakage. A space of approximately 0.5 inch was left at the upper part of the steel pipe (figure (3-18)) to allow for easy pouring of the grout into the pipe [3].

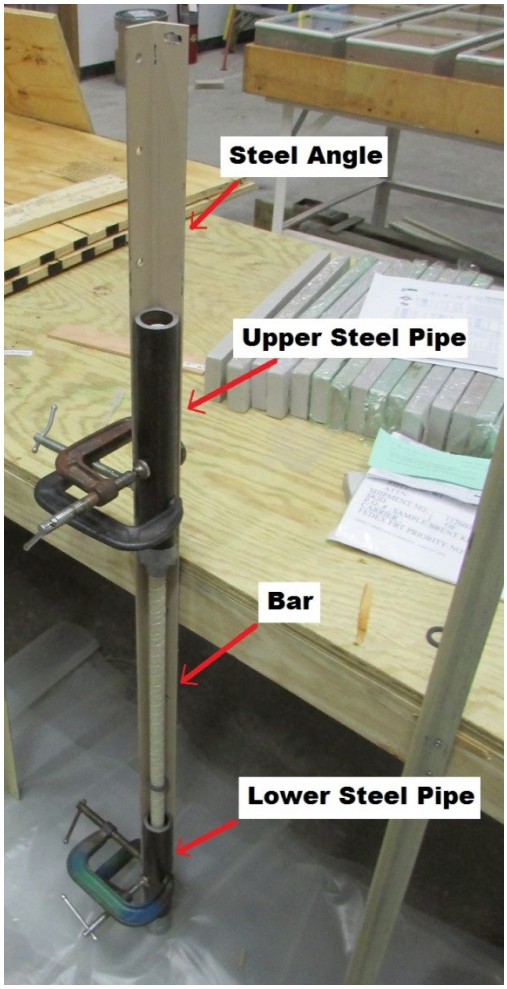

Figure 3-19 Steel angles used to hold the specimens vertical for grout casting

Figure 3-20 (on left) Steel pipe clamped and taped to prevent leakage. (on right) Grout cast into pipe.

After casting, the specimens were left for at least three days before performing the tension test. A 2 inch cube of the grout was tested in compression at three days age (before the test), to insure the required strength was developed. The cube failed at 63.1 MPa.

Tension tests of FS-bars were performed using a Tinius Olsen machine with a loading rate of around 6000-8000 lb/min. Two LVDTs were utilized to obtain the elongation data. The LVDTs were mounted on a fixture (similar to the one used for the DB-samples) which in turn was mounted on the free length of the bar (Fig.(3-21), Fig.(3-22) and Fig. (3-23)). Load and displacement data were recorded and then used

to obtain the stress-strain curves for the bars, as well as their modulus of elasticity. A preliminary test was conducted using a strain gage mounted on one specimen, to relate LVDT measurements to bar strain, and to verify the effective gage length.

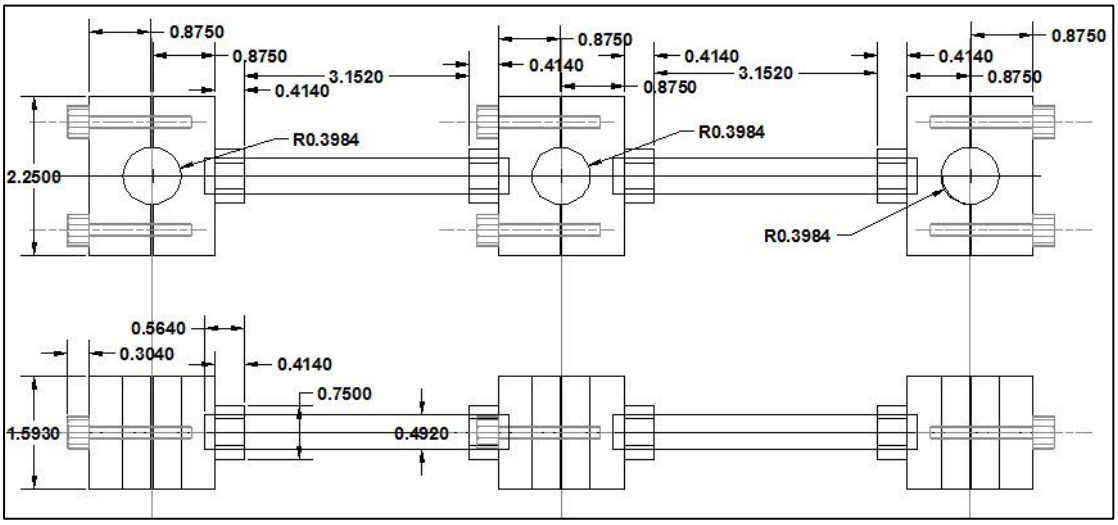

Figure 3-21 Upper fixture used for FS-specimen tension test.

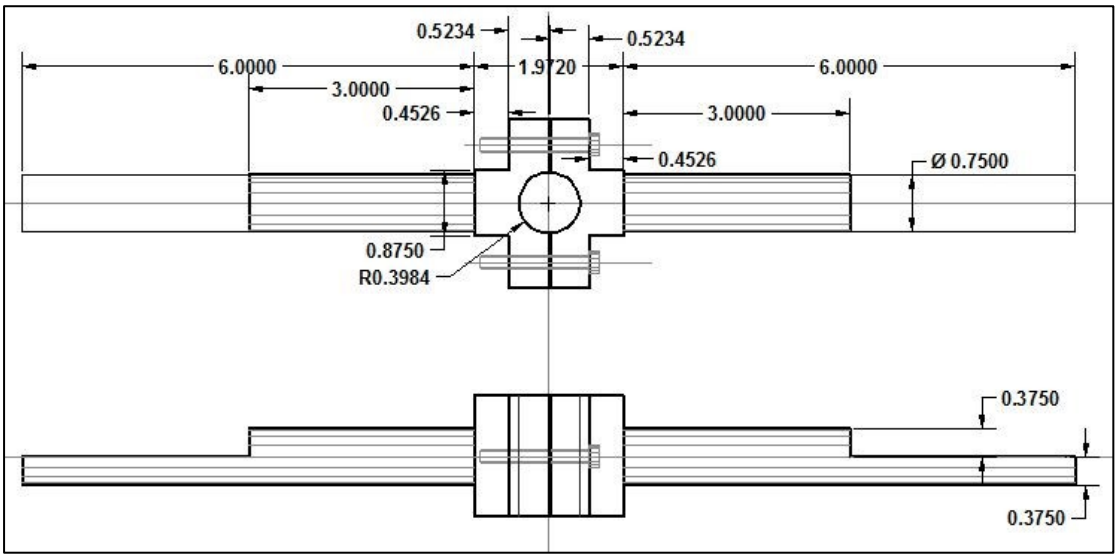

Figure 3-22 Lower fixture used for FS-specimen tension test.

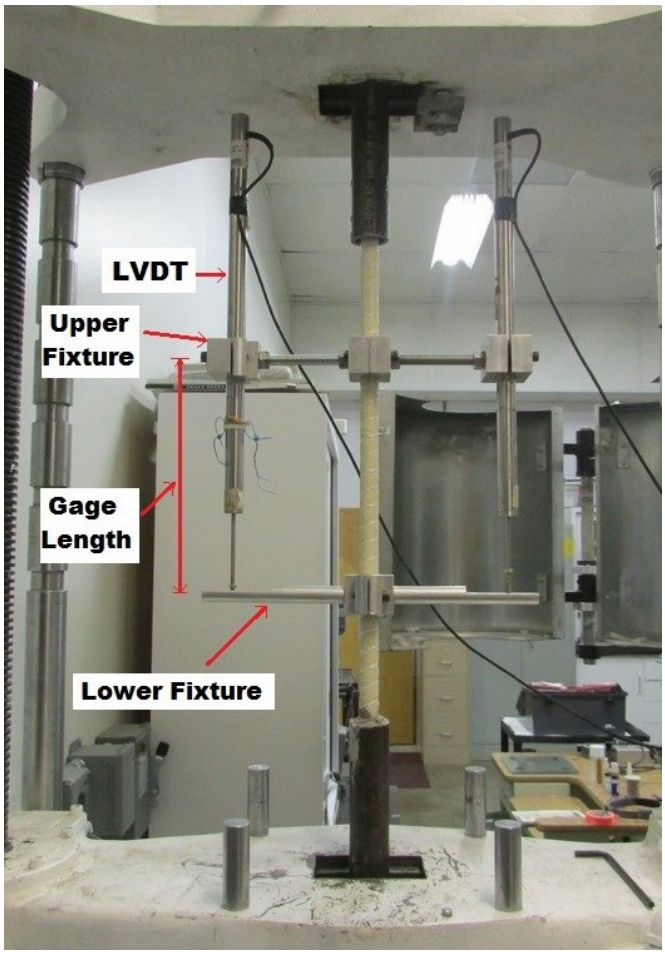

Figure 3-23 Tensile strength test setup.

3.4 Thermogravimetric Analysis TGA:

A thermogravimetric analysis test was run on a sample of an unheated GFRP bar. The original sample used weighed 22.13 mg. And the sample was heated to a temperature of 800^{o}C in air at a rate of 20 ^{o}C min^{-1}. The TGA test is used to study the variation in weight of specimen, and the percentage loss in mass, due to the heating process [18]. This helps better understand the change in properties of the FRP material at elevated temperatures [18].

CHAPTER 4: RESULTS

4.1 DB-Samples

4.1.1 DB-Control Samples

These samples were used as control in the study of the influence of heat on the machined GFRP samples. Results from four control specimens are reported. All specimens failed within the free length. However, due to the transverse pressure from the gripping system of the test machine, most specimens also exhibited cracks in their anchorage areas, from the beginning of the tests. Table (4-1) shows observations on the failure pattern of the control specimens.

Table 4-1 Failure observations of the control dog-bone specimens.

Sample Name	Failure Observations
DB-C-6	Gradual failure, outer fibers detaching from one side of the specimens.
DB-C-7	Fibers detaching from one side of the sample, bending the sample to the other side
DB-C-8	Brittle failure, separation of the out fibers from all sides of the sample
DB-C-10	Fibers detaching from one side of the sample, bending the sample to the other side.

Figure (4-1) Shows the control specimens after failure

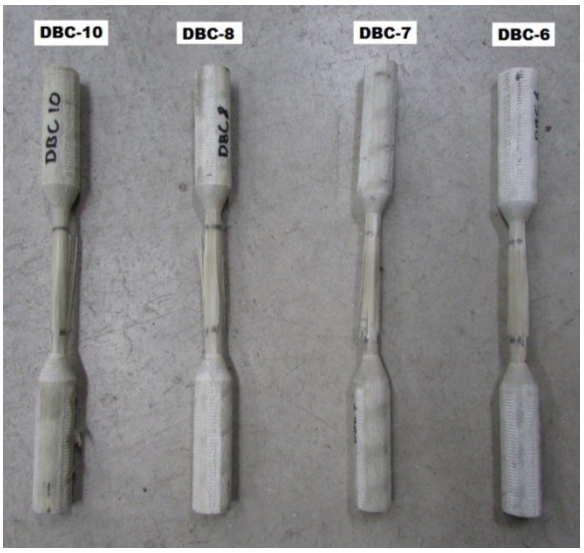

Figure 4-1 DB-control specimens after failure (DB-C-6 on right).

Table (4-2) presents a summary of test result for the control specimens. The average tensile strength of 115 ksi, is 15% higher than the manufacturer's guaranteed strength for this type of bars (100 ksi) [7]. Two values for the modulus of elasticity were calculated for each specimen. The first modulus was calculated based on the slope of the stress-strain curve up to the point of maximum stress (failure point), which is referred to as E (0-max). And the second modulus was based on the slope of the stress-strain curve up to the point of 50 ksi stress, referred to as E (0-50). In general, the E (0-50) modulus gives higher values do the slight bend in the stress-strain curves near failure. Also, two values for strain are given, the strain at maximum stress, which is the recorded strain value at the peak (failure) stress. The second strain term presented is the maximum strain, which is equal to the ultimate strain recorded, and is determined as the strain value correspondent to a (post-failure) stress equal to 90% of the failure stress. For this category of samples, and

due to their brittle failure, both strain values are equal, since there is no post peak elongation in the samples. The ultimate strain of 1.88% compared very well with those of full bars of the similar diameter. According to the manufacturer the ultimate strain of bars of 0.25 inches and 0.375 inches in diameter, are 1.94%, and 1.79%, respectively [7]. The energy density measurement was made through calculation of the area under the stress-strain curve (energy per unit volume), with the use of the trapezoidal rule.

Table 4-2 Summary of the control dog bone samples.

Sample Name	Max Load (lb)	Max Stress (ksi)	E (0-max) (ksi)	E (0-50) (ksi)	Strain at Max. Stress %	Max Strain %	Energy Density (ksi)
DB-C-6	8438	118	5924	6187	1.98	1.98	122
DB-C-7	8032	111	5818	5967	1.88	1.89	107
DB-C-8	8642	122	6344	6479	1.91	1.91	116
DB-C-10	7792	109	6190	6453	1.75	1.75	98
AVERAGE	**8226**	**115**	**6069**	**6272**	**1.88**	**1.88**	**111**
St. Dev.	**333.2**	**5.0**	**208.6**	**209.7**	**0.08**	**0.08**	**9.4**
COV %	**4.1**	**4.4**	**3.4**	**3.3**	**4.4**	**4.4**	**8.5**

As can be seen from the stress-strain curves in figure (4-2), the control samples maintained a linear elastic behavior up until failure, and failed in a sudden and brittle manner. The control samples were consistent and similar in their behavior throughout the test.

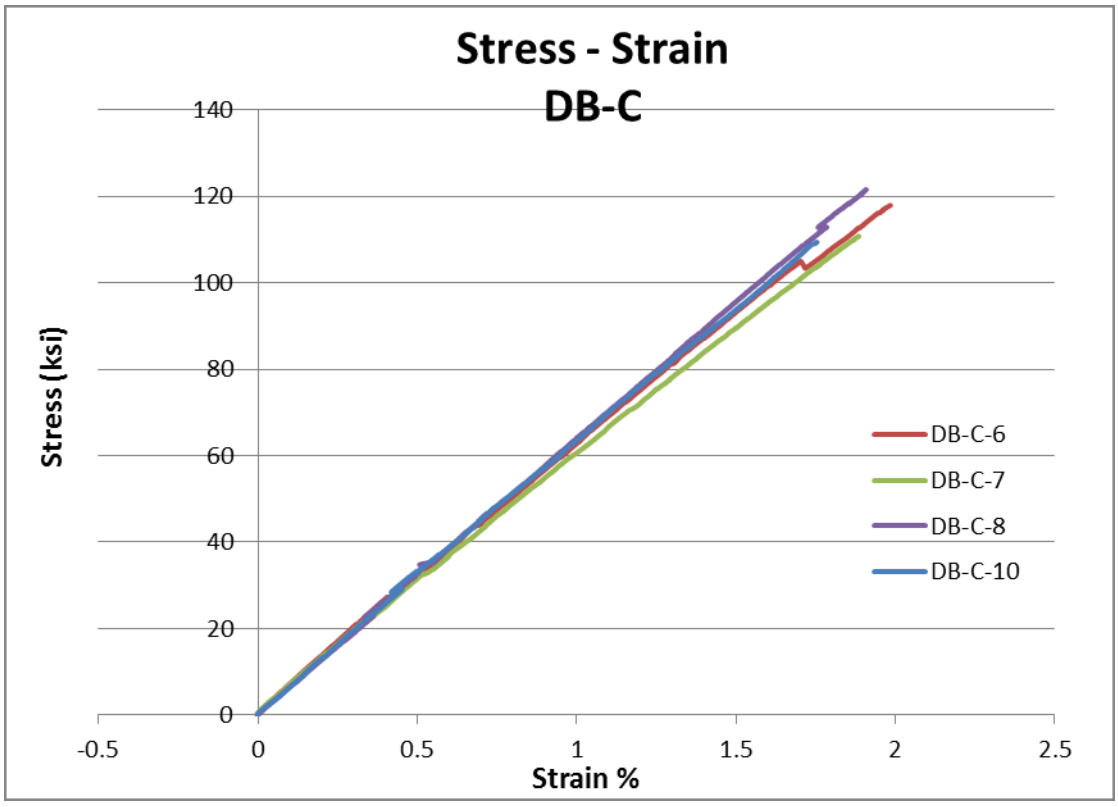

Figure 4-2 Stress-strain curves of the DB-Control samples.

4.1.2 DB-250-0 Samples:

All of the samples in this group failed in the free length. In terms of the color of the pre-heated specimens, no noticeable change (compared to control specimens) was observed in the color of these specimens (figure (4-3)). In general, the specimens in this category were very similar in their failure mode, all exhibiting brittle failure behaviors. Failure was characterized by sounds of fibers breaking, longitudinal fractures in the free length of the specimen, and separation of the outer layers of fiber.

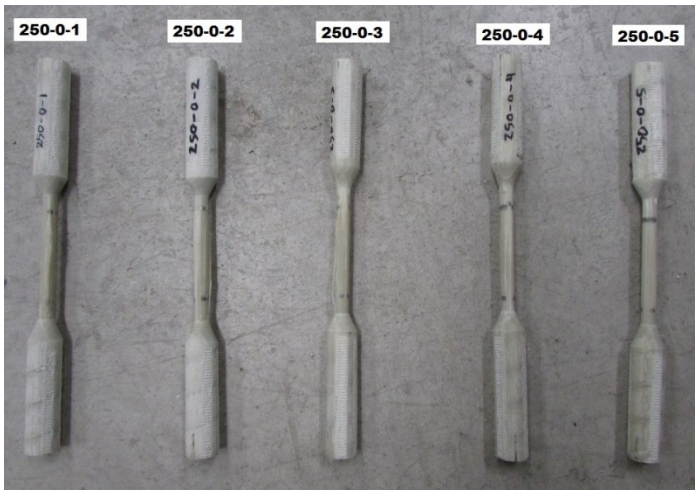

Figure 4-3 DB-250-0 specimens after failure.

The consistency of results across this group can be observed in almost identical stress-strain behaviors (shown in figure (4-4)), as well as low standard deviations for all test results (Table (4-3)).

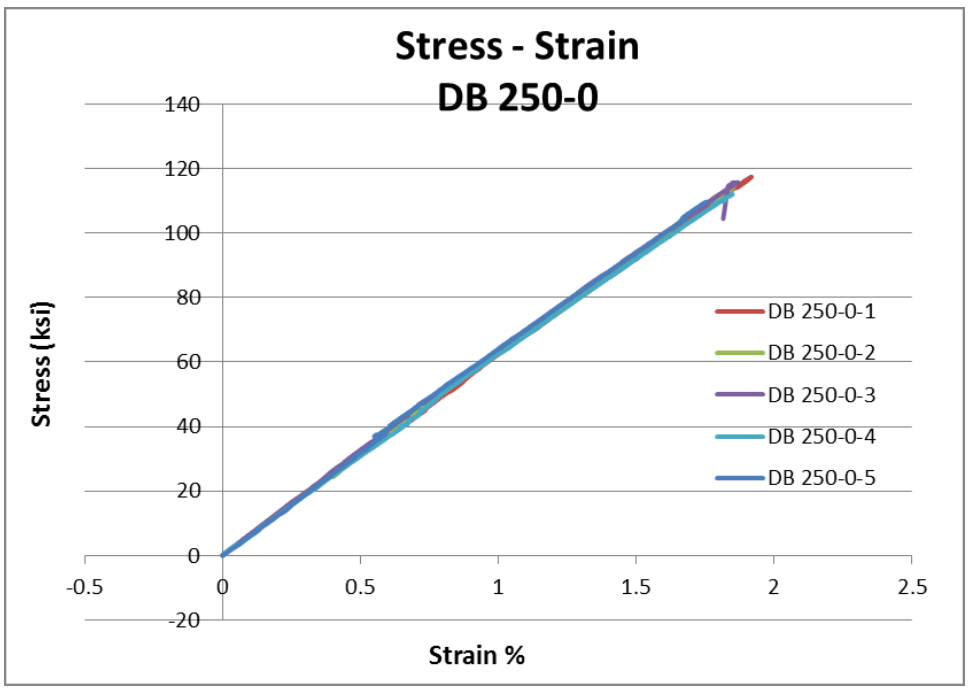

Figure 4-4 Stress-strain curves of the DB-250-0 samples.

Table 4-3 Summary of the test result for DB 250-0 samples.

Sample Name	Max Load (lb)	Max Stress (ksi)	E (0-max) (ksi)	E (0-50) (ksi)	Strain at Max. Stress %	Max Strain %	Energy Density (ksi)
DB 250-0-1	8432	117	6092	6111	1.92	1.92	114
DB 250-0-2	8088	115	6181	6269	1.86	1.86	108
DB 250-0-3	8241	116	6145	6500	1.87	1.87	111
DB 250-0-4	7887	112	6078	6175	1.85	1.85	105
DB 250-0-5	7773	110	6211	6638	1.75	1.75	98
AVERAGE	**8084**	**114**	**6141**	**6339**	**1.85**	**1.85**	**107**
St. Dev.	**237.2**	**2.7**	**50.8**	**199.7**	**0.05**	**0.05**	**5.6**
COV %	**2.9**	**2.4**	**0.8**	**3.1**	**2.88**	**2.88**	**5.2**

The dog bone samples heated to 250^{o}C showed little reduction in the tensile strength, when compared with control samples. As suggested by Ellis [1] this may be related to the "post cure" phenomenon, which in turn enhances some mechanical properties of the FRP material. The elastic modulus somewhat increased with respect to the unheated specimens, and there was some reduction in the ultimate strain of the specimens.

4.1.3 DB-250-5 Samples:

All of the samples in this group failed in the free length. As was the case with the 250-0 specimens, no obvious change in color of the specimens in this category was observed (compared to control). Figure (4-5) shows the specimens after failure

Figure 4-5 DB-250-5 specimens after failure (DB-250-5-1 on left).

The failure behaviors of the specimens in this group were also somewhat similar. Table (4-4) presents observations made during the failure of these specimens:

Table 4-4 Failure observations of the 250-5 samples.

Sample Name	Failure Observations
DB 250-5-1	Outer fibers separating from the middle part of the specimen, followed by breaking of the fibers.
DB 250-5-2	gradual breaking of the fibers, with little separation of the outer ones
DB 250-5-3	Gradual breaking sounds, accompanied by single fibers rupturing at the surface of the specimen.
DB 250-5-4	Gradual breaking of the outer fibers, along the circumference of the specimen.
DB 250-5-5	few breaking sound, with some fiber dust seen, and some longitudinal cracks on the body of the specimen

Apart from one specimen that has an ultimate strain slightly higher than the strain at maximum stress value, all other samples exhibited no signs of ductile behavior. However, the ultimate strain of this group is increased in comparison with the 250-0, and was approximately equal to that of the control group. The average

strength of the DB-250-5 samples remained almost the same as that of the 250-0 specimens. While a reduction in the elastic modulus was observed. Table (4-5) shows detailed test results for the 250-5 group

Table 4-5 Summary of the test result for DB 250-5 samples.

Sample Name	Max Load (lb)	Max Stress (ksi)	E (0-max) (ksi)	E (0-50) (ksi)	Strain at Max. Stress %	Max Strain %	Energy Density (ksi)
DB 250-5-1	8602.8	118.0	5894.0	6009.5	2.00	2.00	120.1
DB 250-5-2	7799.9	107.9	6087.3	6134.5	1.77	1.80	96.1
DB 250-5-3	8296.0	114.3	5850.7	6107.2	1.94	1.94	113.6
DB 250-5-4	7883.4	109.1	5870.2	5747.6	1.84	1.84	99.4
DB 250-5-5	8084.7	115.9	6148.3	6118.6	1.89	1.89	110.1
AVERAGE	**8133.4**	**113.0**	**5970.1**	**6023.5**	**1.89**	**1.89**	**107.9**
St. Dev.	**290.8**	**3.9**	**122.9**	**144.7**	**0.08**	**0.07**	**8.9**
COV %	**3.6**	**3.5**	**2.1**	**2.4**	**4.2**	**3.8**	**8.3**

The stress-strain responses of this group were fairly similar (figure (4-6)). and all stress-strain curves are linear up to the point of failure.

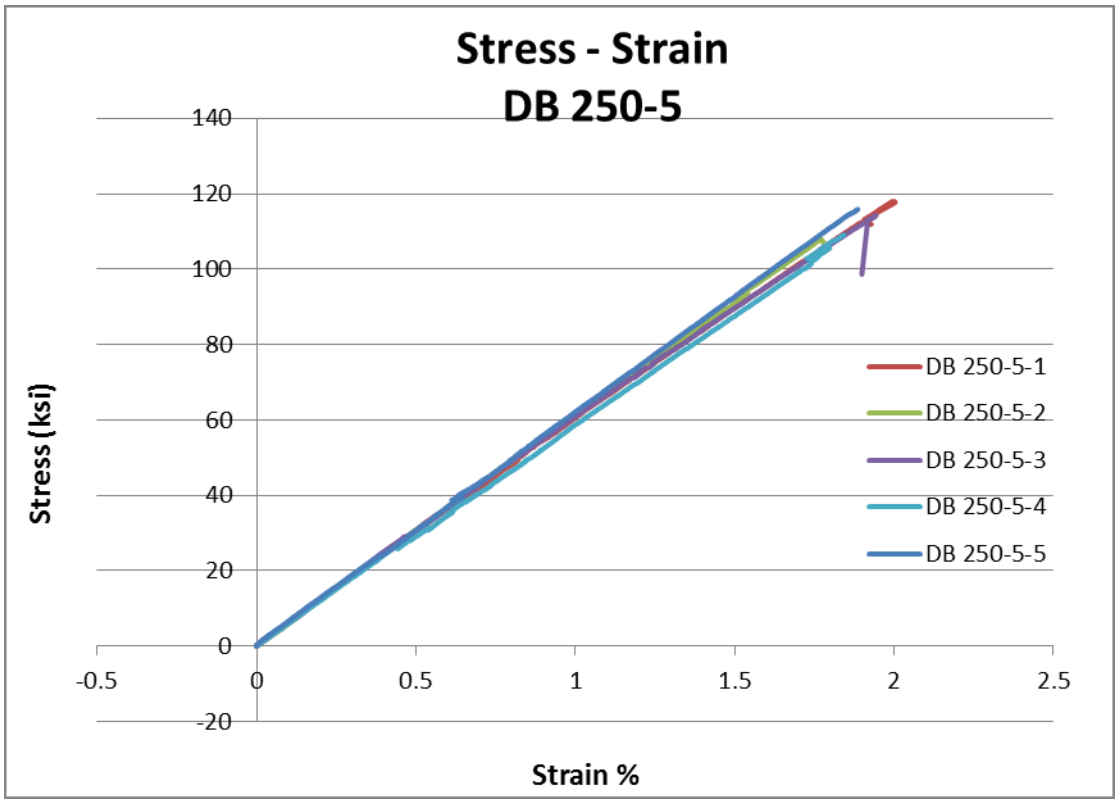

Figure 4-6 Stress-strain curves of the DB-250-5 samples.

4.1.4 DB-250-10 Samples:

All of the samples in this group failed in the free length. The color of the specimens showed very slight change to become more yellowish. The fibers' breaking point in most samples of this category and other categories was at the point of contact of the fixtures that held the LVDTs during the tests. A description of the failure manner for the specimens in this group is given in table (4-6). Figure (4-7) shows a picture of all specimens in this group after failure.

Table 4-6 Failure modes of the 250-10 samples.

Sample Name	Failure Mode
DB 250-10-1	Gradual and slow failure, with longitudinal cracks accompanied by some fiber separation.
DB 250-10-2	Slow failure process, with features similar to that of the 250-10-1 sample, only more separation of fibers noticed.
DB 250-10-3	Sudden failure, with one relative bang, accompanied by fibers breaking on a side of the sample.
DB 250-10-4	Gradual failure, with longitudinal cracks accompanied by some fiber separation.
DB 250-10-5	Quick failure characterized by two breaking sounds.1st accompanied by longitudinal fracture, and the 2nd by dispersal & separation of fibers.

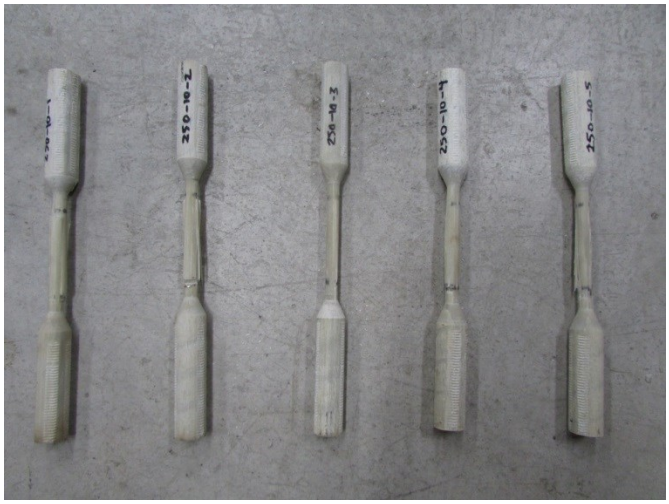

Figure 4-7 DB-250-10 samples after failure (250-10-1 on left)

The stress-strain curves for the specimens in the 250-10 group are shown in figure (4-8). All of them failed in a brittle way, showing no indications of post peak ductile behavior.

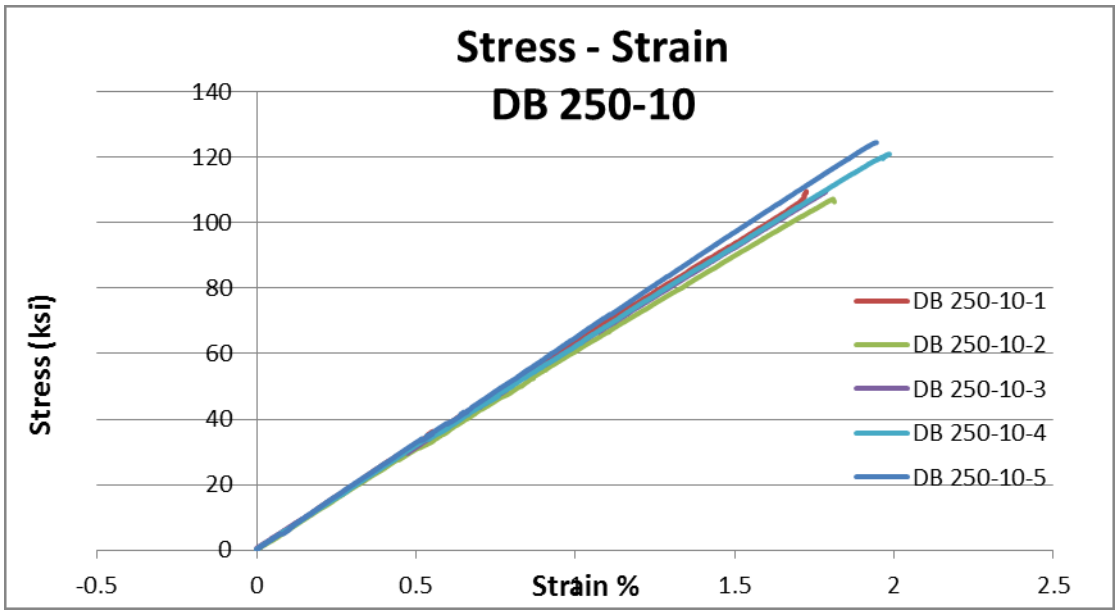

Figure 4-8 Stress-strain curves of the DB-250-10 specimens.

Table (4-7) shows results of tests in the 250-10 group. The 250-10 specimens showed an increase in the modulus of elasticity in comparison with the 250-5 specimens. The average strength did not change with this increase in the heating duration (remained the same as it was in both 250-0 and 250-5 specimens). As for the ultimate strain, it showed a decline compared to the 250-5 specimens, and about the same as the 250-0 specimens.

Table 4-7 Summary of the test result for DB 250-10 specimens.

Sample Name	Max Load (lb)	Max Stress (ksi)	E (0-max) (ksi)	E (0-50) (ksi)	Strain at Max. Stress %	Max Strain %	Energy (ksi)
DB 250-10-1	7790	110	6184	6355	1.72	1.72	94
DB 250-10-2	7813	107	5925	6016	1.81	1.81	99
DB 250-10-3	7802	109	6075	6177	1.78	1.78	99
DB 250-10-4	8663	121	6095	6182	1.98	1.99	122
DB 250-10-5	8934	124	6427	6416	1.94	1.94	122
AVERAGE	**8200**	**114**	**6141**	**6229**	**1.85**	**1.85**	**107**
St. Dev.	**495.7**	**7.0**	**165.6**	**142.2**	**0.10**	**0.10**	**12.4**
COV %	**6.0**	**6.1**	**2.7**	**2.3**	**5.4**	**5.3**	**11.5**

4.1.5 DB-250-30 Specimens:

Heating the dog bone specimens for 30 minutes at 250^{o}C, caused their color to change to a light brown color. And all 250-30 specimens failed in their free length. Figure (4-9) shows a picture of all 250-30 specimens after failure. Table (4-8) shows observations on failure modes of these specimens.

Figure 4-9 DB-250-30 samples after failure (250-30-1 on left)

The specimens of this group show a more dispersed stress-strain curves (figure (4-10)), which is partly due to the fact that the fixture on specimen 250-30-5 appears to have slipped around 40 ksi, causing a shift in the stress-strain curve of that sample. As noticed in the other groups of the 250°C, this group too maintained a linear elastic behavior up to failure, in spite of the considerably longer duration of heat exposure.

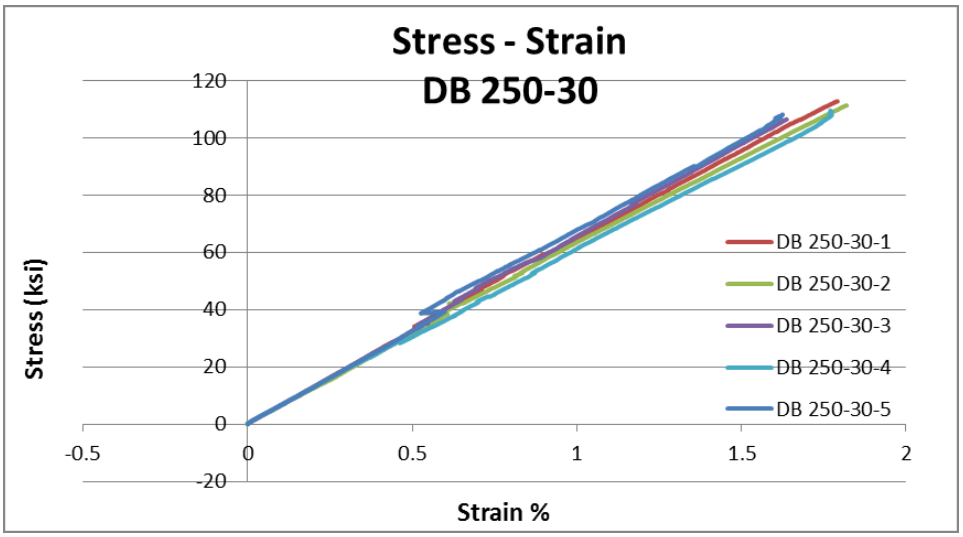

Figure 4-10 Stress-strain curves of the DB-250-30 samples.

Table 4-8 Failure modes of the 250-30 samples.

Sample Name	Failure Mode
DB 250-30-1	Quick failure, surface fibers breaking, and longitudinal cracks forming.
DB 250-30-2	Sudden failure, pushing some of the surface fibers slightly outwards.
DB 250-30-3	Gradual breaking sounds, accompanied by longitudinal fractures in the free length of the specimen.
DB 250-30-4	a low breaking sound, with the separation of a layer of fibers, followed by some quick fiber breakings and separation.
DB 250-30-5	successive breaking of fibers, with little separation observed on the surface of specimen, and fractures being more on one side of the sample

All test results are summarized in table (4-9). The elastic modulus of this group showed a continued increase in comparison with the 250-10 specimens. The ultimate strain continued its decline with regard to the 250-5 and 250-10 groups. The strength of these samples exhibited a small reduction of 4% with respect to the 250-10 group.

Table 4-9 Summary of the test result for DB 250-30 samples.

Sample Name	Max Load (lb)	Max Stress (ksi)	E (0-max) (ksi)	E (0-50) (ksi)	Strain at Max. Stress %	Max Strain %	Energy Density (ksi)
DB 250-30-1	7957	113	6272	6661	1.79	1.79	103
DB 250-30-2	8028	111	6110	6450	1.82	1.82	104
DB 250-30-3	7468	106	6495	6806	1.64	1.64	88
DB 250-30-4	7766	110	6004	5956	1.77	1.77	95
DB 250-30-5*	7663	108	6577	7161	1.62	1.63	89
AVERAGE	**7805**	**110.0**	**6220.3**	**6468.5**	**1.75**	**1.75**	**97.6**
St. Dev.	**216.9**	**2.4**	**185.3**	**321.7**	**0.07**	**0.07**	**6.4**
COV %	**2.8**	**2.2**	**3.0**	**5.0**	**4.0**	**4.0**	**6.6**

(*) Results not included in the averages reported due to LVDT fixture slip.

4.1.6 DB-300-0

No obvious change in the color of the 300-0 specimen (compared to control specimens) was observed. All specimens in this group failed in the free length. Table (4-10) describes the observed failure behaviors of the specimens.

Table 4-10 Failure modes of the 300-0 samples.

Sample Name	Failure Mode
DB 300-0-1	Quick failure, successive breaking of the surface fibers, and longitudinal cracks forming.
DB 300-0-2	Gradual failure, longitudinal fractures forming, followed by breaking of fibers.
DB 300-0-3	Gradual failure, longitudinal fractures forming, followed by breaking of fibers.
DB 300-0-4	Quick failure, breaking sounds accompanied by the formation of longitudinal cracks.
DB 300-0-5	Single fiber breaking sounds, followed by a sudden separation of fibers from the core in the free length, turning the fixtures a bit.

Table (4-11) shows results of the specimen tests of this group. The average strength of the samples in this group was higher than all other dog bone samples in this study, reaching 127 ksi and 128 ksi for some specimens. Aside from the improved strength, this group exhibited the highest ultimate strain values, reaching an average of 2.07 %. Figure (4-12) shows stress-strain responses in all specimens. Despite the brittle failure and the linear elastic behavior up to failure, most specimens exhibited a slightly higher ultimate strain than the strain at failure. On the other hand, this group constituted the lowest modulus of elasticity among all dog-bone specimens.

Table 4-11 Summary of the test result for DB 250-0 samples.

Sample Name	Max Load (lb)	Max Stress (ksi)	E (0-max) (ksi)	E (0-50) (ksi)	Strain at Max. Stress %	Max Strain %	Energy Density (ksi)
DB 300-0-1	9216	127	5702	5758	2.22	2.23	144
DB 300-0-2	8468	118	5574	5769	2.13	2.22	131
DB 300-0-3	8282	116	6299	6145	1.79	1.83	101
DB 300-0-4	9124	128	6176	6207	2.07	2.07	133
DB 300-0-5	8368	116	5885	5955	1.96	1.98	115
AVERAGE	**8691**	**121**	**5927**	**5967**	**2.03**	**2.07**	**125**
St. Dev.	**396.1**	**5.2**	**274.8**	**185.7**	**0.15**	**0.15**	**14.9**
COV %	**4.6**	**4.3**	**4.6**	**3.1**	**7.3**	**7.2**	**11.9**

A picture of all specimens in this group (after failure) is shown in figure (4-11). Specimen 300-0-2 was damaged in the machine after test completion, and the damage shown did not happen during the test.

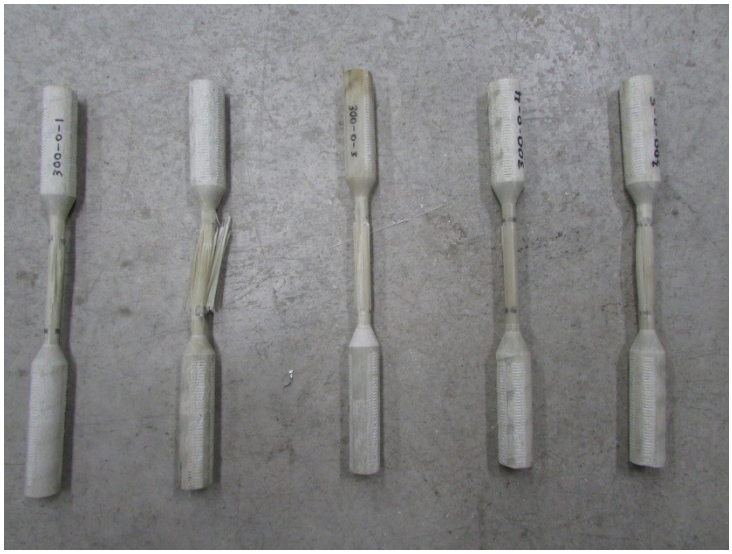

Figure 4-11 DB-300-0 samples after failure (DB-300-0-1 on left).

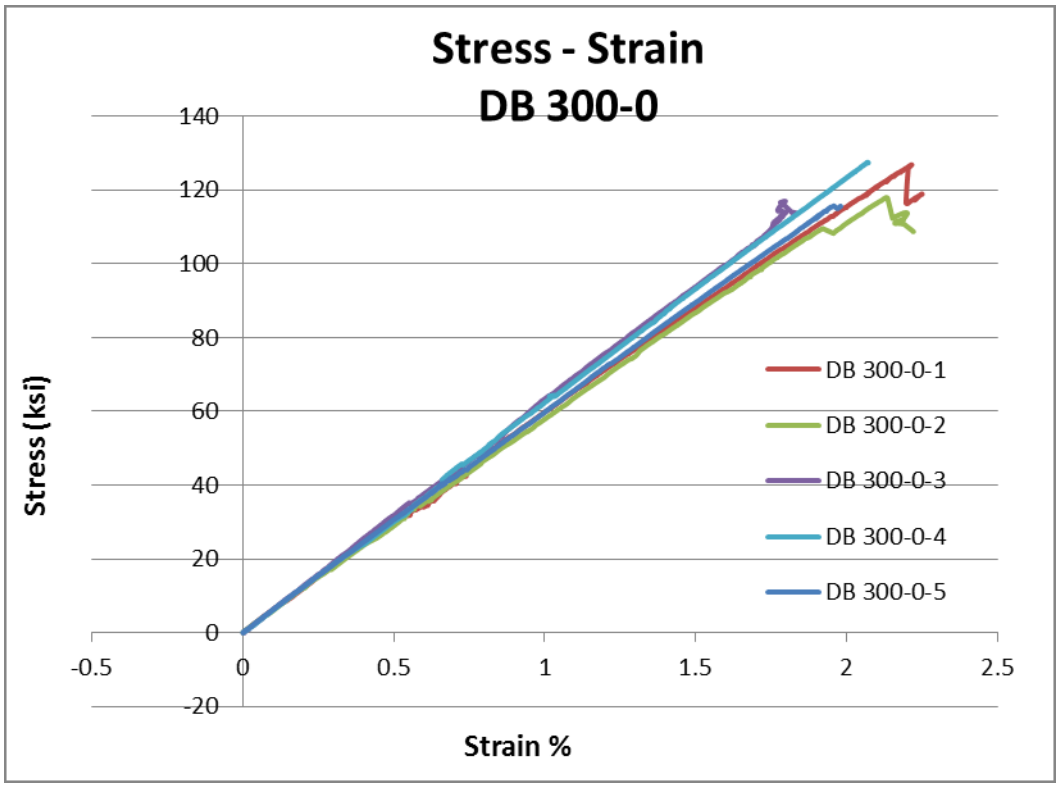

Figure 4-12 Stress-strain curves of the DB-300-0 samples.

4.1.7 DB-300-5

As was the case with the 300-0 specimens, the specimens of this category showed no change in color (compared to control specimens). And all of the specimens failed in the free length. Apart from the first specimen, which showed some ductility in the stress-strain curve (figure (4-13)), all other specimens failed in a brittle manner, and the stress-strain curves of the specimens remained linear up to failure.

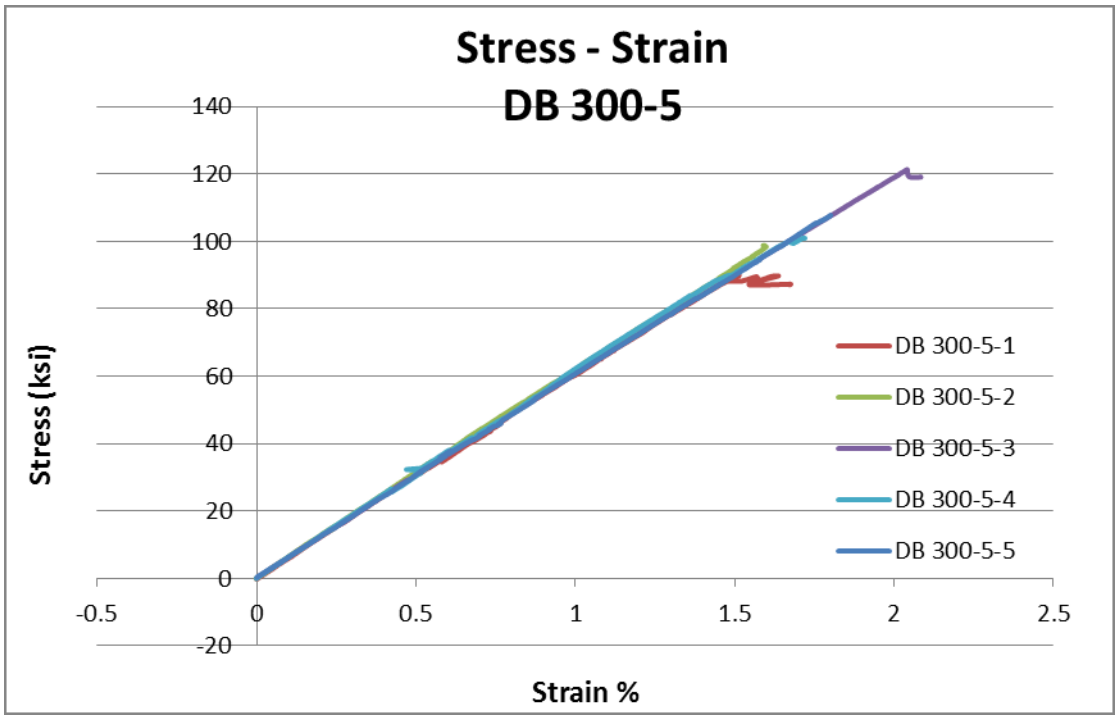

Figure 4-13 Stress-strain curves of the DB-300-5 samples.

Table (4-12) describes the observed failure behaviors of the specimens. The average tensile strength of this group showed a decrease by 14% with respect to the 300-0 results. However, the elastic modulus for this group increased by 2% in comparison with the 300-0 group. All specimens were similar in their tensile strength, apart from specimen 300-5-3 which exhibited a considerably higher strength than the other samples. The properties of this specimen were closer to that of the 300-0 specimens. This large difference caused the COV for the strength, strain, and energy density for the group to be noticeably high. The average ultimate strain for the 300-5 specimens showed a 14.5% reduction in comparison with the 300-0 samples.

Table 4-12 Summary of the test result for DB 300-5 samples.

Sample Name	Max Load (lb)	Max Stress (ksi)	E (0-max) (ksi)	E (0-50) (ksi)	Strain at Max. Stress %	Max Strain %	Energy Density (ksi)
DB 300-5-1	6612	90	5992	6008	1.51	1.67	69
DB 300-5-2	7258	99	6108	6247	1.59	1.59	78
DB 300-5-3	8642	121	5917	6069	2.04	2.08	126
DB 300-5-4	7393	101	6017	6117	1.72	1.72	91
DB 300-5-5	7821	108	5962	6045	1.80	1.80	98
AVERAGE	**7545**	**104**	**5999**	**6097**	**1.73**	**1.77**	**92**
St. Dev.	**671.6**	**10.5**	**63.8**	**82.7**	**0.18**	**0.17**	**19.4**
COV %	**8.9**	**10.1**	**1.1**	**1.4**	**10.6**	**9.5**	**21.0**

Figure (4-14) shows the 300-5 samples after being tested. Most of the specimens were similar in their failure pattern, characterized by longitudinal cracks along the free length of the specimens. The breaking point for these specimens was at the area of contact with the LVDT holding fixtures.

Figure 4-14 DB-300-5 samples after failure (DB-300-5-1 on left).

4.1.8 DB-300-10

There was very little change in color noticed among the specimens heated for 10 minutes at 300°C (figure (3-15)). All specimens failed in a brittle manner, as can be seen from the linear stress-strain curves of these specimens shown in figure (4-16). Also, all specimens failed in the free length. The specimens show a relatively good consistency in the elastic modulus results.

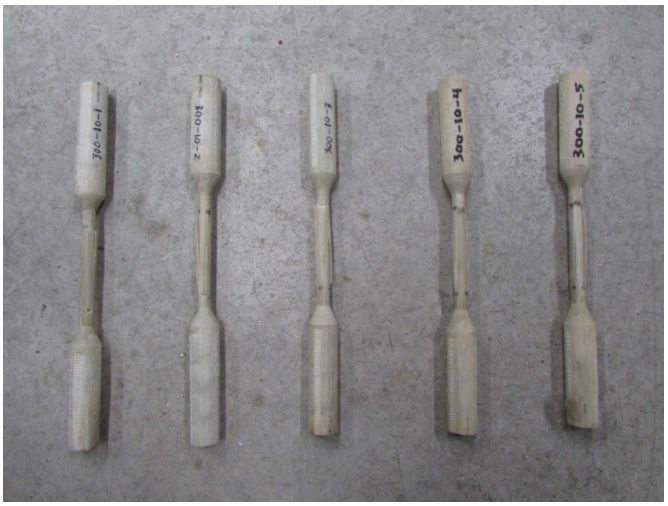

Figure 4-15 DB-300-10 samples after failure (DB-300-10-1 on left).

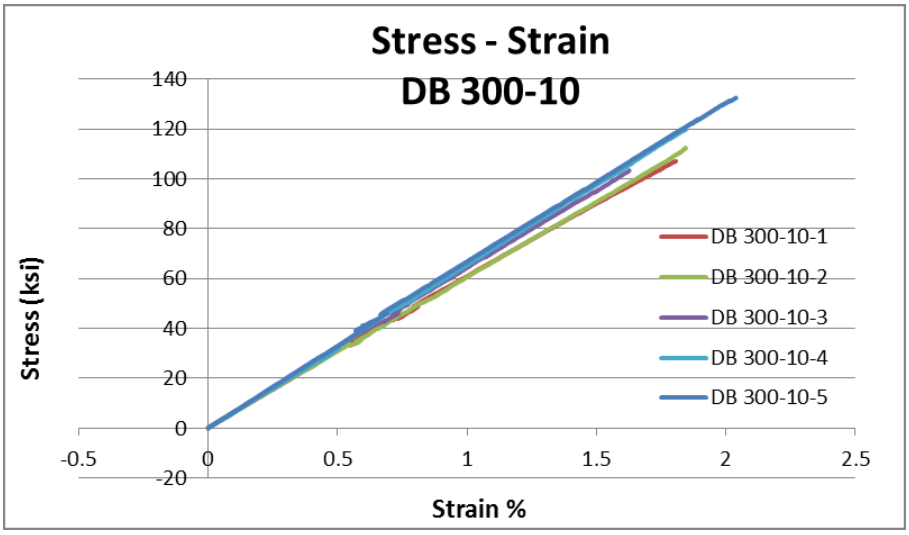

Figure 4-16 stress-strain curves of the DB-300-10 samples.

Table (4-13) shows the detailed results for this group. The modulus of elasticity for these specimens showed an increase of 4.5% in comparison with the 300-5 specimens, while there was a surprising increase in the average strength of this group by 10% with respect to the specimens heated for 5 minutes. This is in contrast to the expected reduction in the strength of the composite material as it is heated longer. Yet, this may be due to the fact that the specimen 300-10-5 exhibited an unusually high strength of 133 ksi, thereby increasing the average tensile strength of the group. This was the highest tensile strength recorded in a specimen reached among all DB-samples. There is also an apparent increase in the average ultimate strain in the 300-10 group compared to the 300-5 group.

Table 4-13 Summary of the test result for DB 300-10 samples.

Sample Name	Max Load (lb)	Max Stress (ksi)	E (0-max) (ksi)	E (0-50) (ksi)	Strain at Max. Stress %	Max Strain %	Energy Density (ksi)
DB 300-10-1	7592	107	5917	6046	1.81	1.81	99
DB 300-10-2	8066	112	6033	6054	1.84	1.84	103
DB 300-10-3	7265	103	6325	6388	1.63	1.63	85
DB 300-10-4	8634	120	6508	6677	1.84	1.85	111
DB 300-10-5	9277	133	6490	6775	2.04	2.04	138
AVERAGE	**8167**	**115**	**6255**	**6388**	**1.83**	**1.83**	**107**
St. Dev.	**721.8**	**10.3**	**239.7**	**304.1**	**0.13**	**0.13**	**17.4**
COV %	**8.8**	**9.0**	**3.8**	**4.8**	**7.2**	**7.2**	**16.2**

4.1.9 DB-300-30

The 300-30 specimens exhibited a noticeable change in color to a light brown color, after being exposed to elevated temperatures for 30 minutes. The color of the specimens resembled that of the specimens heated for 30 minutes at 250^{o}C. The specimens all failed in the free length. Failure was sudden, and was characterized by longitudinal cracks along the free length, with some fibers breaking and partially separating from the body of the specimen. Figure (4-17) shows the 300-30 specimens after being tested.

Figure 4-17 DB-300-30 samples after failure (DB-300-30-1 on left).

Table (4-14) shows the effect of the elevated temperatures on the mechanical properties of the specimens heated for 30 minutes. The average tensile strength displayed a reduction of 7.8% in comparison with the 300-10 average strength;

however the 300-30 was not the lowest strength of all groups heated to 300^{o}C, despite being heated for the longest duration. One the other hand, the average modulus for this group continued to increase relative to the other groups heated for shorter durations, reaching an overall increase of 8 % with respect to the 300-0 specimens. As for the ultimate strain of the specimens, there was a relative reduction in comparison with 300-10 samples. Overall, there was very good consistency between the specimens, indicated by the small standard deviations and low coefficient of variations of the results.

Table 4-14 Summary of the test result for DB 300-30 samples.

Sample Name	Max Load (lb)	Max Stress (ksi)	E (0-max) (ksi)	E (0-50) (ksi)	Strain at Max. Stress %	Max Strain %	Energy Density (ksi)
DB 300-30-1	7881	111	6031	6173	1.83	1.83	102
DB 300-30-2	7533	106	6344	6470	1.68	1.68	91
DB 300-30-3	7350	103	6279	6769	1.63	1.63	86
DB 300-30-4	7849	108	6351	6685	1.69	1.69	91
DB 300-30-5	7428	103	6166	6364	1.66	1.66	87
AVERAGE	**7608**	**106**	**6234**	**6492**	**1.70**	**1.70**	**91**
St. Dev.	**217.9**	**2.9**	**121.4**	**215.7**	**0.07**	**0.07**	**5.8**
COV %	**2.9**	**2.7**	**1.9**	**3.3**	**4.0**	**4.0**	**6.4**

All specimens of this group failed in a brittle manner, as can be seen from figure (4-18) showing the linear stress-strain curves that up to failure:

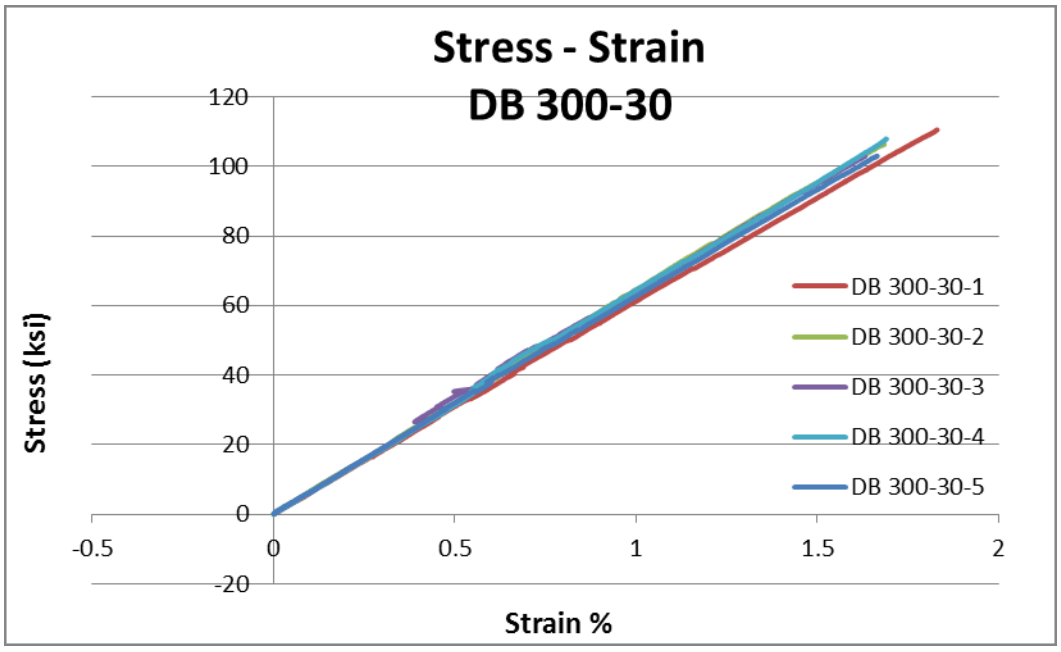

Figure 4-18 Stress-strain curves of the DB-300-30 specimens.

4.1.10 DB-350-0

The color of these specimens was changed to a light brown color, resembling specimens heated to 250^{o}C for 30 minutes. Figure (4-19) shows the 350-0 specimens after failure. All of the specimens failed in the free length. No bending was noticed in any specimen, failure occurred with longitudinal cracks forming along the free length, and breaking of fibers at the surface of the specimens.

Figure 4-19 DB-350-0 specimens after failure (DB-350-0-1 on left).

The specimens failed in a brittle manner, and maintained a straight stress-strain curve up to failure as shown in figure (4-20). The results were very consistent with each other, with coefficient of variation for the elastic modulus being as little as 1.2%. Only the energy density showed a relatively high variation, due to the fact that specimen 350-0-4 had a higher tensile strength than the other specimens, thereby producing a larger area under the stress-strain curve.

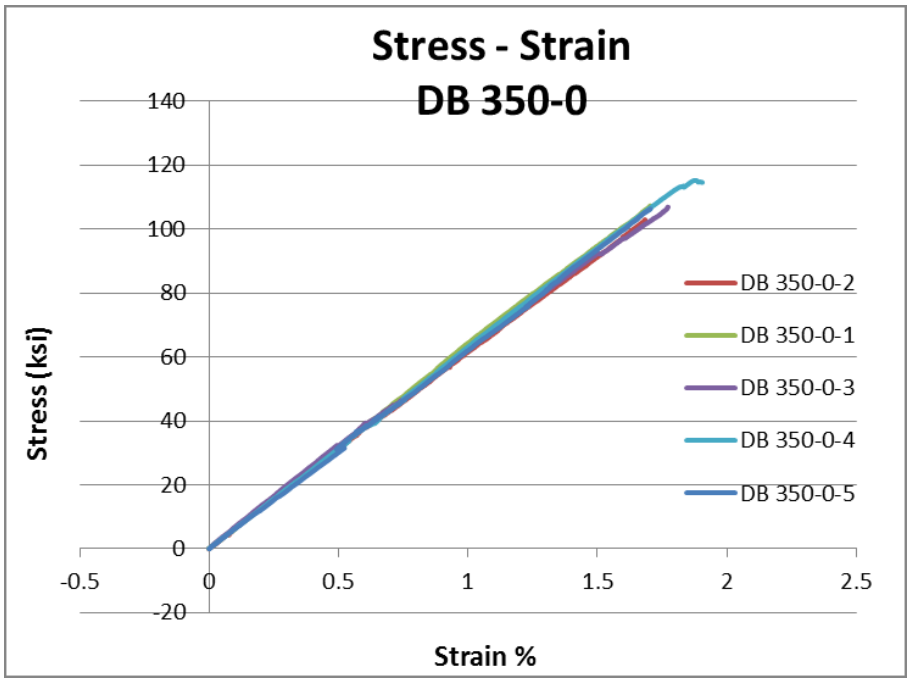

Figure 4-20 Stress-strain curves of the DB-350-0 specimens.

Table (4-15) shows the detailed results for this group There was a reduction of 6% in the average tensile strength of the 350-0 specimens compared to the unheated control samples. The 350-0 specimens also reached the lowest average strength level among the all dog-bone specimens heated to elevated temperatures and removed immediately from the oven. Also, there was very little reduction in the elastic modulus of these samples in comparison with the control samples. It appears that the elastic modulus is not affected much by heating GFRP dog-bones to 350^{o}C when the specimens are taken out of the oven immediately after reaching the target temperature (duration of 0 min).

Table 4-15 Summary of the test result for DB 350-0 specimens.

Sample Name	Max Load (lb)	Max Stress (ksi)	E (0-max) ksi	E (0-50) ksi	Strain at Max. Stress %	Max Strain %	Energy Density (ksi)
DB 350-0-1	7765	107	6304	6374	1.70	1.70	92
DB 350-0-2	7368	103	6050	6142	1.68	1.68	87
DB 350-0-3	7566	107	5962	6224	1.77	1.77	98
DB 350-0-4	8216	115	6250	6219	1.88	1.91	111
DB 350-0-5	7489	106	6250	6250	1.70	1.70	90
AVERAGE	**7678**	**108**	**6163**	**6242**	**1.75**	**1.75**	**96**
St. Dev.	**298.5**	**4.0**	**132.6**	**75.4**	**0.07**	**0.08**	**8.2**
COV %	**3.9**	**3.7**	**2.2**	**1.2**	**4.1**	**4.7**	**8.6**

4.1.11 DB-350-5

As it is shown in figure (4-21), some of the specimens heated to 350^{o}C for 5 minutes look darker than others. All specimens were heated to the same temperature and for the same duration, yet the variation in color may be due to the fact that the lighter specimens were heated together, and the darker specimens were heated together at a later time.

Apart from specimen 350-5-3 which failed slowly, all other specimens failed in a sudden way. All specimens showed longitudinal breaks in their free length, with little partial separation of fibers in the free length, except for specimen 350-5-4 which showed more separation and some bending along its longitudinal axis.

Figure 4-21 DB-350-0 specimens after failure (DB-350-5-1 on left).

The failure behavior of all of the specimens was brittle, characterized by the linear elastic stress-strain curves, as well as the fact that the strain at maximum stress was equal to the ultimate strain. Figure (4-22) shows the stress-strain curves for all specimens in this group.

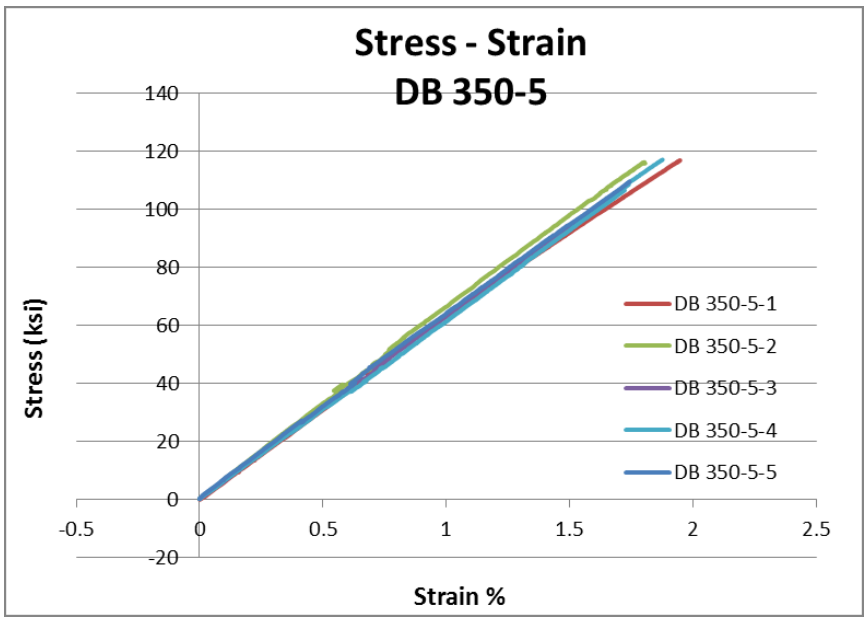

Figure 4-22 Stress-strain curves of the DB-350-5 specimens.

Table (4-16) shows results of tests on the 350-5 specimens. The tensile strength for the 350-5 specimens exhibited an increase (by about 5%) in comparison with the 350-0 specimens. The elastic modulus also showed an increase with respect to the 350-0 specimens; however the magnitude of the increment was smaller. The ultimate strain showed an increase of about 4% compared to the 350-0 group. Good consistency among the specimens was observed.

Table 4-16 Summary of the test result for DB 350-5 specimens.

Sample Name	Max Load (lb)	Max Stress (ksi)	E (0-max) ksi	E (0-50) ksi	Strain at Max. Stress %	Max Strain %	Energy Density (ksi)
DB 350-5-1	8532	117	5999	6325	1.95	1.95	117
DB 350-5-2	8318	116	6449	6538	1.80	1.81	107
DB 350-5-3	7653	106	6240	6284	1.72	1.72	93
DB 350-5-4	8363	117	6242	6041	1.88	1.88	109
DB 350-5-5	7809	110	6244	6410	1.74	1.74	97
AVERAGE	**8137**	**113**	**6231**	**6320**	**1.82**	**1.82**	**105**
St. Dev.	**342.2**	**4.4**	**137.2**	**164.2**	**0.09**	**0.09**	**8.8**
COV %	**4.2**	**3.9**	**2.2**	**2.6**	**4.7**	**4.7**	**8.4**

4.1.12 DB-350-10

As shown in figure (4-23), the color of the specimens heated for 10 minutes at 350^{o}C, changed to a darker shade of brown in comparison with the specimens heated for 5 minutes. All specimens failed in the free length with longitudinal cracks forming in the middle part of the specimens. Some of the specimens exhibited a slower failure process than others. The specimen 350-10-1 was bent along its longitudinal axis following the test.

Figure 4-23 DB-350-10 specimens after failure (DB-350-10-1 on left).

Table (4-17) shows the results of this group. All of the measured mechanical properties of the 350-10 specimens showed reduction in their magnitude in comparison to the 350-5 specimens. The reduction of the tensile strength was about 3.8 %, while the ultimate strain was reduced by approximately 2.2 % with respect to the 350-5 specimens. The reduction in the elastic modulus was only 1.4 %.

Table 4-17 Summary of the test result for DB 350-10 specimens.

Sample Name	Max Load (lb)	Max Stress (ksi)	E (0-max) ksi	E (0-50) ksi	Strain at Max. Stress %	Max Strain %	Energy Density (ksi)
DB 350-10-1	7893	110	6143	6381	1.78	1.78	98
DB 350-10-2	8119	113	6018	6081	1.88	1.88	108
DB 350-10-3	7588	107	6267	6174	1.72	1.72	93
DB 350-10-4	8026	114	6119	6252	1.87	1.87	108
DB 350-10-5	7349	101	6104	6256	1.65	1.65	84
AVERAGE	**7795**	**109**	**6130**	**6229**	**1.78**	**1.78**	**98**
St. Dev.	**286**	**4.6**	**80.4**	**99.2**	**0.09**	**0.09**	**9.2**
COV %	**3.7**	**4.2**	**1.3**	**1.6**	**4.8**	**4.9**	**9.3**

A very good consistency can be seen among the specimens of this group, which manifests in the similar stress-strain curves shown in figure (4-24). The specimens failed in a brittle manner, and the stress-stain curves remained linear up to failure.

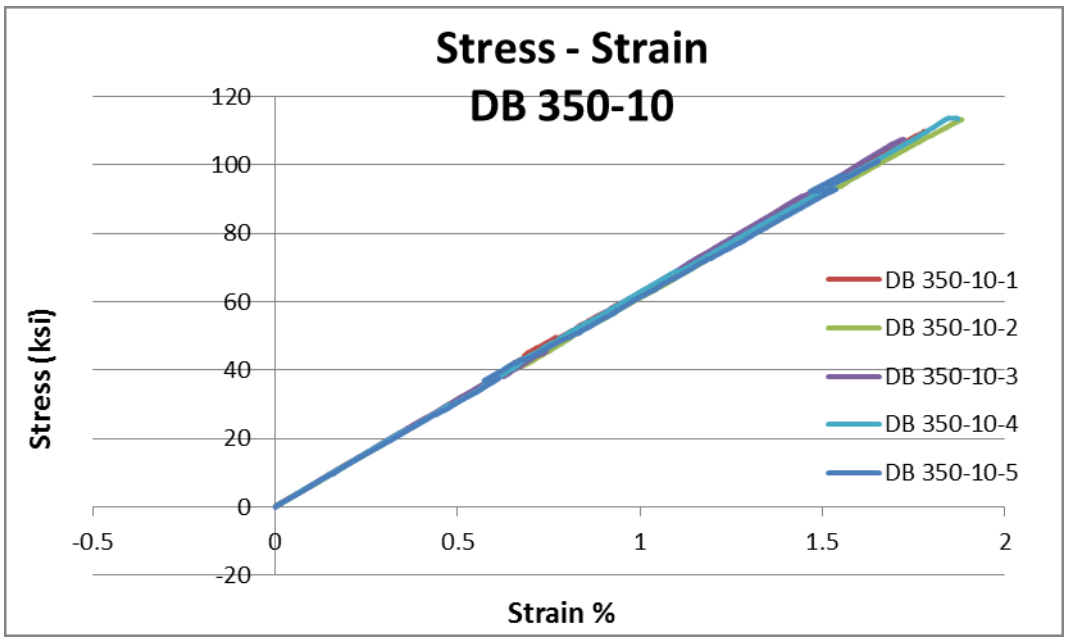

Figure 4-24 Stress-strain curves of the DB-350-10 specimens.

4.1.13 DB-350-30

In this group, the number of specimens was increased from five to seven. This was done because two of the specimens were damaged by the heat, where the aluminum foil had been torn and the area of the bars under it had swelled. Since a large portion of the resin had evaporated and left the fibers weakened, these two specimens failed prematurely, and were discarded.

In general, the exposure to high heat for 30 minutes changed the color of the specimens to a dark brown color as can be seen in figure (4-25). It's interesting to

note that after failure, the fibers in the 350-30 specimens seemed to be blackened, where in lower temperatures, or shorter durations, fibers under the surface of the specimen remained white, similar to the color of an unheated fiber. However in the 350-30 specimens, the intense heat and the long duration of exposure caused disintegration of a large portion of the resin, thereby allowing the heat to reach the core of the specimen, and allowing the bare fibers to be darkened by the heat.

Figure 4-25 DB-350-30 specimens after failure (DB-350-30-1 on left).

All of the specimens failed in the free length, but failure commenced in early stages of the tests, characterized by some surface fibers breaking gradually, until the end of the failure process, where some breaking sounds could be heard, and some dust was released. The specimens took a broom like shape after full failure had occurred. The specimens were somewhat similar in their tensile strength**,** however, the rest of the results showed a lower consistency, and a noticeable variation in the stress-strain curves could be seen, thus producing evident differences in the

corresponding elastic modulus. As it is obvious from the stress-strain curves in figure (4-26), some of the samples failed in a brittle manner (specimens 350-30-4 and 350-30-5). Others exhibited more ductile behavior in their failure, as is the case with specimens 350-30-1 and 350-30-6.

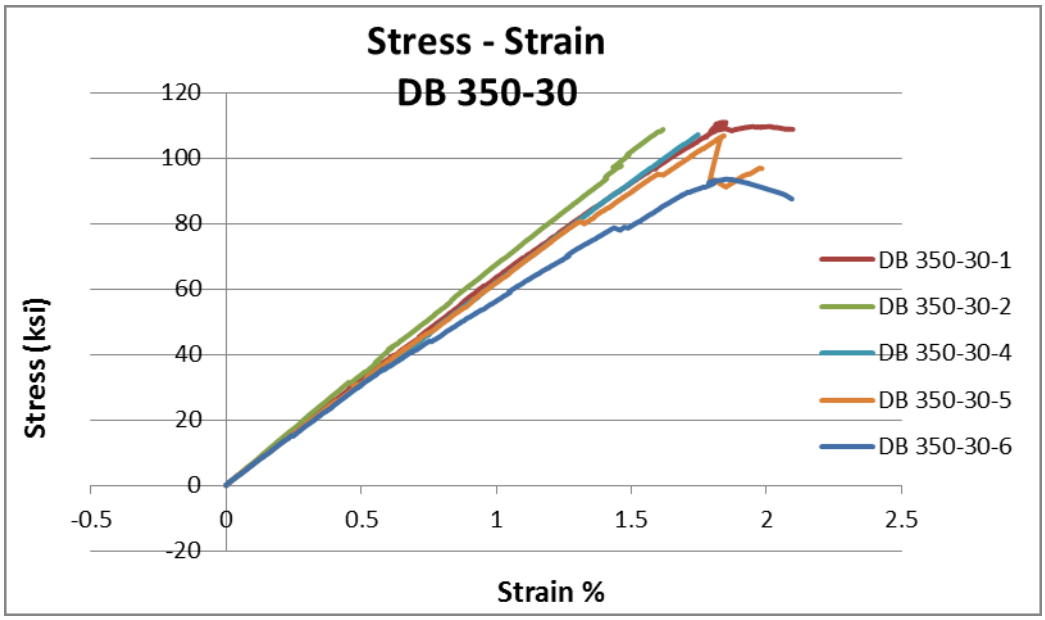

Figure 4-26 Stress-strain curves of the DB-350-30 specimens.

Table (4-18) shows the detailed results of all specimens in this group. The average elastic modulus of this group showed little variation in comparison with the 350-10 specimens. On the other hand, the average ultimate strain for this category showed an increase of 6.8 % with respect to the 350-10 specimens. While the average strength in for the 350-30 specimens decreased by 3.4 % with respect to the 350-10 specimens.

Table 4-18 Summary of the test result for DB 350-10 specimens.

Sample Name	Max Load (lb)	Max Stress (ksi)	E (0-max) ksi	E (0-50) ksi	Strain at Max. Stress %	Max Strain %	Energy Density (ksi)
DB 350-30-1	7750	110	5962	6308	1.85	2.10	106
DB 350-30-2	7574	109	6694	6753	1.62	1.62	88
DB 350-30-4	7600	107	6151	6071	1.75	1.75	94
DB 350-30-5	7592	107	5770	6201	1.84	1.98	103
DB 350-30-6	6679	94	5076	5732	1.85	2.09	95
AVERAGE	**7623**	**108**	**6137**	**6273**	**1.76**	**1.91**	**97**
St. Dev.	**64.2**	**1.4**	**308.7**	**258.6**	**0.08**	**0.19**	**6.6**
COV %	**0.8**	**1.3**	**5.0**	**4.1**	**4.8**	**10.1**	**6.8**

4.2 FS-Specimens:

4.2.1 FS-Control Specimens:

The FS control specimens, were tested for comparison with the heated specimens, to explore the effect of elevated temperatures on the GFRP bars.

All of the four control FS specimens failed in the free length. Figure (4-27) shows the specimens after failure. The failure of CONTROL-1 sample commenced with a few cracking sounds, followed by a faint breaking sound. Apart from slight peeling of a part of the bar surface, no other obvious signs of failure can be seen on this specimen. And the helical fiber strand wrapped around the bar was kept mostly intact.

Figure 4-27 FS-CONTROL specimens after failure

The CONTROL-3 specimen's failure started with several breaking sounds of single fibers, followed by several noticeably louder breaking sounds of the helical strand failing at multiple places across the free length. And finally, the core failed with a very loud and sudden bang, splitting the bar into strands in the middle part of the free length. Figure (4-28) shows the CONTROL-3 specimen before and after the failure.

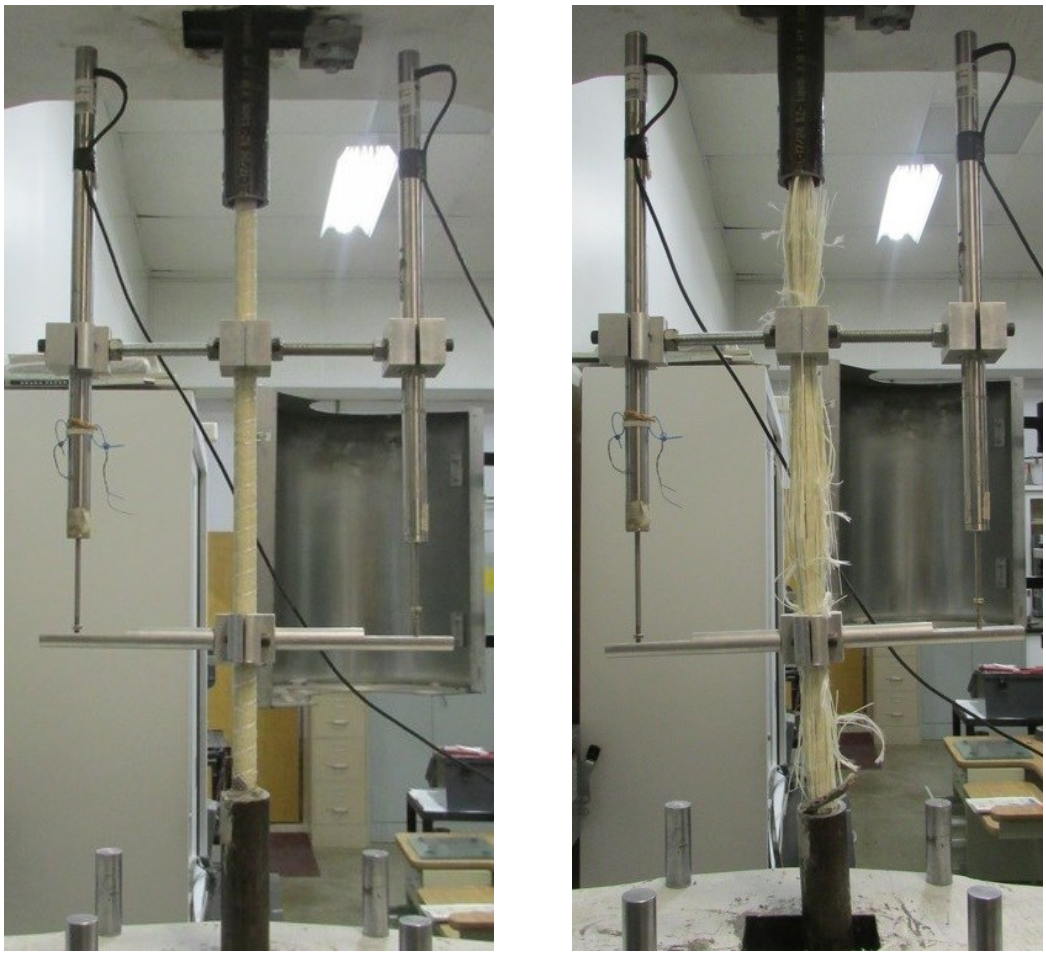

Figure 4-28 (on left) CONTROL-3 before failure. (on right) CONTROL-3 after failure

As for the specimen CONTROL-5, the failure occurred in two successive loud stages. In the first stage the fiber strands broke. In the second, the bar split into two parts along its longitudinal axis. Figure (4-29) shows the specimen after failure.

Figure 4-29 CONTROL-5 after failure.

In CONTROL-6, the failure initiated through a loud sound accompanying a break of the helical strand, followed by several breaking sounds of the fibers near and at the surface of bar. After this another sound marked the break of the core of the bar. Table (4-19) presents a summary of results of the FS-Control specimens:

Table 4-19 Summary of the FS-Control specimens.

Sample Name	Max Load (lb)	Max Stress (ksi)	E (0-max) ksi	E (0-50) ksi	Strain at Max. Stress %	Max Strain %	Energy Density (ksi)
FS-Control 1	50827	107	6193	6198	1.72	1.72	92
FS-Control 3	54044	112	5545	6050	1.97	1.97	113
FS-Control 5	54884	114	6008	6235	1.91	1.91	112
FS-Control 6	54605	117	5912	6093	2.01	2.01	122
AVERAGE	**53590**	**113**	**5913**	**6144**	**1.90**	**1.90**	**109**
St. Dev.	**1623.6**	**3.6**	**237.6**	**75.0**	**0.11**	**0.11**	**11.1**
COV %	**3.0**	**3.2**	**4.0**	**1.2**	**5.6**	**5.8**	**10.2**

The average tensile strength of the control-FS specimens was 113 ksi. The strength obtained is higher than the manufacturer's guaranteed tensile strength of 100 ksi. As for the modulus of elasticity for these specimens, an average value of 6144 ksi was obtained, which is lower than the manufacturer's reported value of 6700 ksi. The stress-strain behavior of the control bars was mostly linear up to failure, except for CONTROL-3 which exhibited slight curvature. This average peak strain of 1.9% is noticeably higher than the manufacturer's reported ultimate strain of 1.49. Figure (4-30) shows the stress-strain curves for the FS-control specimens. In the appendix, the stress-strain curves for individual specimens are provided.

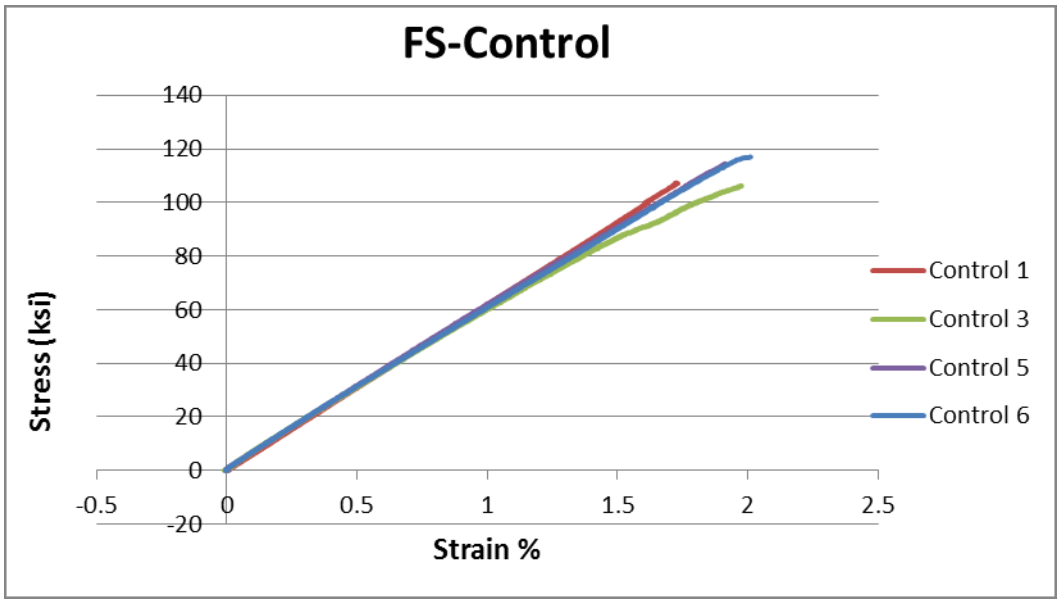

Figure 4-30 Stress-strain curves of the FS-control specimens.

4.2.2 FS-AFR-350 Specimens:

As presented in the previous chapter, these FS-specimens were heated to 350^{o}C, and tested after cool down. All FS-AFR-350 specimens failed in the free length of bar. Figure (4-31) shows the stress-strain curves for these specimens:

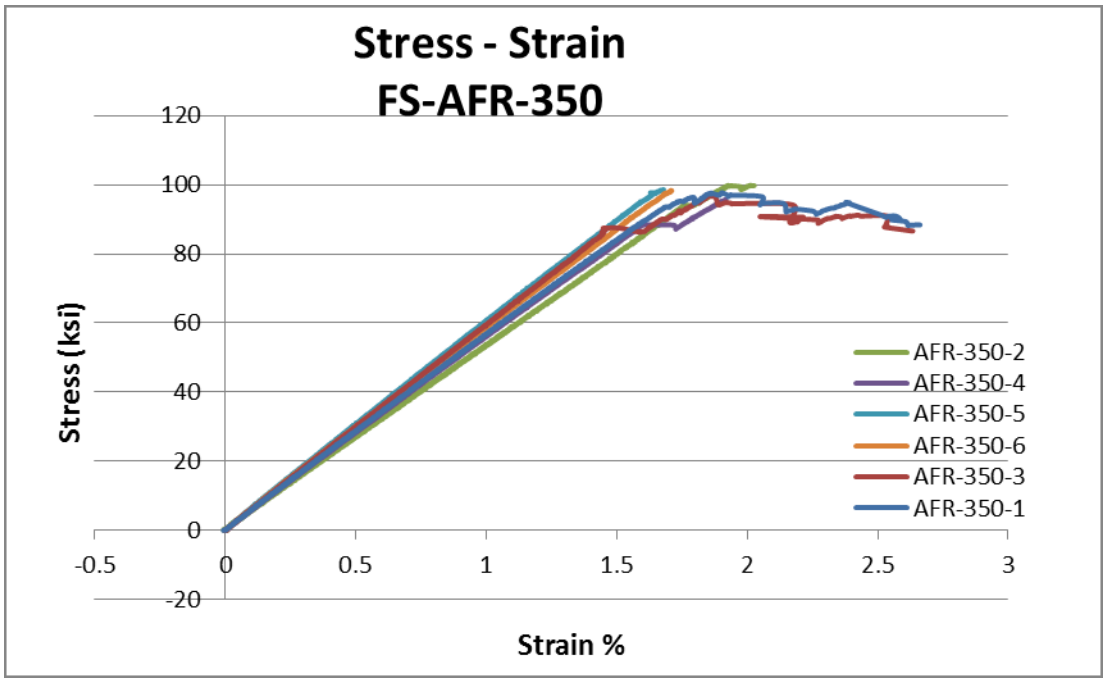

Figure 4-31 Stress-strain curves of the FS-AFR-350 specimens.

Based on their stress-strain curves, the specimens in this category can be classified into two groups. The specimens of each group being similar in their failure mode, and the shape of the stress-strain curve:

1- Specimens FS-AFR-350-1, and FS-AFR-350-3:

Specimen FS-AFR-350-1 failed in approximately 25 seconds, during which the sound of fibers breaking could be heard, after which a loud bang was heard accompanied by a drop in the load. Specimen FS-AFR-350-3 was similar in its failure mode to the first specimen, where low sounds of breaking fibers could be heard near failure, after which louder continuous fiber breaking sounds could be heard for 20 seconds, with the failure ending with a bang. Interesting to note is that both of these specimens exhibited similar stress-

strain curves, characterized by a plateau in the curve after peak stress had occurred, as can be seen from figure (4-34). A noticeably high ultimate strain of 2.66%, and 2.63% was recorded for the first and third specimens, respectively. Figure (4-32) and (4-33) show the specimens after failure.

Figure 4-32 FS-AFR-350-1 after failure.

Figure 4-33 FS-AFR-350-3 after failure.

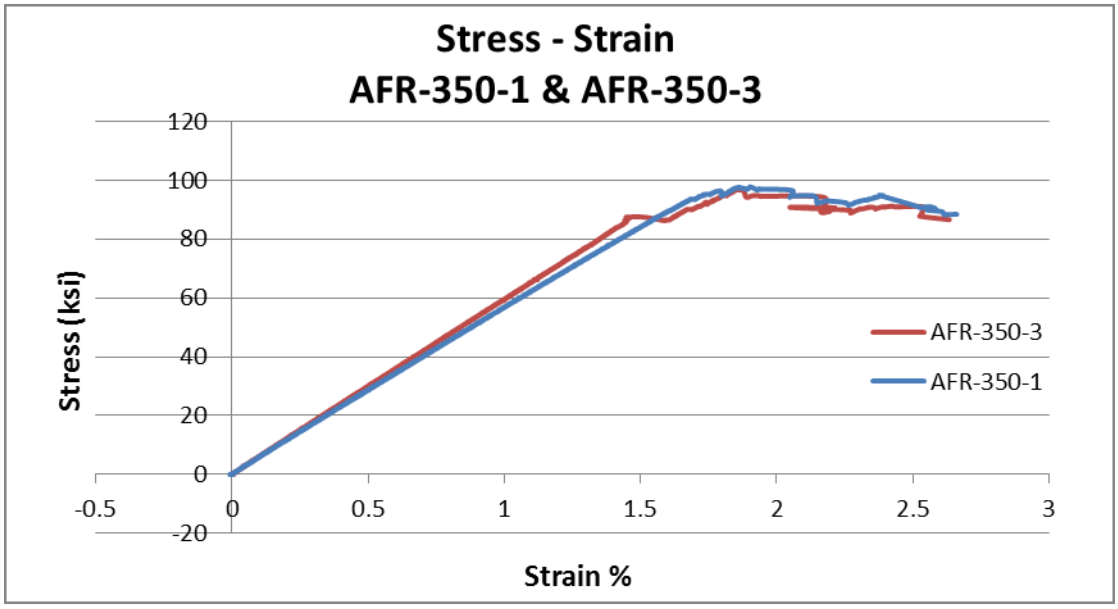

Figure 4-34 Stress-strain curves for specimens FS-AFR-350-1 & FS-AFR-350-3.

2- Specimens FS-AFR-350-2, 4, 5, and 6:

Unlike the first and third specimens, specimens FS-AFR-350-2, 4, 5, and 6 did not exhibit any ductility (post-peak plateau) in the stress-strain curves. Instead, the curves were similar to that of the control specimens (linear up to failure). These four specimens were also similar in their failure behavior. The failure of this group can be characterized by two bangs, the first being usually louder than the second, with fiber breaking sounds heard between the two bangs in two of the four specimens. The failure processes were generally more sudden than the first group. Figure (4-35) shows the stress-strain curves for this group.

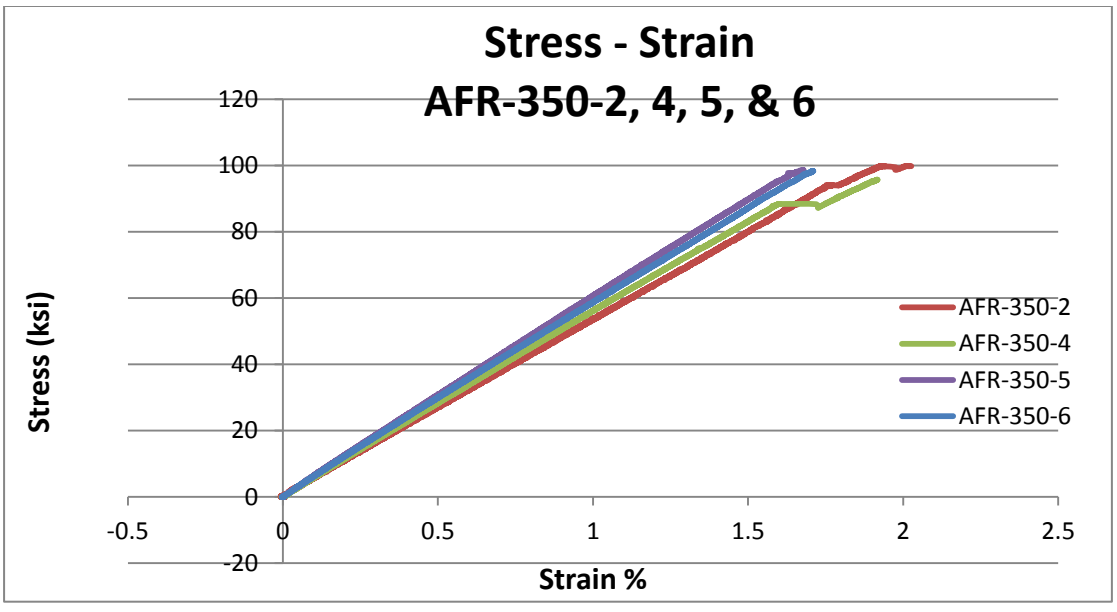

Figure 4-35 Stress-strain curves for specimens FS-AFR-350-2, 4, 5, and 6

Figure (4-36) presents all FS-AFR-350 specimens after failure.

Figure 4-36 FS-AFR specimens after failure (1-6 from left to right).

Table (4-20) shows results of all of the FS-AFR-350 bar tests. In general, the tensile strength of the FS-specimens heated to 350^{O}C was reduced by 13% in comparison with the control specimens. Ellis [1] reported a reduction in strength of 17% for specimens heated to 400^{o}C. The reduction in the tensile strength is expected as a result of the heating process of the bars. Little scatter was noticed in the tensile strength values, as can be seen in the COV of 1.4%. An average reduction of about 6.2 % is noticed in the modulus of elasticity of the bars with respect to the control specimens. A relatively good agreement in the elastic modulus was observed among the heated specimens. Ellis's [1] reported a reduction inelastic modulus of about 17% for the category heated to 400^{o}C.

The strain at maximum stress was reduced in comparison with the control specimens by 3.15 %. However, the ultimate strain is increased by 9.5 % with respect to the unheated temperatures. The coefficient of variation for the ultimate strain is high due to the fact that only two of the specimens exhibited the pseudo-ductile behavior in their failure, causing a scatter in the results. Lastly, the average energy density of the specimens was also reduced by 11.7%.

Table 4-20 Summary of the FS-AFR-350 specimens.

Sample Name	Max Load (lb)	Max Stress (ksi)	E (0-max) (ksi)	E (0-50) (ksi)	Strain at Max. Stress %	Max Strain %	Energy Density (ksi)
FS-AFR-350-1	48400	98	5508	5679	1.90	2.66	101
FS-AFR-350-2	49858	100	5251	5325	2.01	2.03	107
FS-AFR-350-3	45860	97	5551	5963	1.85	2.63	98
FS-AFR-350-4	47823	96	5281	5626	1.92	1.92	100
FS-AFR-350-5	47551	99	5939	6061	1.68	1.68	85
FS-AFR-350-6	47181	98	5759	5873	1.71	1.71	86
AVERAGE	**47779**	**98**	**5548**	**5754**	**1.84**	**2.10**	**96**
St. Dev.	**1211.2**	**1.4**	**244.6**	**244.4**	**0.12**	**0.40**	**8.2**
COV %	**2.5**	**1.4**	**4.4**	**4.2**	**6.3**	**19.1**	**8.5**

4.3 TGA Results

Figure (4-37) presents the results of the TGA test of a small (22.13 mg) sample of the GFRP bar used in the experiments. It shows the reduction in weight of the sample as temperature is increased up to 800^{o}C.

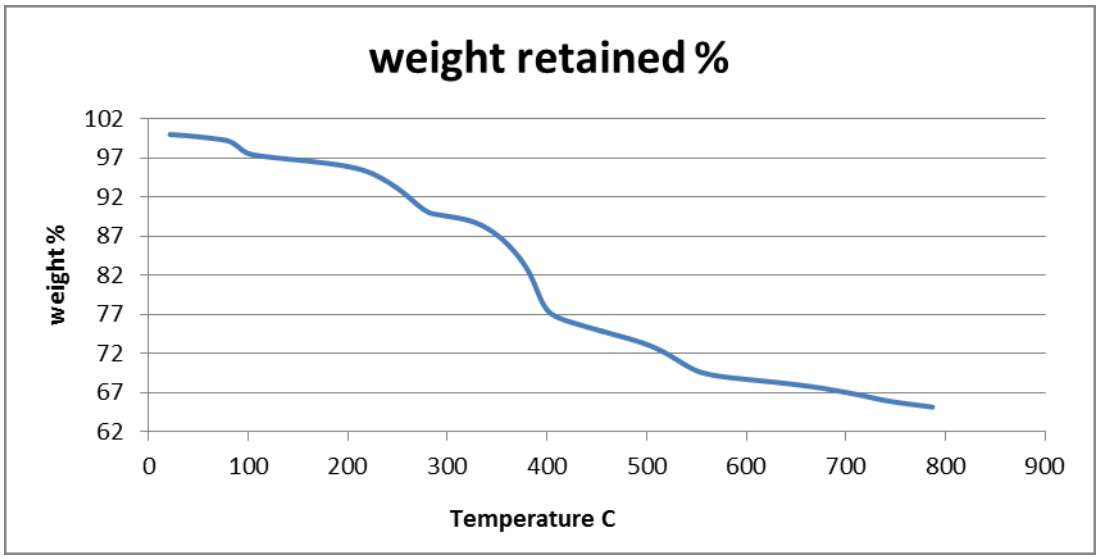

Figure 4-37 TGA of a sample of GFRP bar.

As can be seen from the TGA, there are a number of reductions in the mass occurring at different stages of the heating process. First drop was at about 90^{o}C, while the second occurred at about 270^{o}C. The third commenced at 350^{o}C and continued to about 400^{o}C. The first two drops are believed to be caused by dissipation of moisture from the GFRP material, namely the fiber itself. The third and subsequent drops are signs of the decomposition of the vinyl ester resin in the composite material. Gibson et al [21, 22] ran TGA on vinyl ester, polyester and phenolic resins, and reported very comparable curves for the polyester and vinyl ester resin, characterized by the start of the decomposition process at about 350^{o}C; leaving only about 7% of the material as char by the time the temperature had reached 480^{o}C. Robert et al. [18], also conducted TGAs on a GFRP sample, however their results showed only two drops, first one occurring after the sample reached 150^{o}C which was a very small loss in the mass, while the second very large drop

happened at about 300^{o}C and continued to 450^{o}C, comprising a roughly 18% total mass loss.

DISCUSSION

5.1 Changes in Mechanical Properties with Temperature

5.1.1 Tensile Strength Variation with Temperature

Figure (5-1) shows the changes in tensile strength for the DB-samples with temperature (results normalized with respect to the unheated control samples) (**t** is duration of exposure).

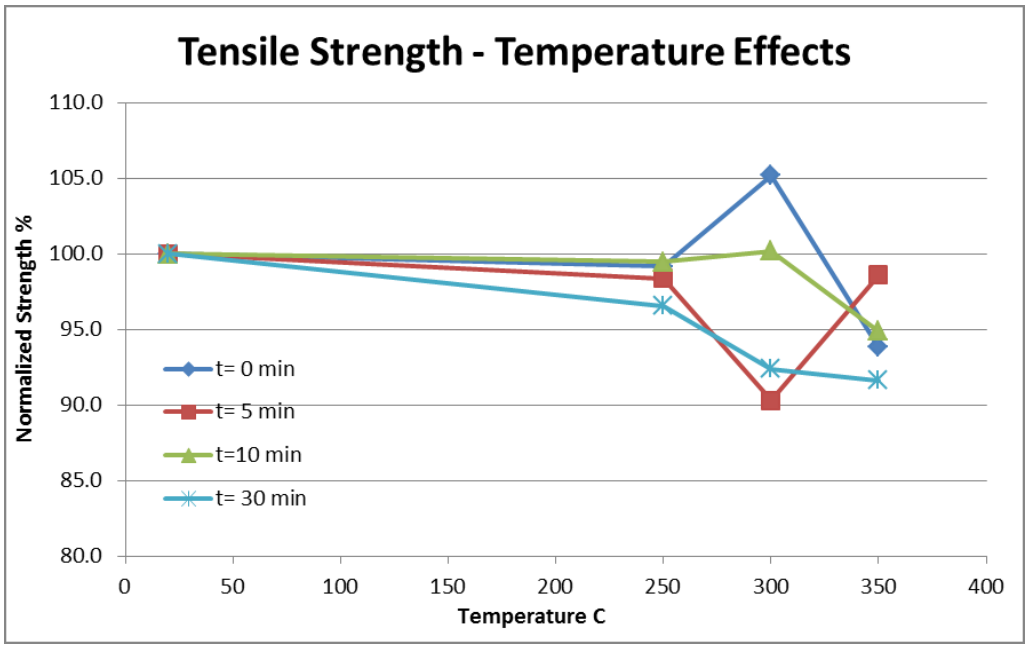

Figure 5-1 Changes in tensile strength with temperature

The tensile strength for the specimens exhibited changes within 10 % (with respect to control specimens) throughout the different temperatures included in this study. Little change is observed in the tensile strength for most specimens heated to 250^{o}C, except for the specimens heated for 30 min at 250^{o}C. Thomason et al. [12]

reported little reduction taking place in the tensile strength of single glass fibers at temperatures lower than 250^{o}C. The tensile strength is more dependent on the fibers' strengths which are not highly affected by these temperatures [18]. This explains why the change in the tensile strength of the DB-specimens was not high.

The tensile strength follows a pattern with duration. This can be noticed for durations of 0, 10, and 30 minutes, where the tensile strength is reduced with longer durations of heating. However, specimens heated for 5 minutes (especially at 300^{o}C) do not follow the same pattern. This could be due to the relatively high variation in strength between the specimens (see table (5-1)). Specimens heated for 30 min exhibit a clear reduction across all temperatures. This can be attributed to the degrading effect of the long exposures to high temperatures on FRP materials. The reduction in the strength for specimens heated to 350^{o}Cwas about 7 % (for t=0 min). Ellis [1] reported a reduction of about 2% at 200^{o}C and 17 % at 400^{o}C in the post-heat strength of GFRP bars.

Figure (5-2) shows the changes in tensile strength at different durations (results normalized with respect to t = 0 min exposure duration). There is not much difference between the behaviors of the DB-specimens at 250^{o}C and 350^{o}C. Both show slight reduction with increasing durations, apart from the 5 minute exposure period. However, for the samples heated to 300^{o}C, there is a clear reduction of tensile strength with duration, reaching about 87% (for t=30 min) compared to samples immediately removed from oven (t=0 min). It is unclear why the material's

behavior is different at 300°C. However, this could be due to the fact that the effect of the compaction phenomenon in the glass fibers begins to manifest at around this temperature. Yang and Thomason [13] reported "significant fibre length shrinkage above 300°C". The authors [13] also noted that "the length contraction was found to follow a logarithmic function of time". This combined with the initiation of the decomposition of the vinyl ester resin could be contributing to this observed behavior.

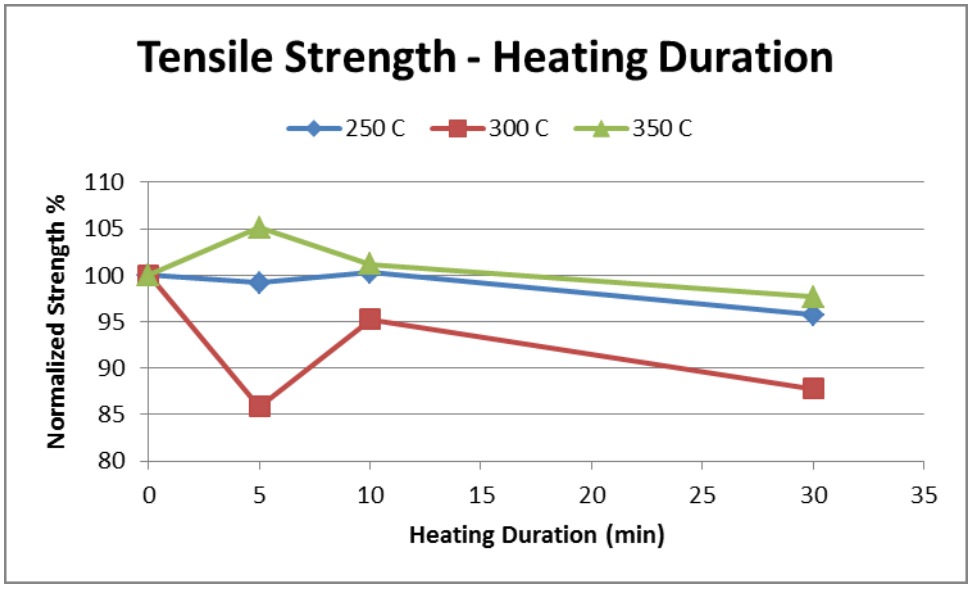

Figure 5-2 Changes in tensile strength with durations

Table 5-1 Coefficient of variation for tensile strength results

Temperature C	Duration (min)	Tensile Strength
		COV %
250	0	2.41
	5	3.5
	10	6.1
	30	2.0
300	0	4.3
	5	10.1
	10	9.0
	30	2.7
350	0	3.7
	5	3.9
	10	4.2
	30	1.3

5.1.2 Elastic Modulus Variation with Temperature

Figure (5-3) shows changes in the elastic modulus (0-50 ksi) for the DB-specimens versus temperature (results normalized with respect to the unheated control specimens) (**t** is duration of exposure). In term of the "narrow" range within which the change in elastic modulus is occurring, other researchers have reported similar narrow scales of change too. Alsayed et al [16] reported very little reduction (not exceeding 5 %) in the elastic modulus of vinyl ester based GFRP bars (heated to temperatures up to 300^{o}C for durations up to 3 hours). Alsayed et al. [16], suggested that the reason for the unchanged moduli might be related to the way these bars are degraded with heat, where most of the damage, under the conditions considered in their experiments, is done to the matrix material. Also, Yang et al. [13] reported an

increase in elastic modulus of single glass fiber specimens not exceeding 5 %, for fibers heating for 30 minutes to temperatures below 400^{o}C. This compares well with the limit of change noticed for the GFRP dog-bones heated for 30 minutes in this study.

The change in elastic modulus with temperature has a certain pattern (for heating durations of 10 min and 30 min). For these durations, it seems that the longer the duration of heating, the more upward cambered the curve becomes. This is supported by the pattern reported by Thomason [12] for single APS sized glass fiber specimens (heated for 15 minutes). However, the material doesn't seem to follow the same pattern for durations of heating of 0 minutes and 5 minutes. It is unclear why the elastic modulus follows an unusual pattern for 0 min and 5 min curves. With the low coefficient of variation (COV) for the 250-5 samples (2.4 %), 300-0 samples (3.1 %), and 300-5 samples (1.4 %), this does not appear to be a problem related to scatter in the data.

When comparing the behavior of the single fibers from the work of Thomason et al [12] with the GFRP behavior (for the 10 min and 30 min heating durations) reported here, it is observed that the decline in the dog-bone moduli for temperatures above 300^{o}C is steeper than that of the single fibers. This is believed to be caused by the decomposition of the resin that takes place at such temperatures. This effect is not applicable to, and is not seen in the single fibers. The same type of decline can be seen in the GFRP specimens heated for 30 minutes. Data also

suggests that all specimens heated to 350°C exhibit approximately the same modulus, regardless of the duration of heating.

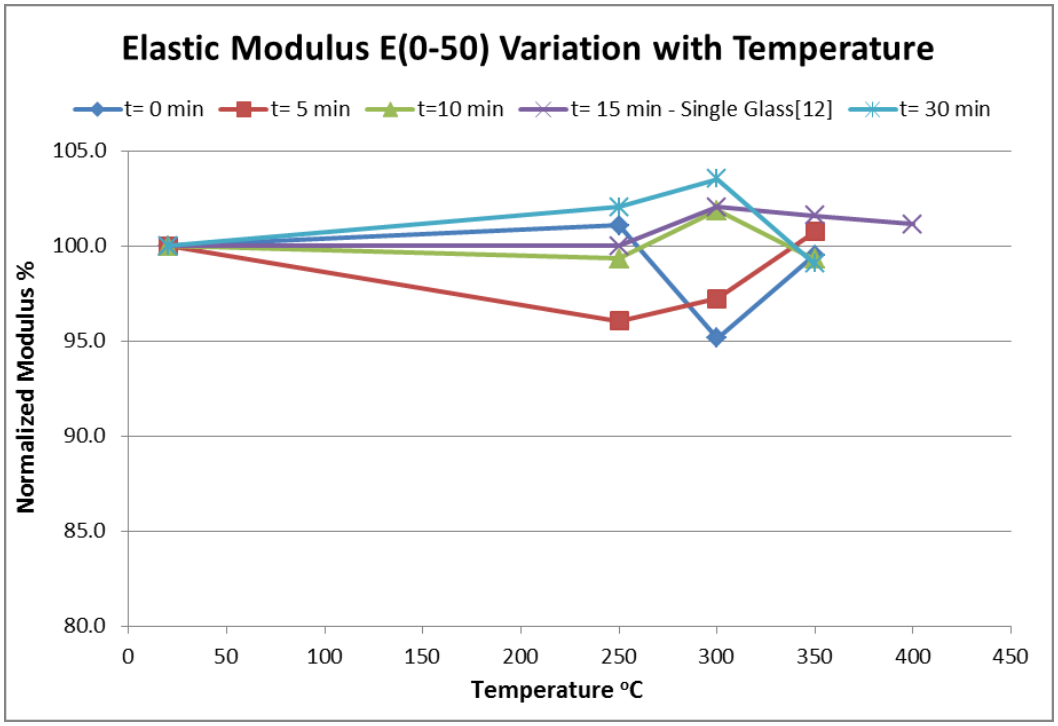

Figure 5-3 Changes in elastic modulus for the DB-specimens with temperature

Figure (5-4) and figure (5-5) show the changes in elastic modulus at different durations (results normalized with respect to t = 0 min exposure duration). The "E (0-50)" data (elastic modulus based on 50 ksi stress upper limit) exhibit larger increases with respect to the "0 min duration" in comparison to the "E (0-max)" curves (elastic modulus based on the stress at failure). The lower elastic modulus in the "E (0-max)" curve (for specimens heated to 530°C for 30 min) compared to the "E (0-50)" curve is due to the near-peak reduction as well as pseudo-ductile behavior observed in some specimens. For the 250°C 300°C data, the elastic modulus shows an overall increase with exposure duration of 30 minutes. This increase may be due to the fact that

some water is forced out of the glass fibers with longer exposures to elevated temperatures. According to Thomason et al [12], "Water can be present in significant quantities in glass and can act as plasticizer. Removal of the water from the network may stiffen the structure and contribute to the increase of the fiber modulus". For the 350°C data, prolonging the exposure periods (up to 30 min) did not show significant change in modulus.

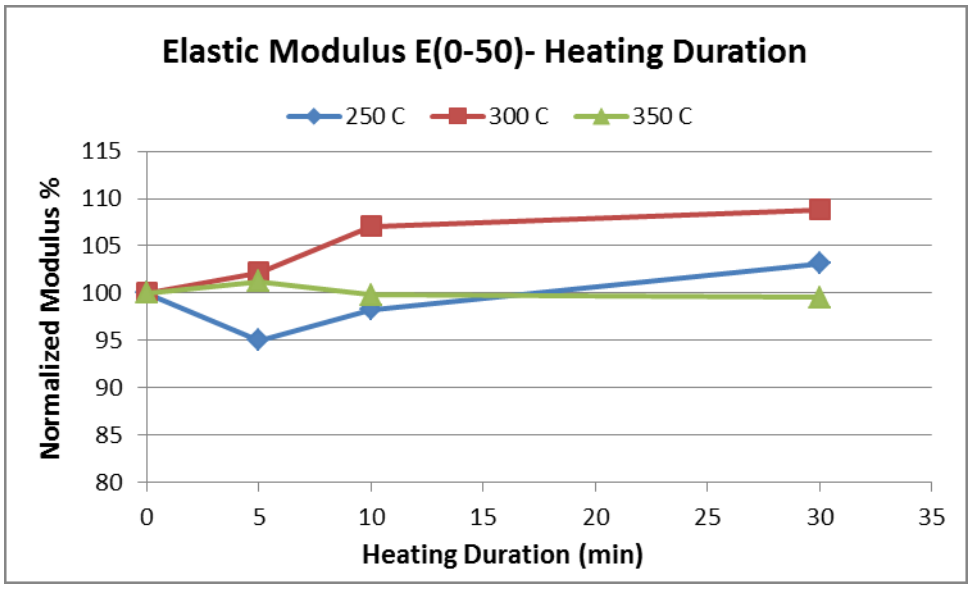

Figure 5-4 Changes in elastic modulus E(0-50) with duration of exposure.

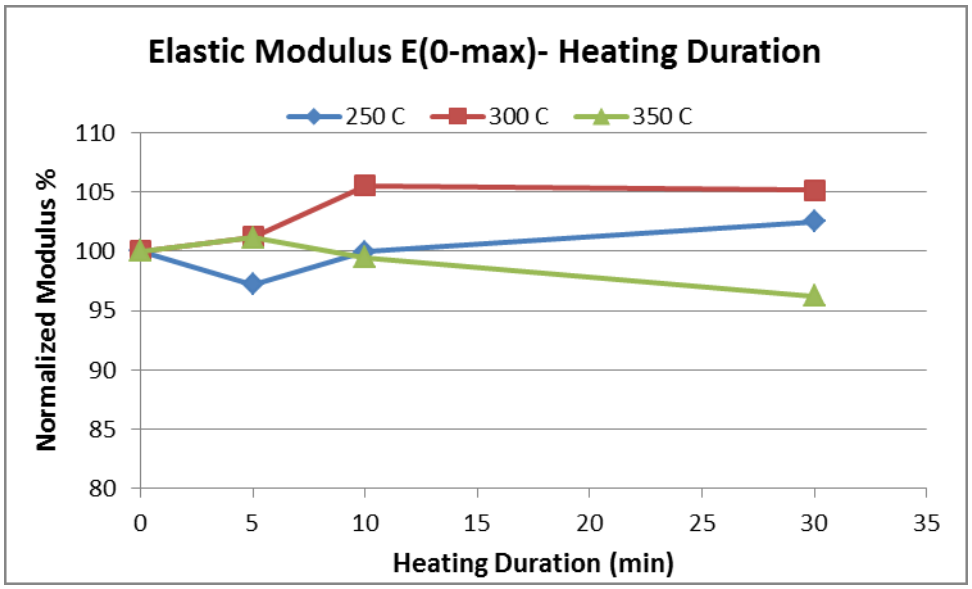

Figure 5-5 Changes in elastic modulus (0-max) with duration of exposure

Table (5-2) shows the coefficients of variation in elastic modulus for the different temperatures and durations:

Table 5-2 Coefficient of variation in elastic modulus results

Temperature C	Duration (min)	COV %	
		E (0-max) ksi	E (0-50) ksi
250	0	0.8	3.1
	5	2.1	2.4
	10	2.7	2.3
	30	3.5	6.0
300	0	4.6	3.1
	5	1.1	1.4
	10	3.8	4.8
	30	1.9	3.3
350	0	2.2	1.2
	5	2.2	2.6
	10	1.3	1.6
	30	5.0	4.1

5.1.3 Ultimate Strain Variation with Temperature

Figure (5-6) and Figure (5-7) show the changes in failure strain (strain at peak stress) and ultimate strain, respectively, for the DB-specimens with temperature (results normalized with respect to the unheated control specimens). (Variable **t** is duration of exposure to elevated temperatures).

Apart from the 30 min exposure data, the changes in both strains resemble those of the tensile strength. Thomason et al [12] also reported similarity between failure strain and fiber strength changes. Since almost all DB-specimens exhibited a linear stress-strain response up to failure (except for a few specimens heated to 350^{o}C for 30 minutes), the failure strain data are similar to the corresponding ultimate strains. Alsayed et al [16] also reported linear stress-strain responses and brittle failures for all temperatures up to 300^{o}C, and for all durations of up to 3 hours.

The longest exposure (30 minutes) seems to have an effect in reducing the ultimate strains of GFRP specimens at 250^{o}C and 300^{o}C (8% and 10% reduction, respectively). However at 350^{o}C, a pseudo-ductile failure behavior was observed in some specimens (figure (5-7)). The strain at 300^{o}C is significantly affected by the duration of heating. Regardless of the duration of exposure, as was the case with the elastic modulus, all specimens exhibited similar failure strains at 350^{o}C. The unusual behavior exhibited at 300^{o}C might be related to significant changes in resin

properties as well as higher variation among the results at this temperature (see table (5-3)).

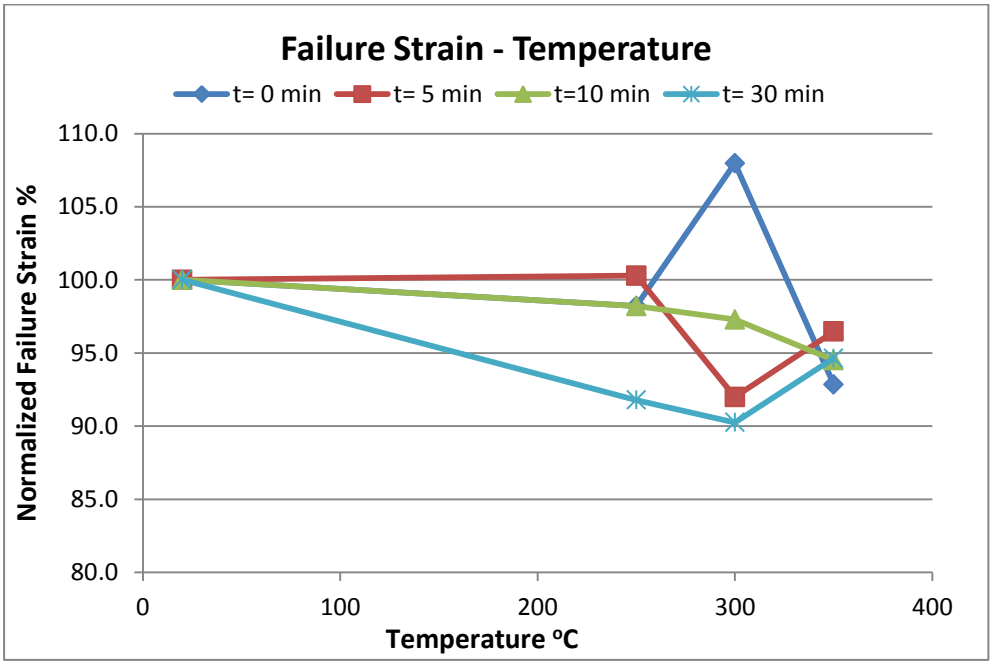

Figure 5-6 Changes in failure strain with temperature.

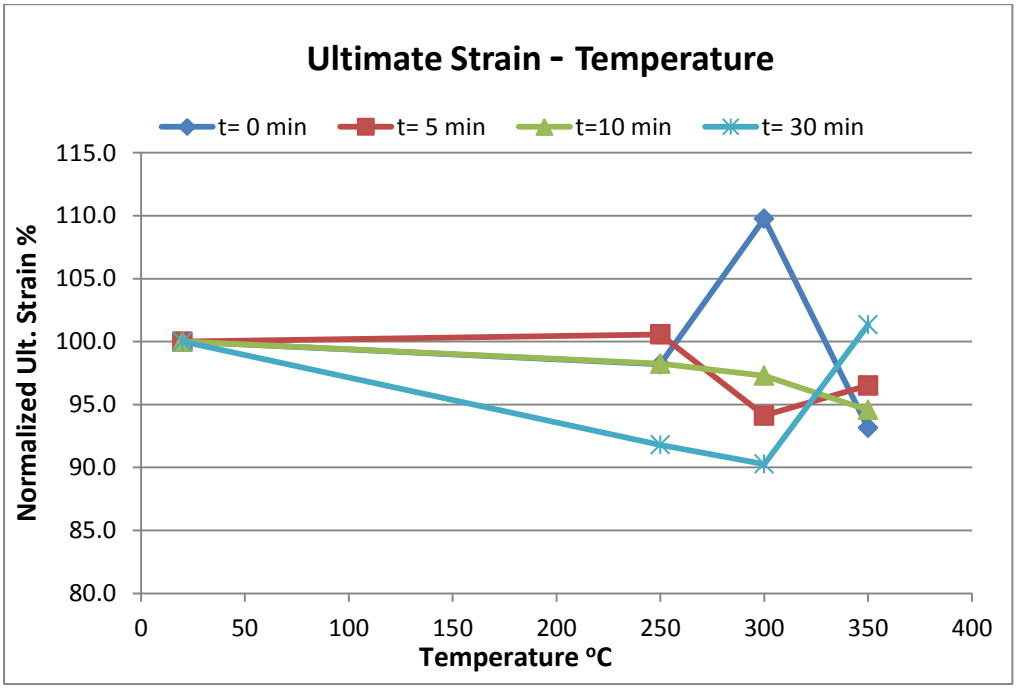

Figure 5-7 Changes in ultimate strain with temperature

Figure (5-8) and figure (5-9) show changes in failure strain and ultimate strain, respectively, at different durations (results normalized with respect to t = 0 min exposure duration**).** From Figure (5-8) and figure (5-9) it is noticed that for 250^{o}C and 300^{o}C, increasing the duration of heating reduces the strain (achieving 6% and 17 % reduction, respectively). On the other hand an increase of 9% is observed in the ultimate strain for 30 minutes exposure at 350^{o}C (associated with the pseudo-ductility effect).

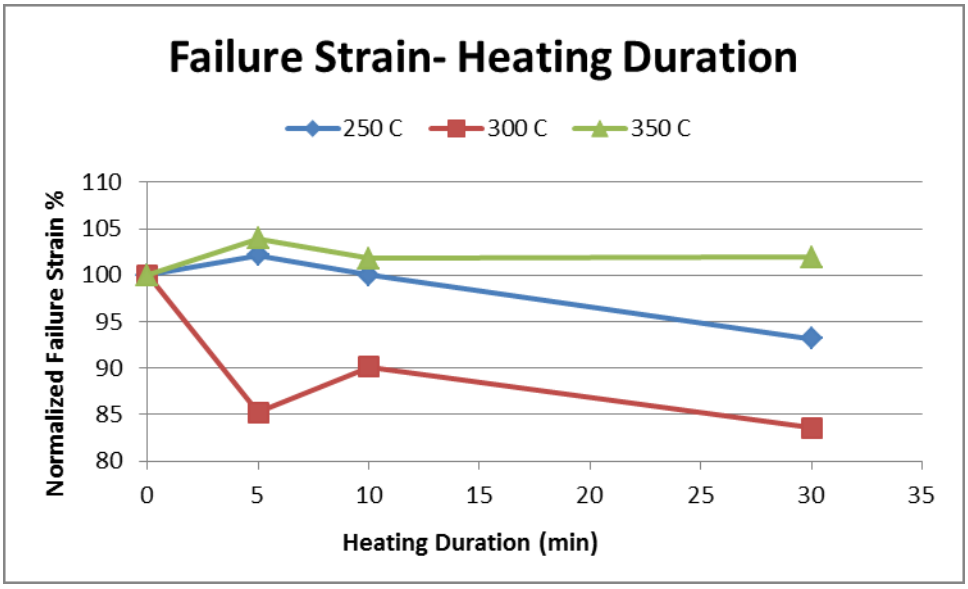

Figure 5-8 Changes in failure strain at different durations of heating

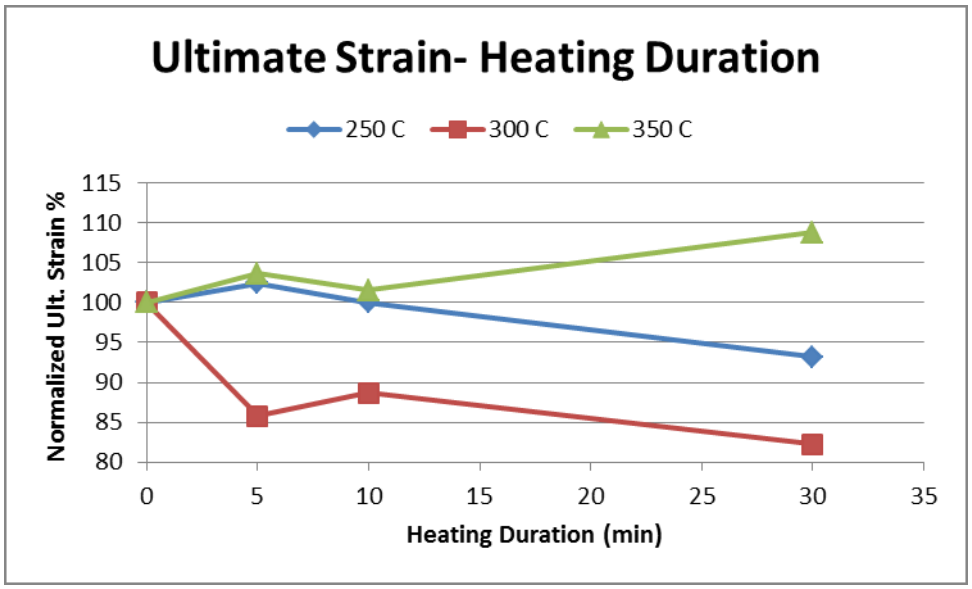

Figure 5-9 Changes in ultimate strain at different durations of heating

Table 5-3 Coefficient of variation for the strain results

Temperature C	Duration (min)	COV %	
		Failure Strain %	Ultimate Strain %
250	0	**2.88**	**2.88**
	5	**4.2**	**3.8**
	10	**5.4**	**5.3**
	30	**4.7**	**4.7**
300	0	**7.3**	**7.2**
	5	**10.6**	**9.5**
	10	**7.2**	**7.2**
	30	**4.0**	**4.0**
350	0	**4.1**	**4.7**
	5	**4.7**	**4.7**
	10	**4.8**	**4.9**
	30	**4.8**	**10.1**

It is worth noting that the responses of these materials and the changes in their mechanical properties are complex and require an in-depth study. For instance, in the subject of modulus of elasticity, a number of studies were conducted to

investigate the changes that occur in this regard with different temperatures. However, different researchers reported completely different results. For example, Ellis [1] reported a reduction in the post treatment elastic modulus with increasingly higher temperatures up to 400^{o}C; while Alsayed et al [16] reported that the post treatment modulus of GFRP bars heated to temperatures up to 300^{o}C, and for durations up to 3 hours, exhibited no significant change with temperature or duration of heating. Feith et al. [14] also reported no change occurring in the modulus of single glass fibers when heated up to temperatures reaching 650^{o}C. Other researchers such as Thomason et al [12], Yang et al [13], and Otto [15] reported increase in the elastic modulus of single glass fibers when heated to elevated temperatures.

5.2 FS-Specimens

As show in table (5-4), a reasonably good agreement was observed between the results of FS-control specimens and the DB-control specimens. The strength and elastic modulus of the dog-bone specimens are slightly higher.

Table 5-4 Comparison of FS and DB control specimens.

Sample Type	Max Stress (ksi)	E (0-max) ksi	E (0-50) ksi	Strain at Max. Stress %	Max Strain %	Energy Density (ksi)
DB-C	114.9	6068.8	6271.6	1.88	1.88	110.9
FS-C	112.8	5913.4	6144.1	1.90	1.90	109.0

Table (5-5) shows a comparison between the FS-specimens heated to 350^{o}C and the dog bone DB-350-0 specimens of the same category. A clear difference is noticed

between the DB-samples and FS-specimens in terms of tensile strength and elastic modulus (the DB-specimens exhibited higher magnitudes)

Table 5-5 Comparison between the FS-specimens heated to 350^{o}C, the DB-350-0 and the DB-350-30 specimens

Group Name	Max Stress (ksi)	E (0-max) ksi	E (0-50) ksi	Failure Strain %	Ultimate Strain %	Energy Density (ksi)
DB-350-0	107.7	6163.4	6241.6	1.75	1.75	95.6
DB-350-30	108	6137	6273	1.76	1.91	97
FS-AFR-350	98	5548	5754	1.84	2.10	96

On the other hand the average ultimate strain of the FS-350 specimens was higher than the DB- specimens. No signs of pseudo-ductile behavior can be noticed in any of the (350-0) DB specimens. However, some of the DB-specimens heated for 30 minutes at 350^{o}C also exhibited a somewhat pseudo-ductile failure behavior, with an average ultimate strain of 1.91% (see figure (4-26)). Ellis [1] also reported bilinear stress-strain curves and a pseudo-ductile failure behavior in GFRP bars (identical to the FS-specimens) heated to 200^{o}C and 400^{o}C. Ellis [1] reported a mean rupture strain of 1.85% and 2.29% for 200^{o}C and 400^{o}C, respectively.

Figure (5-10) shows the stress-strain curves of some of the DB-350-30 and FS-AFR-350 specimens that exhibited a pseudo-ductile behavior. Also, figure (5-11) and figure (5-12) show the stress-strain curves from Ellis's [1] study.

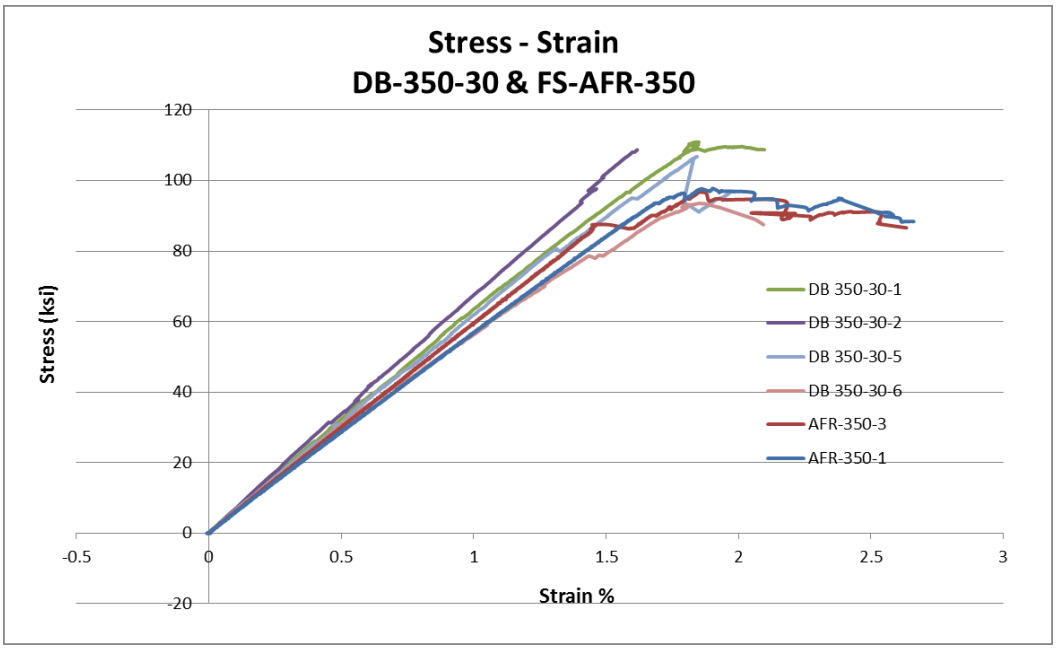

Figure 5-10 Stress-strain curves of DB-350-30 and FS-AFR-350 specimens.

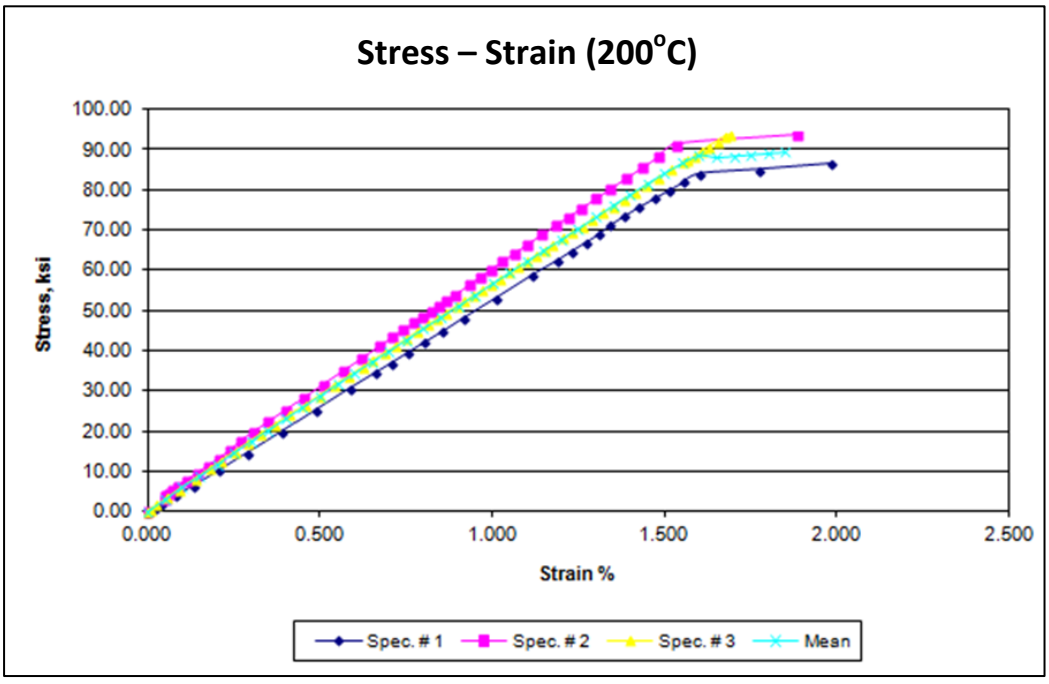

Figure 5-11 Stress-strain curves of FS bars heated to 200°C [1].

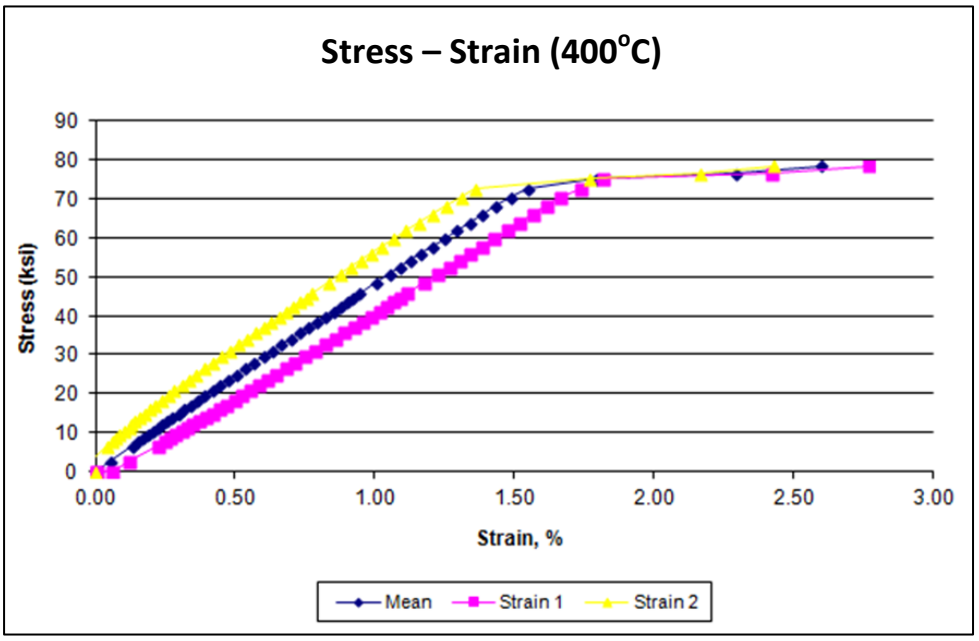

Figure 5-12 Stress-strain curves of FS bars heated to 400°C [1].

The heater used for the FS-specimens raised the temperature to 350°C in about 36.7 minutes (on average), while the oven used for the dog-bone specimens had a higher rate of heating, reaching 350°C in 24 minutes. Figure (5-13) shows the heating rates of the two heaters used.

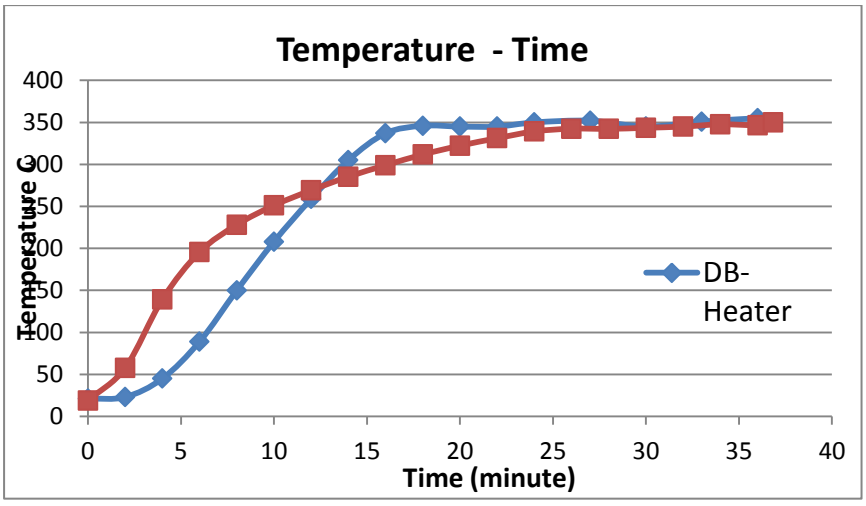

Figure 5-13 The heating rates of the two heaters used in the experiments

The large variation among the 350-30 specimens in terms of stress-strain behaviors, and the pseudo-ductile behavior suggests that the properties are fluid under these exposure conditions, and more research is needed to identify the causes and mechanisms of the pseudo-ductile response. Based on TGA results, the temperature $350^{o}C$ is at the beginning of a sharp declining curve of mass (and thereby degradation). It is possible that some of these specimens were near the lower part of this curve, in terms of the degree of degradation, while others were more close to the up top of the curve, resulting in different types of behaviors.

SUMMARY, CONCLUSIONS, AND RECOMMENDATIONS FOR FUTURE STUDIES

6.1 Summary

In this work, an experimental investigation was conducted on the mechanical properties of GFRP bars (with E-glass fiber and vinyl ester resin) that were previously exposed to elevated temperatures for various durations. The study included evaluation of changes in the post-heat elastic modulus, failure strain, and the tensile strength of GFRP specimens. The possibility of generating a pseudo-ductile material behavior in GFRP bars through heat treatment was also explored.

This work included load tests on sixty-four (64) dog-bone-shaped GFRP specimens and ten (10) full-size (3/4-in-diameter) GFRP reinforcing bars (that are typically used in concrete). The dog-bone specimens were machined from the full-size bars. The mechanical properties of the test specimens were measured after subjecting them to elevated temperatures for different exposure durations.

6.2 Conclusions:

The following conclusions were reached after analyzing the test results:

1- The tensile strength for the DB-samples exhibited changes within approximately ±10 % of the control (unheated) specimens. In most cases, the tensile strength of GFRP dog-bone specimens reduced further with longer exposure to elevated temperatures. The post-heating tensile strength of FS-

specimens heated to 350^{o}C was reduced by approximately 13% in comparison to their control specimens.

2- Little variation is observed in the post-heat modulus of elasticity of the GFRP specimens heated to 250^{o}C to 350^{o}C, and for exposure durations up to 30 minutes. Changes in the elastic modulus did not exceed 8% of the corresponding control modulus. Also, all specimens pre-heated to 350^{o}C exhibited approximately the same elastic modulus, regardless of the duration of heating.

3- All DB-specimens (for all target temperatures except 350^{o}C) exhibited a linear stress-strain response up to failure, and failed in a brittle manner. Some of the DB-specimens pre-heated to 350^{o}C for 30 minutes exhibited some pseudo-ductile behavior after the peak stress was reached. Two out of six FS-specimens also exhibited pseudo-ductile behaviors with an apparent "yield plateau". It should be noted that Ellis [1] had also reported similar pseudo-ductile behavior in his FS tests.

4- Apart from the 30-minutes-duration exposure data, the changes in failure strain data with temperatures are similar to those of the tensile strength. Also, the failure strain at 300^{o}C is very sensitive to the duration of heating. For DB-250 and DB-300 specimens, increasing the duration of heating to 30 minutes reduces the strain (6% and 17 % reduction, respectively) in comparison with specimens taken out immediately from the oven. However, duration of exposure has little effect on failure strain for a heating

temperature of 350^{o}C. An increase of 9% is observed in the ultimate strain of DB-350 specimens kept in the oven for additional 30-minutes after reaching target temperature (compared to specimens taken out of the oven upon reaching 350^{o}C).

6.3 Recommendations for Future Studies

Further investigations are recommended to better understand the behavior of GFRP and CFRP bars, and the changes in mechanical properties of these composite materials after being heated to elevated temperatures. Recommended studies may include:

1. Conducting a study on the effect of pre-heating carbon fiber reinforced polymer bars and sheets.
2. The potential for achieving pseudo-ductile behavior in composite bars should be explored further. The mechanism for this behavior is not clear at this stage. The study reported in this thesis indicates that variation in modulus (layering effect as suggested by Ellis [1]) may not be the likely factor.
3. Conducting a study on the effect of different rates of heating on the ultimate strain of GFRP bars.
4. Conducting a study on the influence of existence of loads on the bars (while they are being heated) on their post-heat mechanical properties.

REFERENCES

1. Ellis, Devon, "Evaluation of Post-Fire Strength of Concrete Flexural Members Reinforced With Glass Fiber Reinforced Polymer (GFRP) Bars" *PhD Thesis, University of Wisconsin-Milwaukee,* 2009

2. Wang, Y. C., Wong, P. M. H. and Kodur, V., "Mechanical Properties of Fiber Reinforced Polymer Reinforcing Bars at Elevated Temperatures" *SFPE/ASCE Specialty Conference: Designing Structures for Fire,* Baltimore, MD., Sept. 30-Oct. 1, 2003, pp. 183-192

3. Castro, Protasio F. and Carino Nicholas J., "Tensile and Nondestructive Testing of FRP Bars" *Journal of Composites for Construction,* Vol. 2, No. 1, February 1998, pp. 17-27

4. Malvar, Javier L., "Tensile and Bond Properties of GFRP Bars", *ACI Materials Journal*, Vol.92, No.3, May-June 1995, pp.276-285

5. ACI Committee 440, " Guide for the Design and Construction of Concrete Reinforced with FRP Bars", *American Concrete Institute*, ACI 440.1R-03, 2003

6. Katz, Ammon, Berman, Neta and Bank, Lawrence C., "Effect of High Temperature on Bond Strength of FRP Rebars", *Journal of Composites for Construction*, Vol.3, No.2, May 1999, pp. 73-81

7. *Glass Fiber Reinforced Polymer (GFRP) Rebar – Aslan 100 series*, Hughes Brothers, Inc., Seward, NE, 2011

8. Harris, H. G., Somboonsong, W., Ko, F. K., "New Ductile Hybrid FRP Reinforcing Bar for Concrete Structures", Journal of Composites for Construction, Vol. 2, No. 1, 1998, pp 28-37

9. Young-Jun You, Young-Hwan Prak, Hyeong-Yeol Kim, Ji-Sun Park, "Hybrid Effect on Tensile Properties of FRP Rods with Various Material Compositions", *Composite Structures*, Vol. 80, 2007, pp 117-122

10. Bakis, C. E., Nanni, A., Terosky, J. A., "Smart, Pseudo-ductile, Reinforcing Rods for Concrete: Manufacture and Test", *First International Conference on Composites in Infrastructure,* 1996, pp 95-108

11. Cui, Y. H., Tao, J., "A New Type of Ductile Composite Reinforcing Bar with High Tensile Elastic Modulus for Use in Reinforced Concrete Structures", *Canadian Journal of Civil Engineering,* Vol. 36, 2009, pp 672-675

12. Thomason, J. L., Yang, L., Meier, R., "The Properties of Glass Fiber After Conditioning at Composite Recycling Temperatures", *Compos Part A Appl Sci Manuf*, Vol. 61, June 2014, pp 201-208

13. Yang, L., Thomason, J. L., "The Thermal Behaviour of Glass Fiber Investigated by Thermomechanical Analysis", *Journal of Materials Science*, Vol. 48, 2013, pp 5768-5775

14. Feih, S., Boiocchi, E., Mathys, G., Mathys, Z., Gibson, A. G., Mouritz, A. P., "Mechanical Properties of Thermally-treated and Recycled Glass Fibres", *Composites Part B: Engineering*, Volume 42, 2011, pp 350-358

15. Otto, W. H., "Compaction Effects in Glass Fibers", Journal of the American Ceramic Society, Volume 44, No. 2, February 1961, pp 68-72

16. Alsayed, S., Al-Salloum, Y., Almusallam, T., El-Gamal, S., Aqel, M., "Performance of Glass Fiber Reinforced Polymer Bars Under Elevated Temperatures", *Composites Part B: Engineering,* 2012, pp 2265-2271

17. Nanni, A., Henneke, M. J., Okamoto, T., "Tensile Properties of Hybrid Rods for Concrete Reinforcement", *Construction and Building Materials*, Volume 8, 1994, pp 27-34

18. Robert, M., Benmokrane, B., "Behavior of GFRP Reinforcing Bars Subjected to Extreme Temperatures", *Journal of Composites for Construction,* Volume 14, 2010, pp 353-360

19. Blontrock, H., Taerwe, L., Matthys, S., "Properties of Fiber Reinforced Plastics at Elevated Temperatures with Regard to Fire Resistance of Reinforced

Concrete Members", *Fourth International Symposium on Fiber Reinforced Concrete Structures*, Volume 188, 1999, pp 44-54

20. Kumahara, S., Masuda, Y., Tanano, H., Shimizu, A., "Tensile Strength of Continuous Fiber Bar Under High Temperature", *Proc. Fiber-Reinforced Plastic Reinforcement for Concrete Structures-International Symposium*, Detroit, 1993, pp 731-742

21. Gibson, A. G., Wright, P. N. H., Wu, Y. -S., Mouritz, A. P., Mathys, Z., Gardiner, C. P., "Modelling Residual Mechanical Properties of Polymer Composites After Fire", *Plastics, Rubber and Composites,* Volume 32, 2003, pp 81-90

22. Gibson, A. G., Wright, P. N. H., Wu, Y. -S., Mouritz, A. P., Mathys, Z., Gardiner, C. P., "The Integrity of Polymer Composites During and After Fire", *Journal of Composite Materials,* volume 38, 2004, pp 1283-1307

23. ASTM D3039 / D3039M-00, "Standard Test Method for Tensile Properties of Polymer Matrix Composite Materials", ASTM International, West Conshohocken, PA, 2000

24. Sorathia, U., Beck, C., Dapp, T., "Residual strength of composites during and after fire exposure", *Journal of Fire Sciences*, Volume 11, 1993, pp 255-270

25. Dodds, N., Gibson, A. G., Dewhurst, D., Davies, J. M., "Fire Behavior of Composite Laminates", *Composites: Part A*, Volume 31, Issue 7, 2000, pp 689-702

26. Sayed-Ahmed, E. Y., Shrive, N. G., "Smart FRP Prestressing Tendons: Properties, and Prospects", *Proceedings of the Second Middle East Symposium on Structural Composites for Infrastructure Applications*, 1999, pp 80–93.

27. Somboonsong, W., "Development of Ductile Hybrid Fiber Reinforced Polymer (D-H-FRP) Reinforcement for Concrete Structures", *PhD thesis*, Drexel University, December-1997, pp 7-26

28. David Cripps, Gurit , “Glass Fibre/Fiber”, *http://www.netcomposites.com/guide/glass-fibrefiber/32*, viewed on 4-Nov-2014©

29. David Cripps, Gurit , “*Aramid Fibre/Fiber",* *http://www.netcomposites.com/guide/aramid-fibrefiber/33*, viewed on 5-Nov-2014©

30. David Cripps, Gurit , “Carbon Fibre/Fiber” *http://www.netcomposites.com/guide/carbon-fibrefiber/34*, viewed on 5-Nov-2014©

31. Lund, M. D., Yue, Y., " Impact of Drawing Stress on the Tensile Strength of Oxide Glass Fibers", *Journal of the American Ceramic Society*, Volume 93, Issue 10, 2010, pp 3236–3243

APPENDIX A: STRESS-STRAIN FIGURES

8.1 DB-CONTROL:

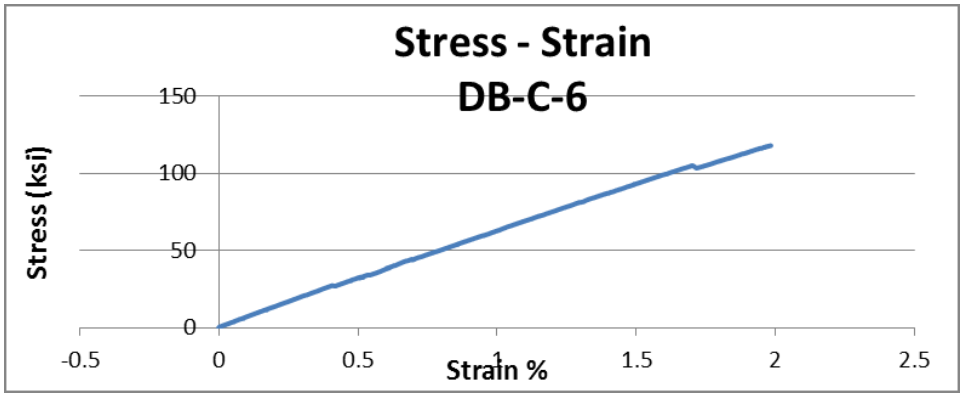

Figure 8-1 Stress – Strain curve for specimen DB –C—6

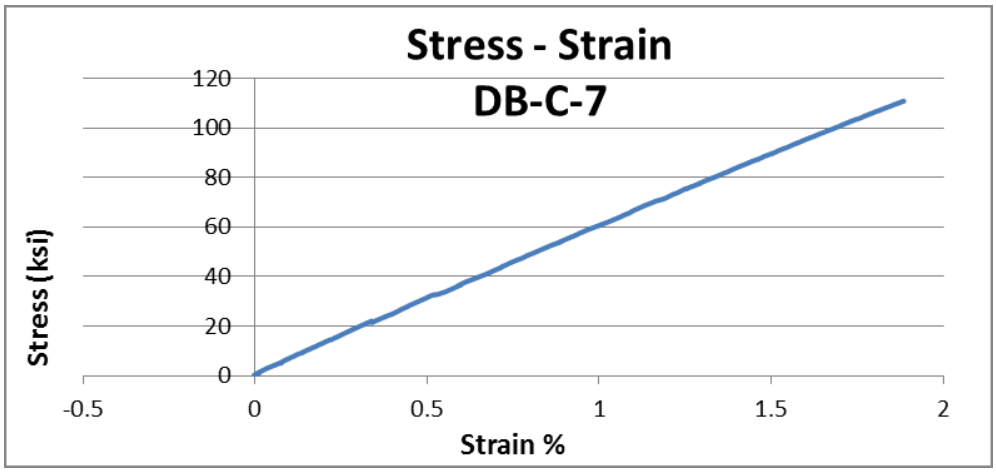

Figure 8-2 Stress – Strain curve for specimen DB –C—7

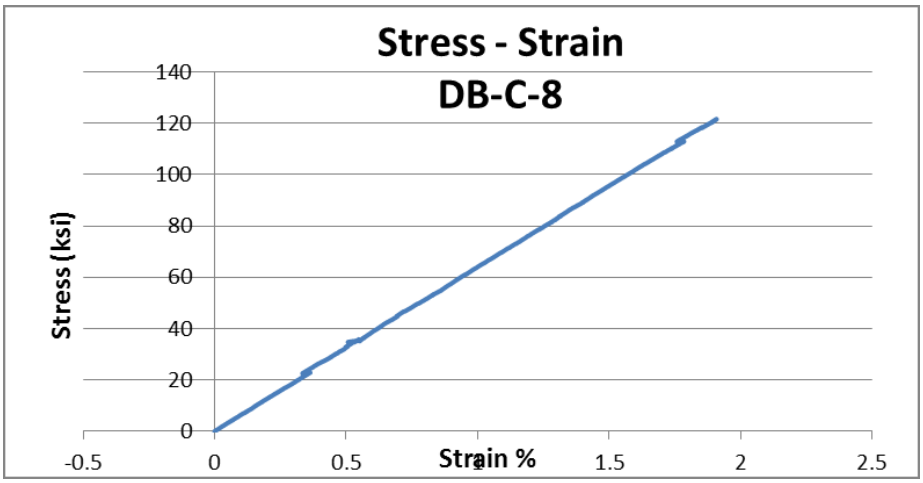

Figure 8-3 Stress – Strain curve for specimen DB –C—8

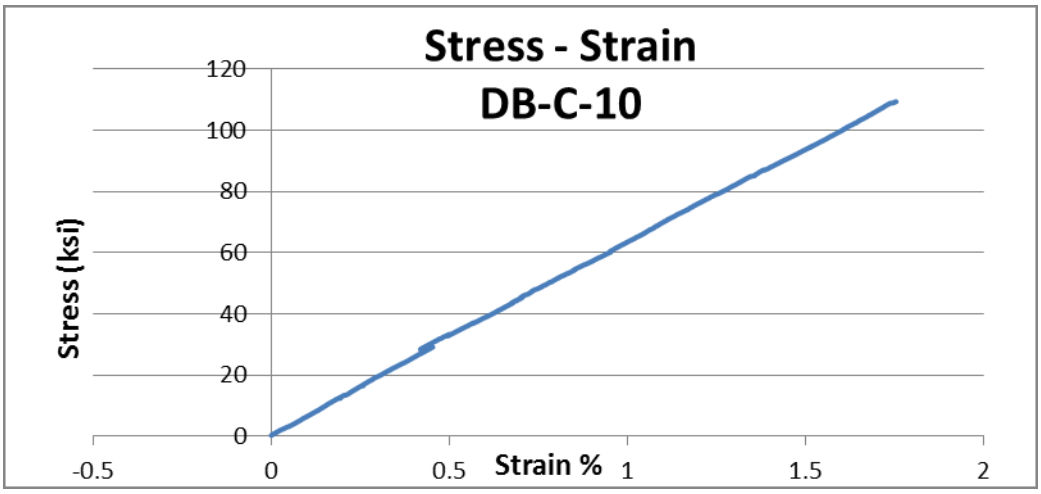

Figure 8-4 Stress – Strain curve for specimen DB –C—10

8.2 DB-250-0:

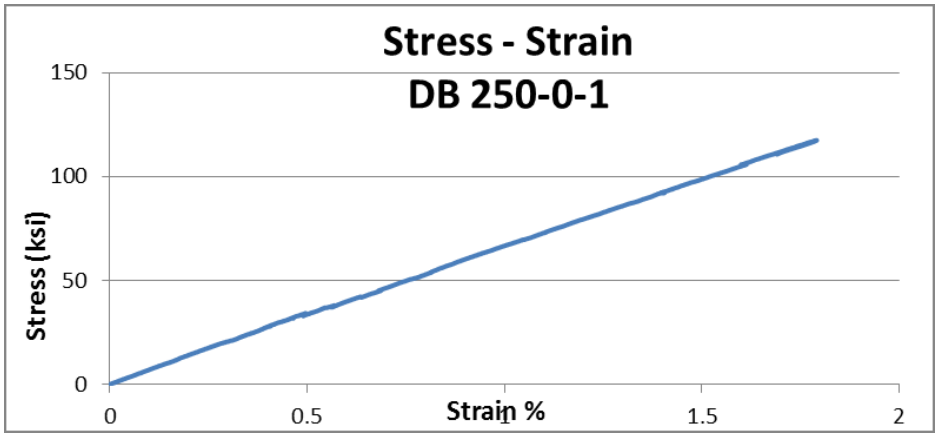

Figure 8-5 Stress – Strain curve for specimen DB 250-0-1

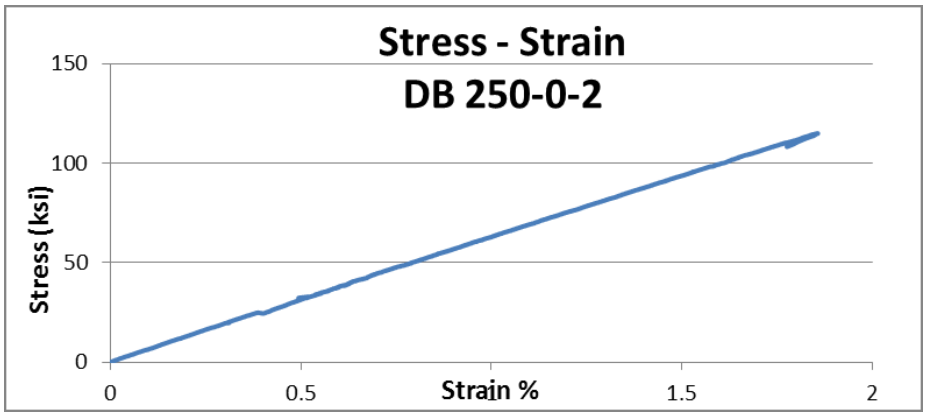

Figure 8-6 Stress – Strain curve for specimen DB 250-0-2

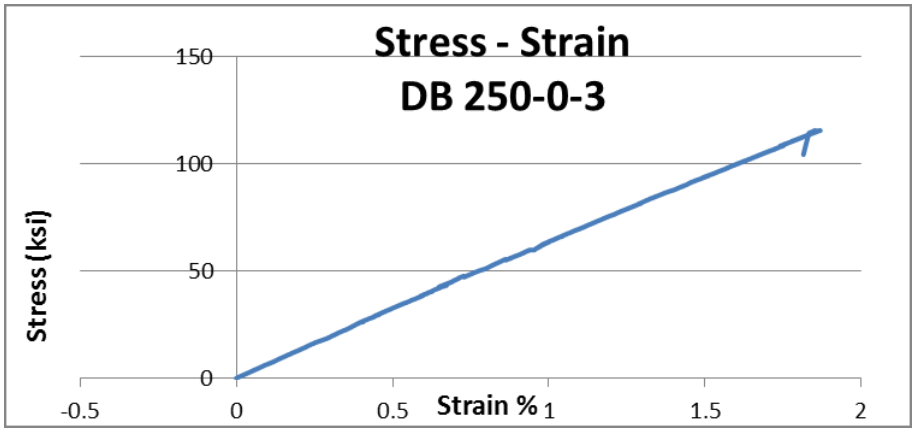

Figure 8-7 Stress – Strain curve for specimen DB 250-0-3

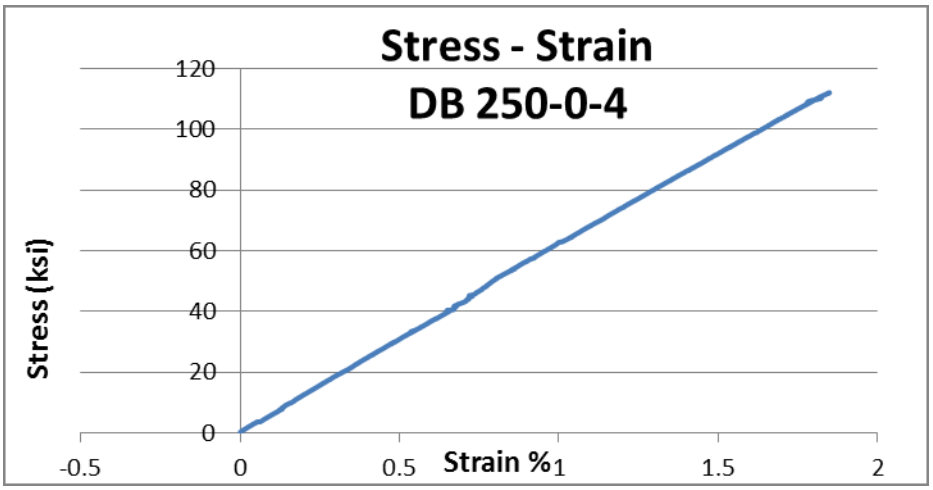

Figure 8-8 Stress – Strain curve for specimen DB 250-0-4

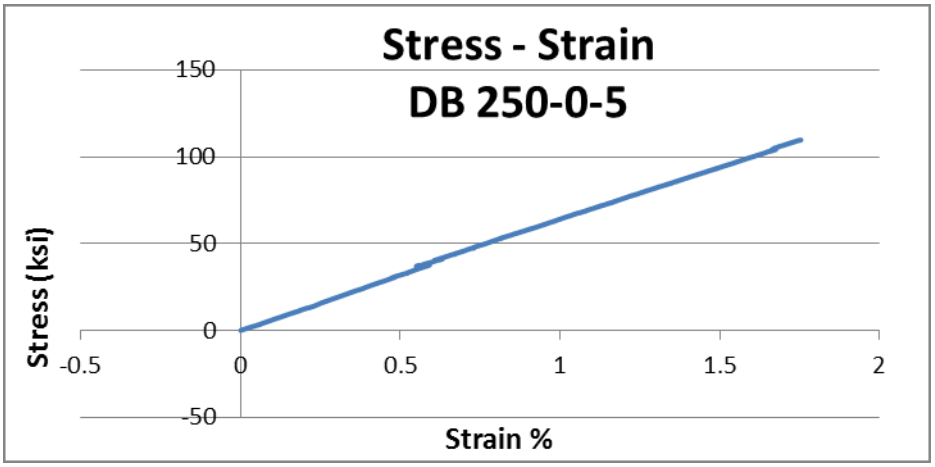

Figure 8-9 Stress – Strain curve for specimen DB 250-0-5

8.3 DB-250-5:

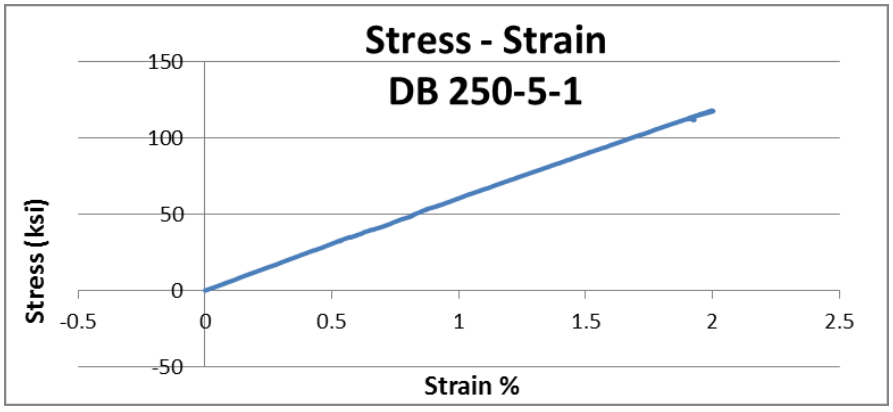

Figure 8-10 Stress – Strain curve for specimen DB 250-5-1

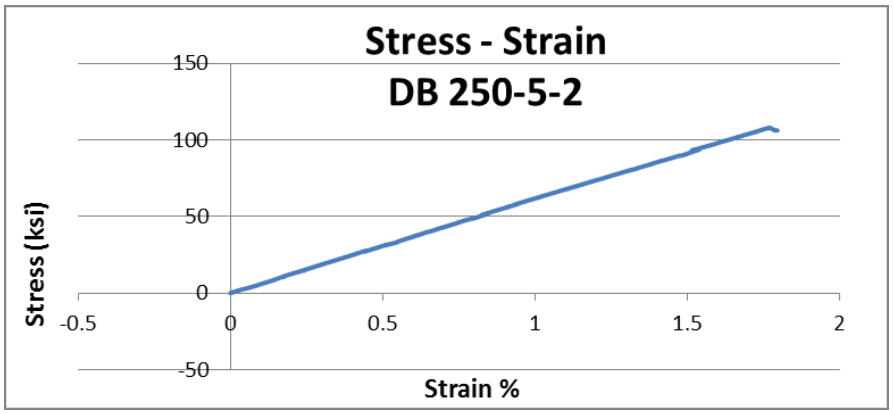

Figure 8-11 Stress – Strain curve for specimen DB 250-5-2

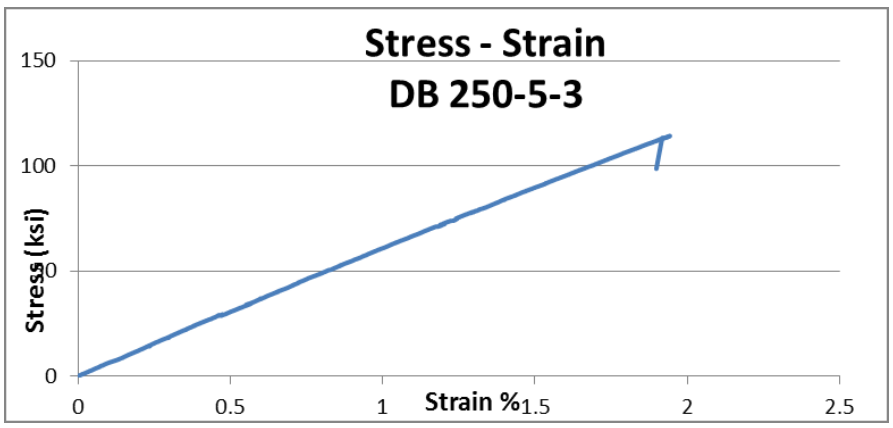

Figure 8-12 Stress – Strain curve for specimen DB 250-5-3

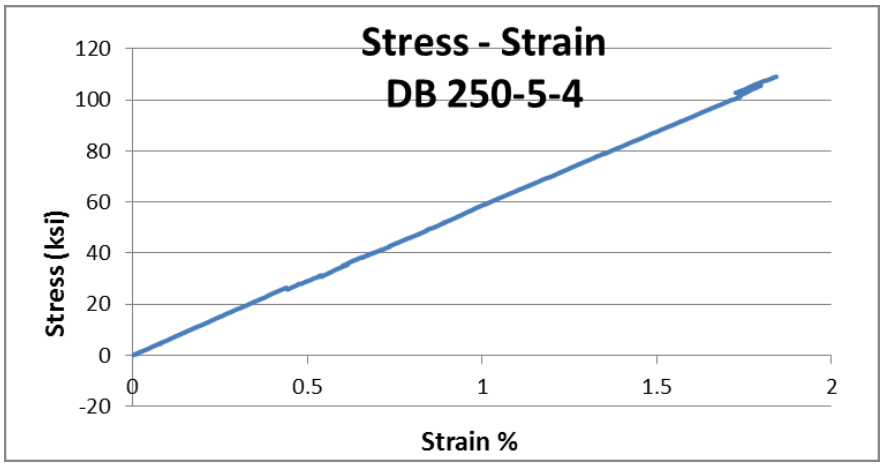

Figure 8-13 Stress – Strain curve for specimen DB 250-5-4

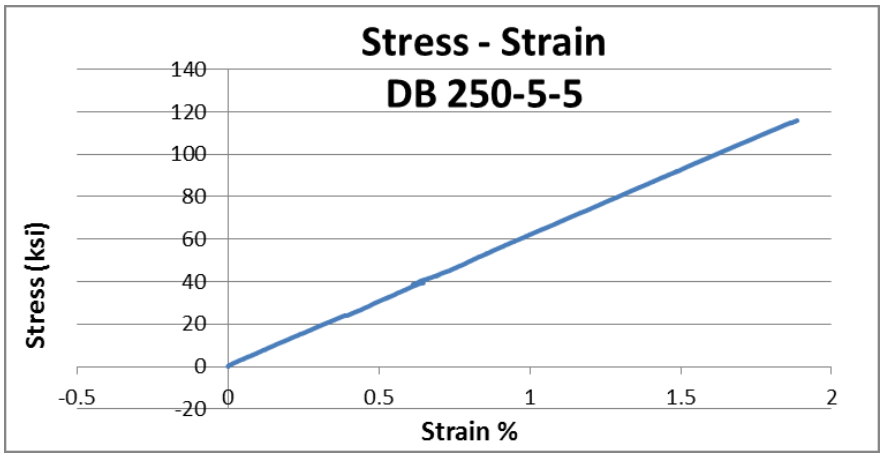

Figure 8-14 Stress – Strain curve for specimen DB 250-5-5

8.4 DB-250-10:

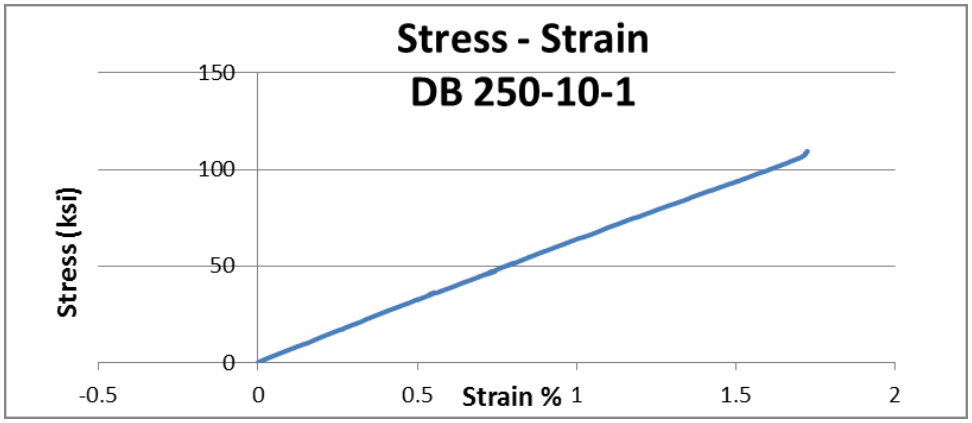

Figure 8-15 Stress – Strain curve for specimen DB 250-10-1

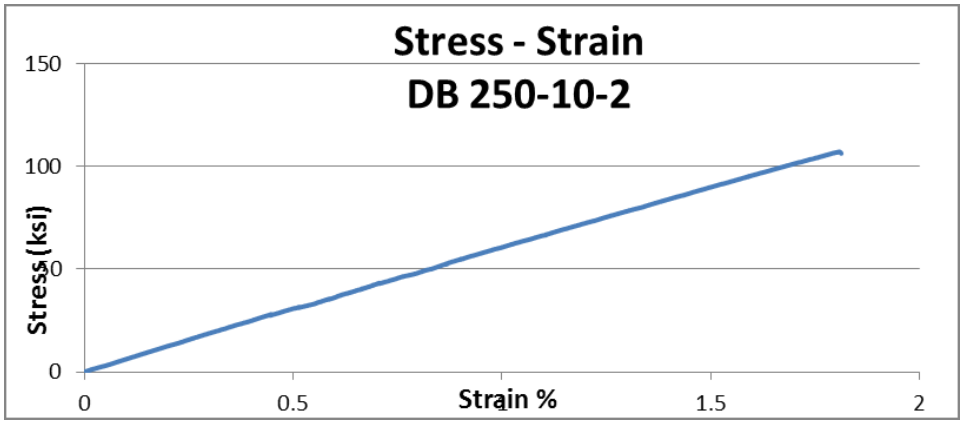

Figure 8-16 Stress – Strain curve for specimen DB 250-10-2

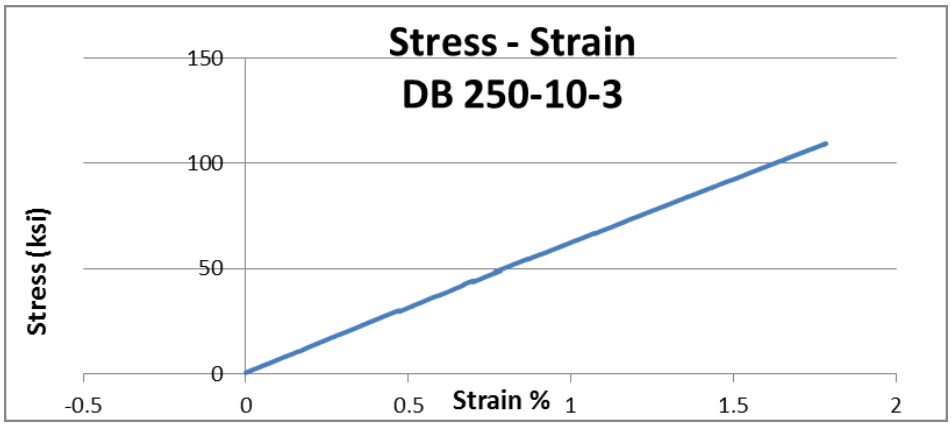

Figure 8-17 Stress – Strain curve for specimen DB 250-10-3

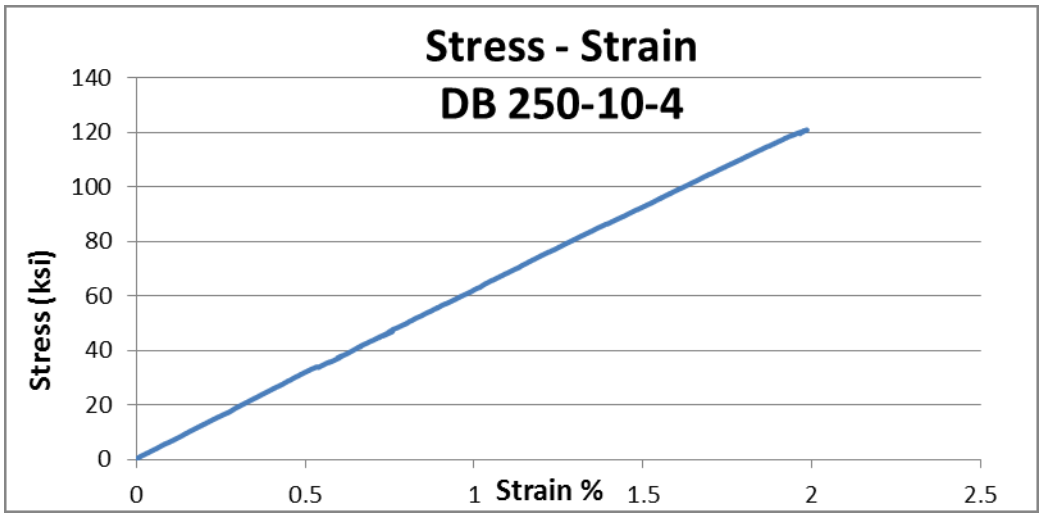

Figure 8-18 Stress – Strain curve for specimen DB 250-10-4

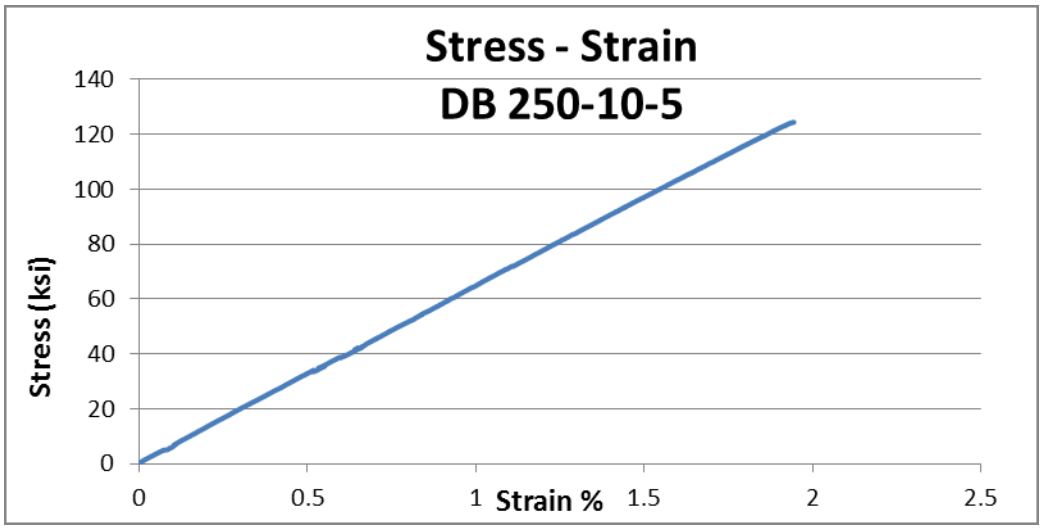

Figure 8-19 Stress – Strain curve for specimen DB 250-10-4

8.5 DB-250-30:

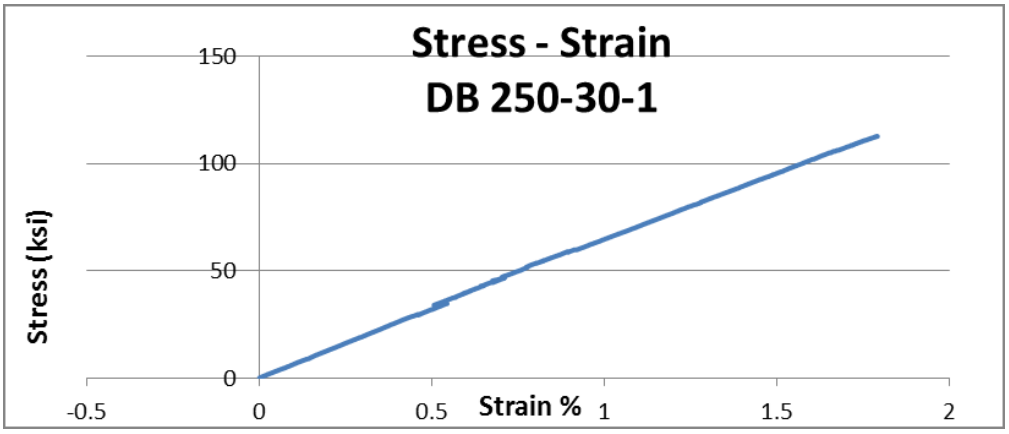

Figure 8-20 Stress – Strain curve for specimen DB 250-30-1

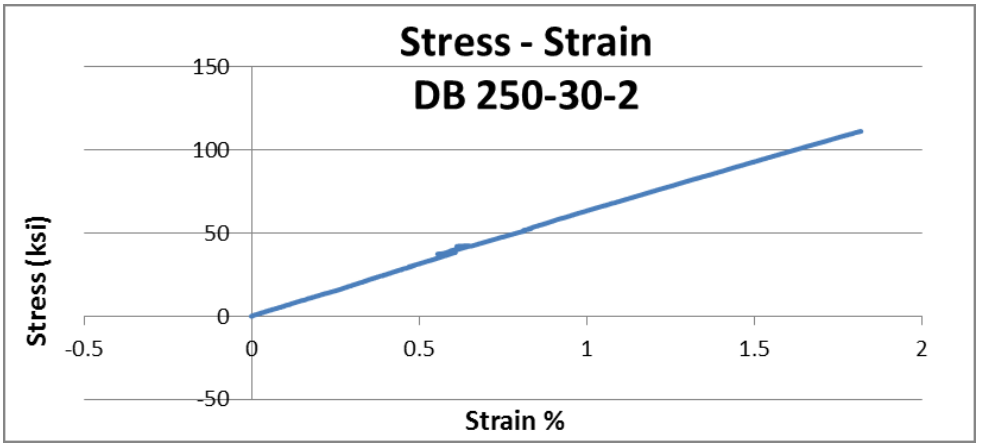

Figure 8-21 Stress – Strain curve for specimen DB 250-30-2

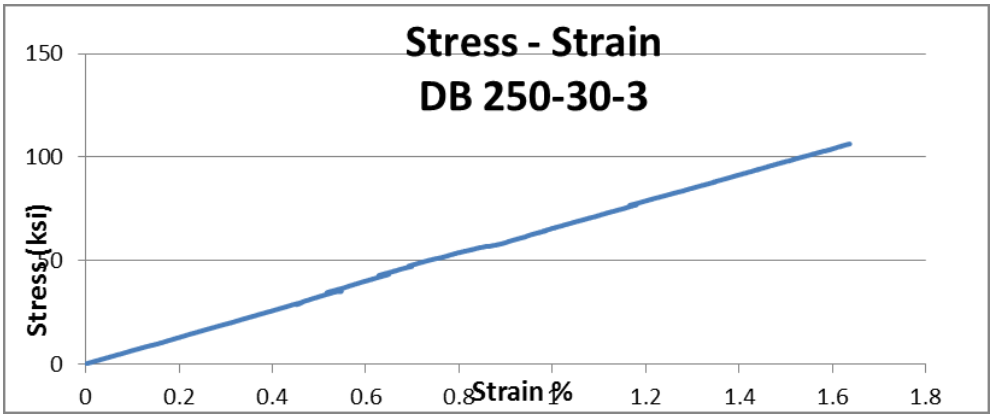

Figure 8-22 Stress – Strain curve for specimen DB 250-30-3

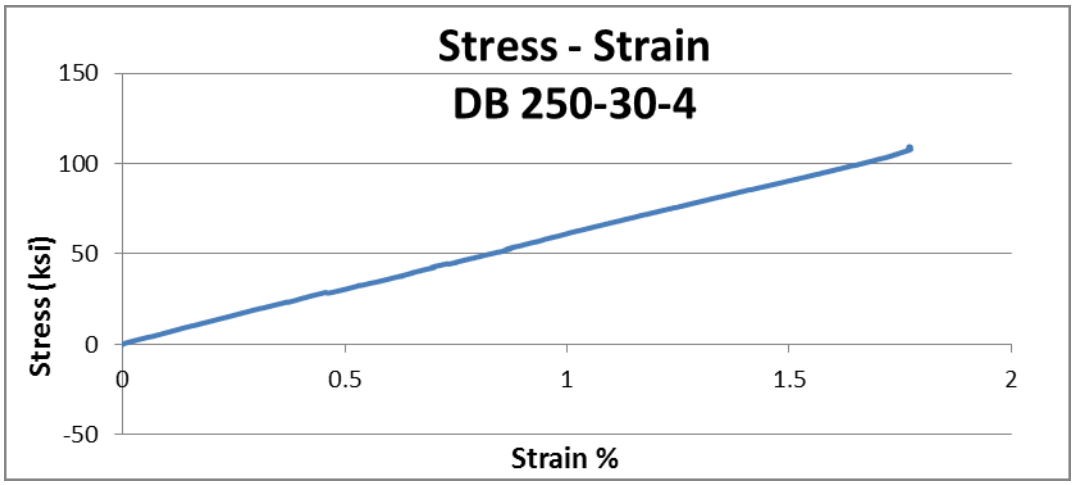

Figure 8-23 Stress – Strain curve for specimen DB 250-30-4

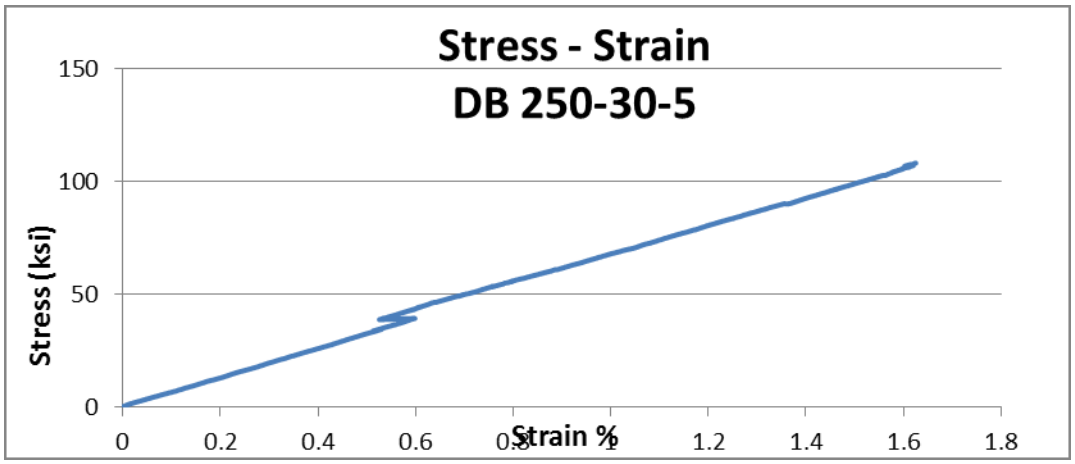

Figure 8-24 Stress – Strain curve for specimen DB 250-30-5

8.6 DB-300-0:

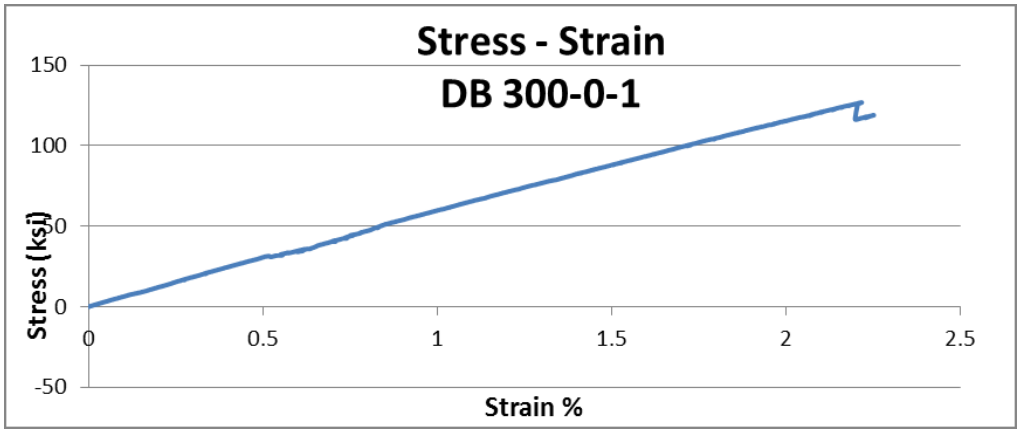

Figure 8-25 Stress – Strain curve for specimen DB 300-0-1

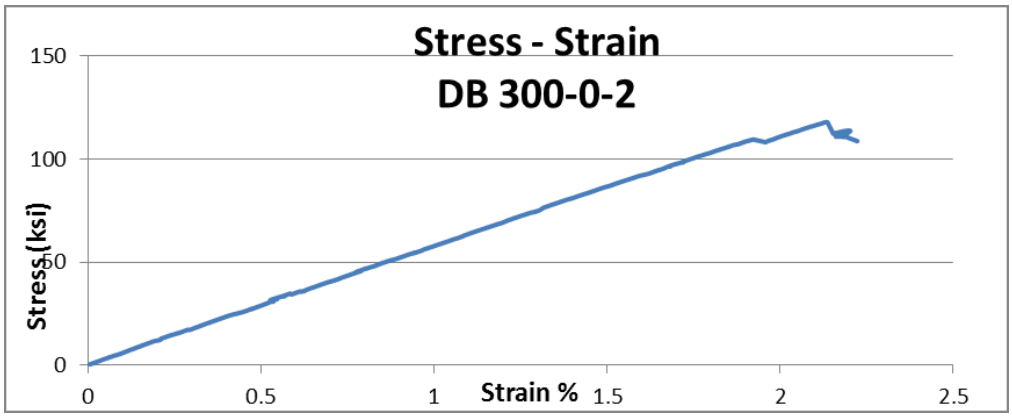

Figure 8-26 Stress – Strain curve for specimen DB 300-0-2

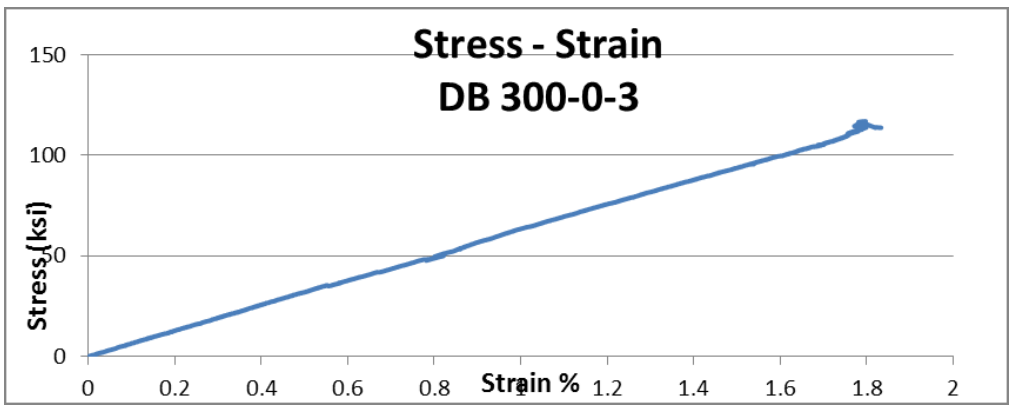

Figure 8-27 Stress – Strain curve for specimen DB 300-0-3

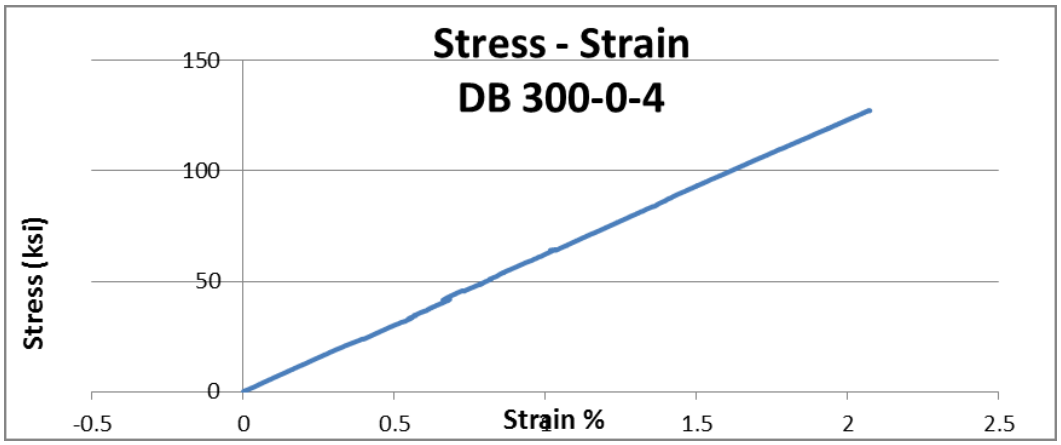

Figure 8-28 Stress – Strain curve for specimen DB 300-0-4

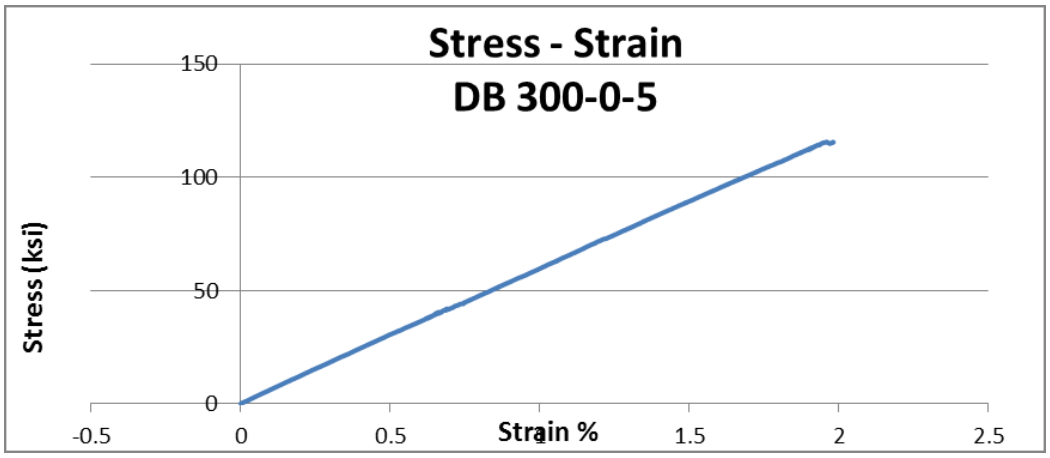

Figure 8-29 Stress – Strain curve for specimen DB 300-0-5

8.7 DB-300-5:

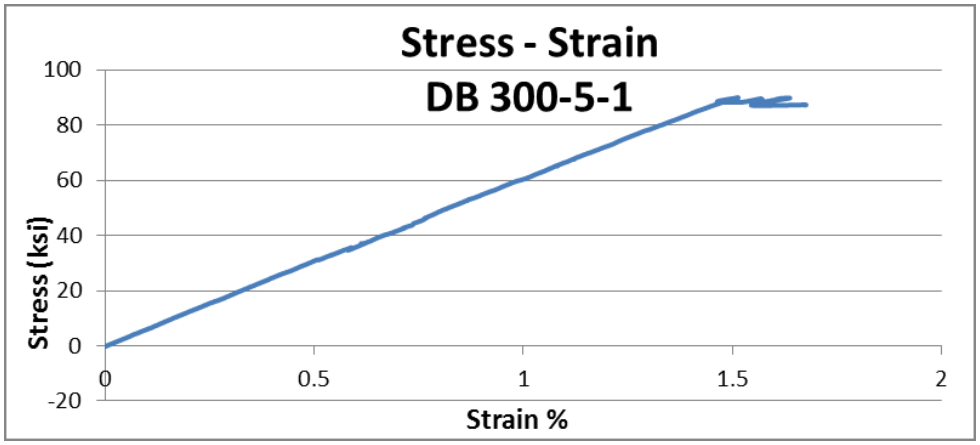

Figure 8-30 Stress – Strain curve for specimen DB 300-5-1

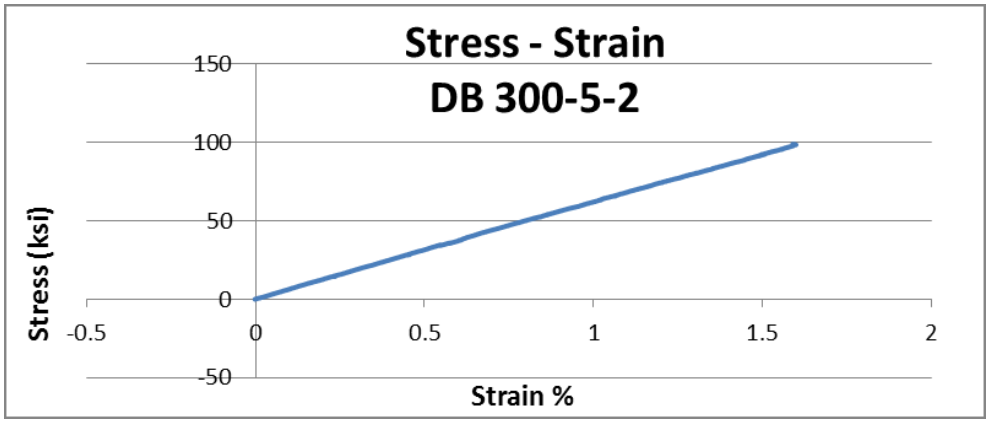

Figure 8-31 Stress – Strain curve for specimen DB 300-5-2

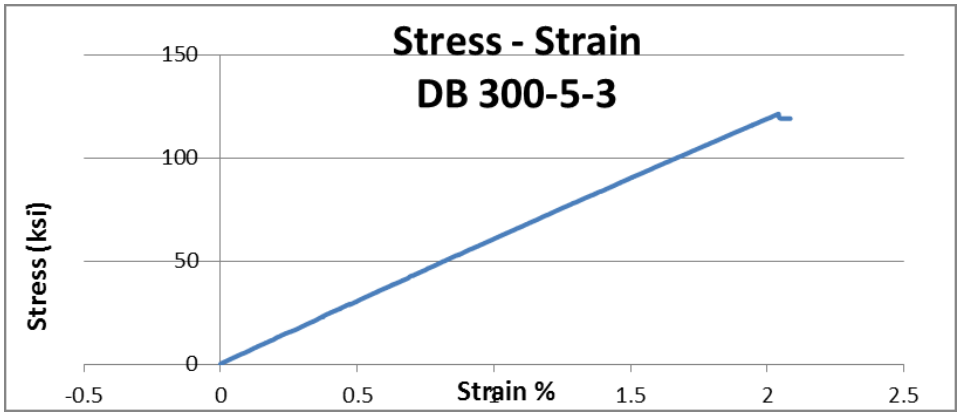

Figure 8-32 Stress – Strain curve for specimen DB 300-5-3

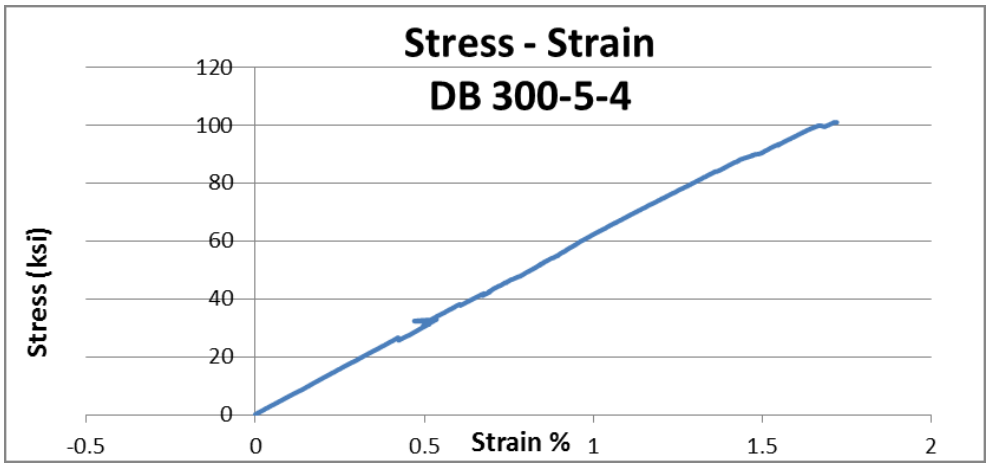

Figure 8-33 Stress – Strain curve for specimen DB 300-5-4

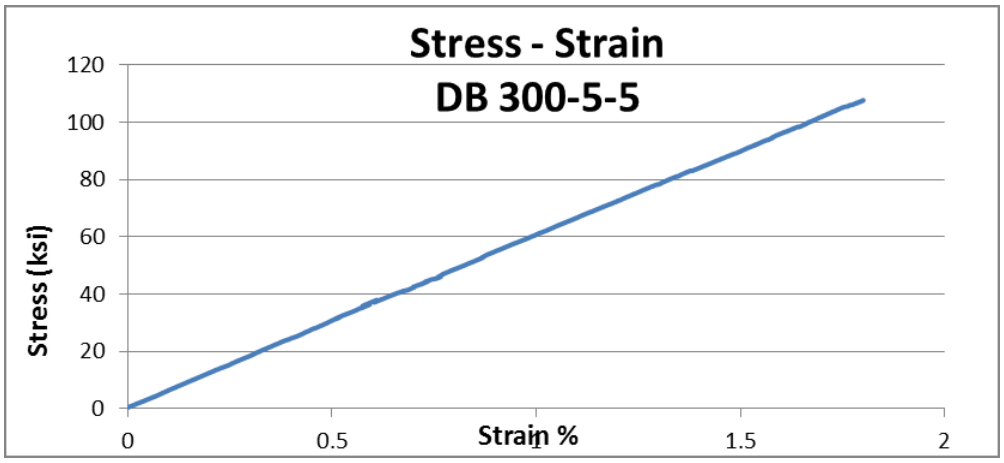

Figure 8-34 Stress – Strain curve for specimen DB 300-5-5

8.8 DB-300-10:

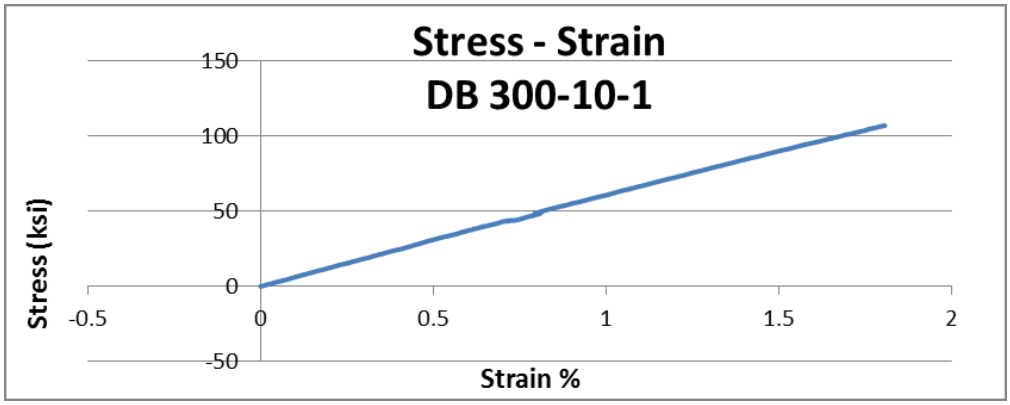

Figure 8-35 Stress – Strain curve for specimen DB 300-10-1

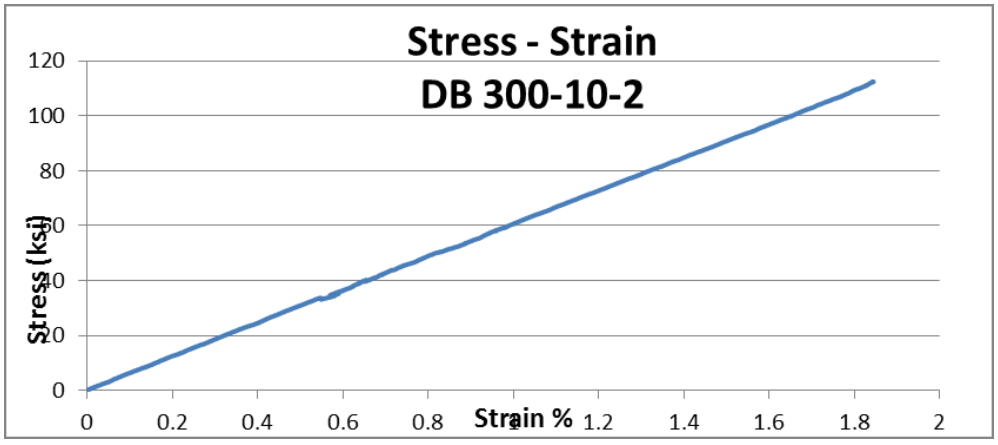

Figure 8-36 Stress – Strain curve for specimen DB 300-10-2

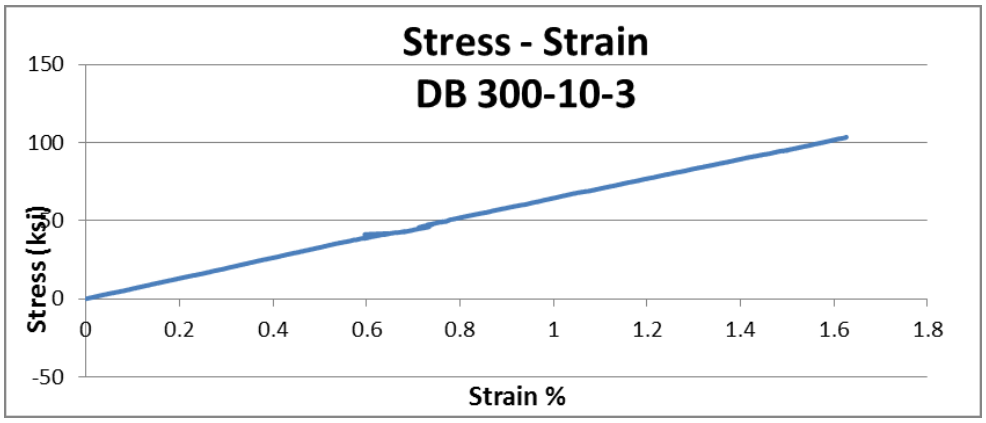

Figure 8-37 Stress – Strain curve for specimen DB 300-10-3

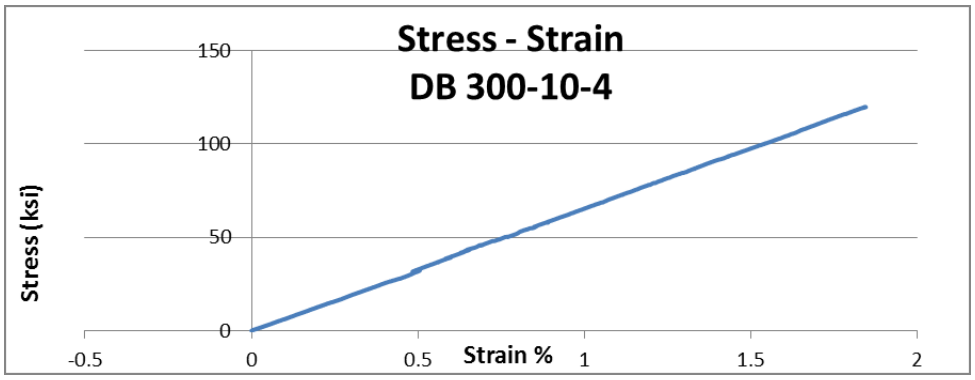

Figure 8-38 Stress – Strain curve for specimen DB 300-10-4

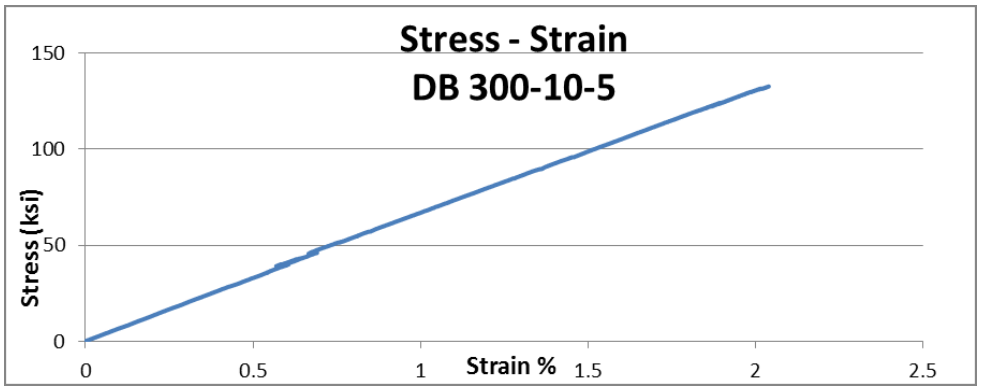

Figure 8-39 Stress – Strain curve for specimen DB 300-10-5

8.9 DB-300-30:

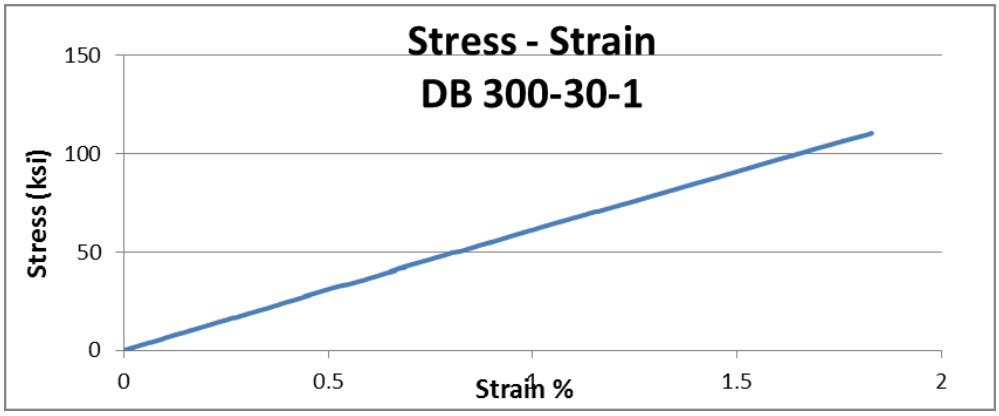

Figure 8-40 Stress – Strain curve for specimen DB 300-30-1

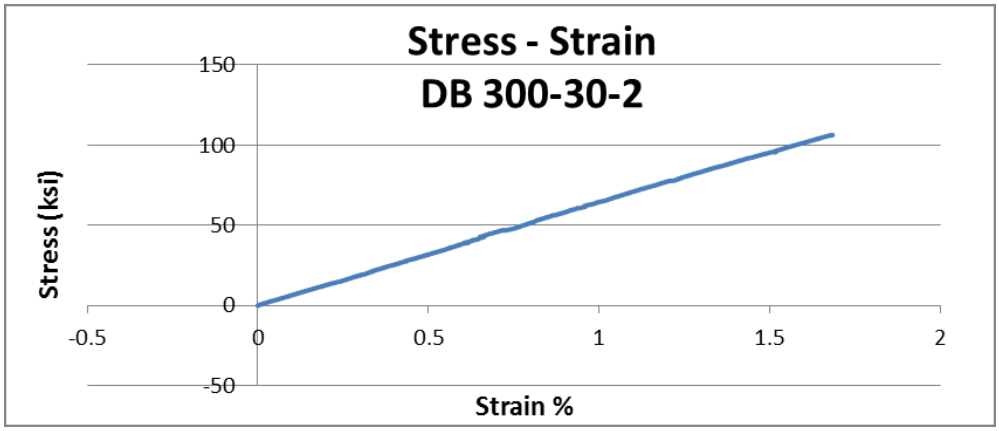

Figure 8-41 Stress – Strain curve for specimen DB 300-30-2

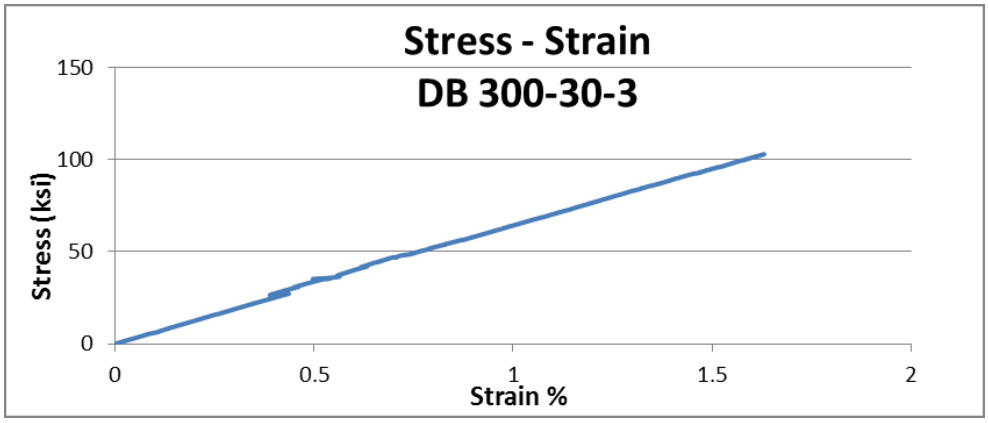

Figure 8-42 Stress – Strain curve for specimen DB 300-30-3

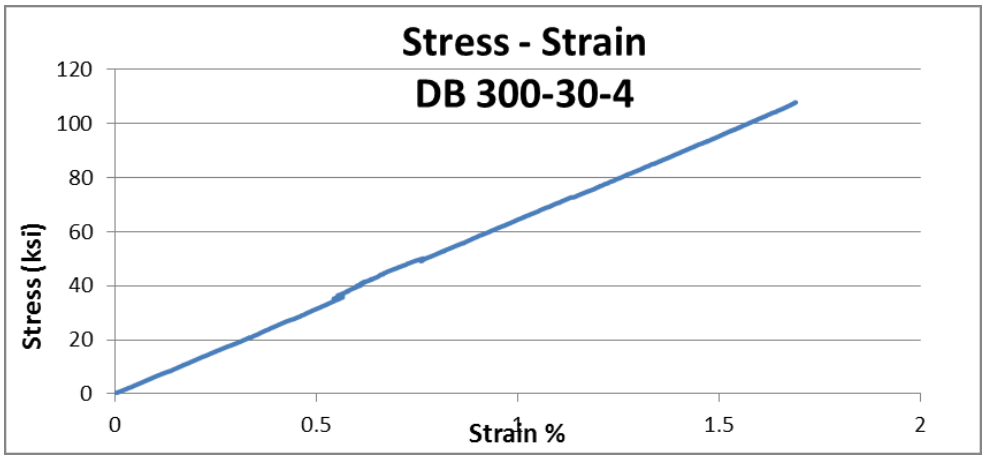

Figure 8-43 Stress – Strain curve for specimen DB 300-30-4

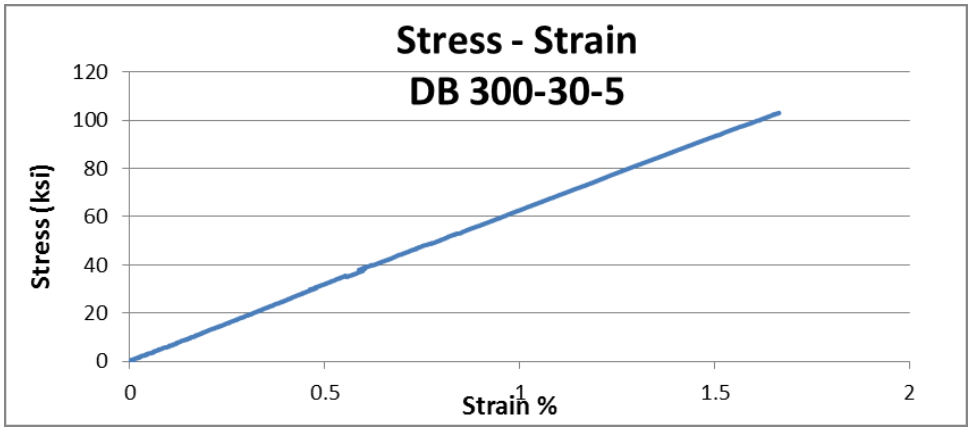

Figure 8-44 Stress – Strain curve for specimen DB 300-30-5

8.10 DB-350-0:

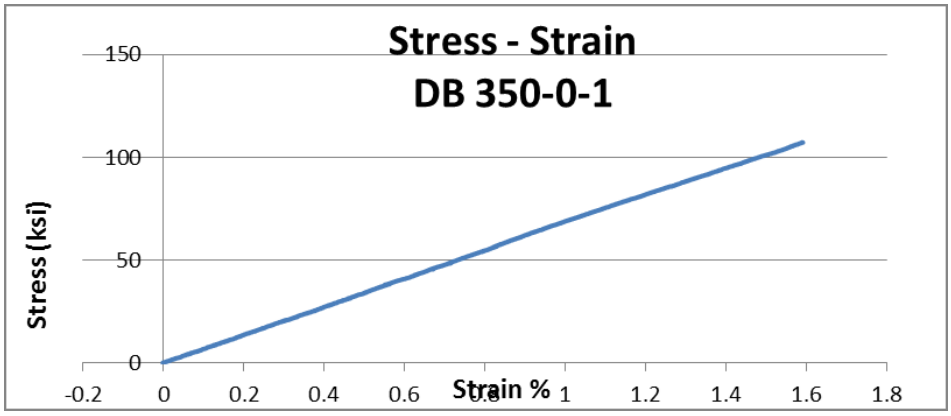

Figure 8-45 Stress – Strain curve for specimen DB 350-0-1

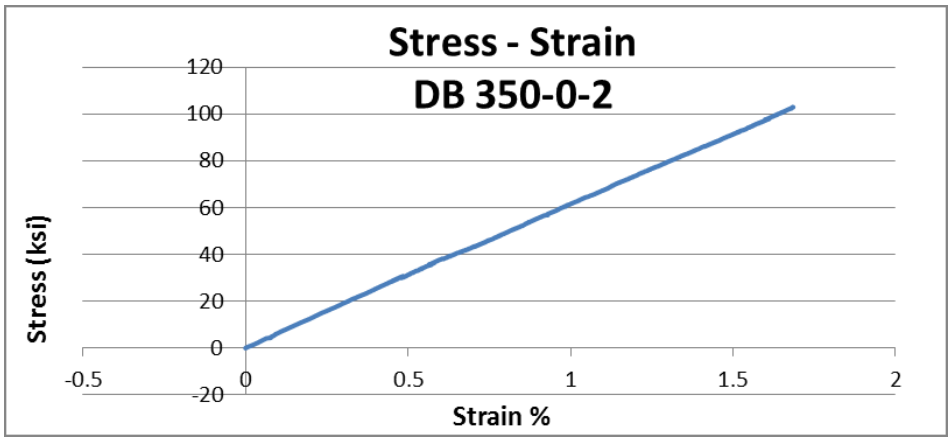

Figure 8-46 Stress – Strain curve for specimen DB 350-0-2

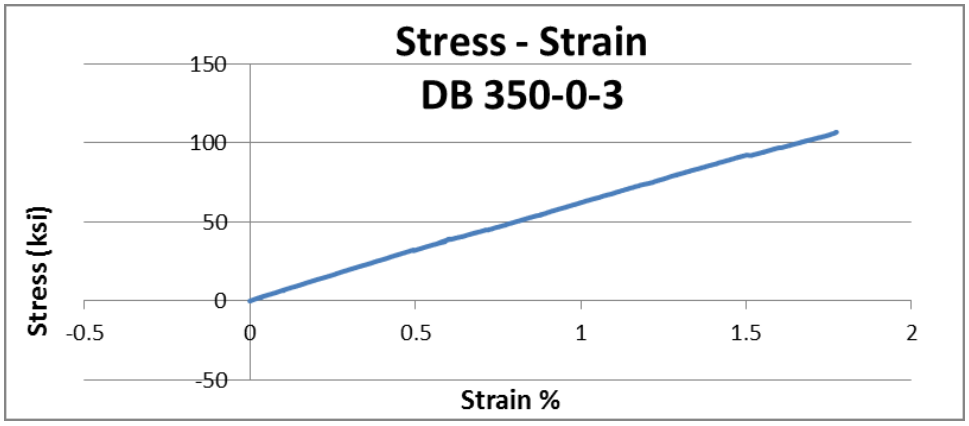

Figure 8-47 Stress – Strain curve for specimen DB 350-0-3

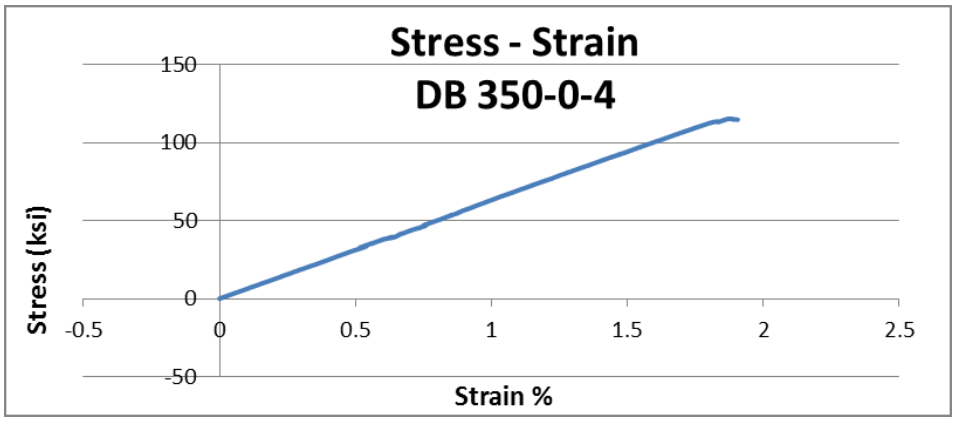

Figure 8-48 Stress – Strain curve for specimen DB 350-0-4

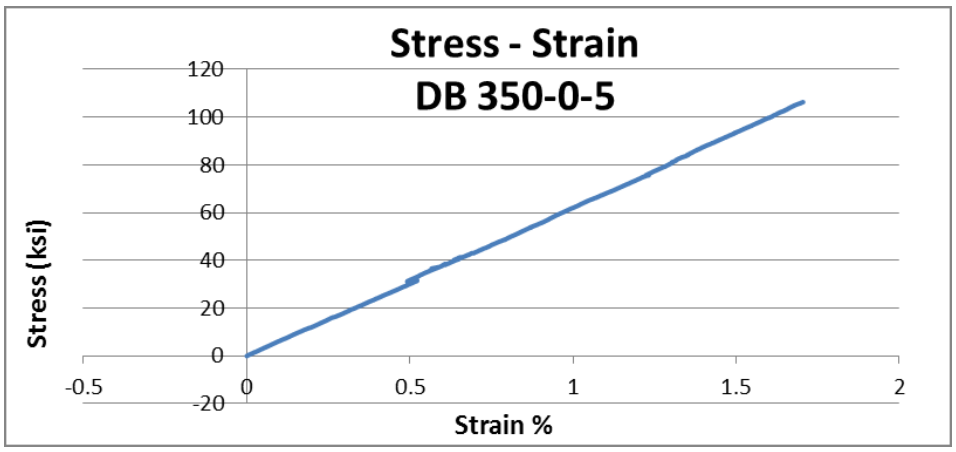

Figure 8-49 Stress – Strain curve for specimen DB 350-0-5

8.11 DB-350-5:

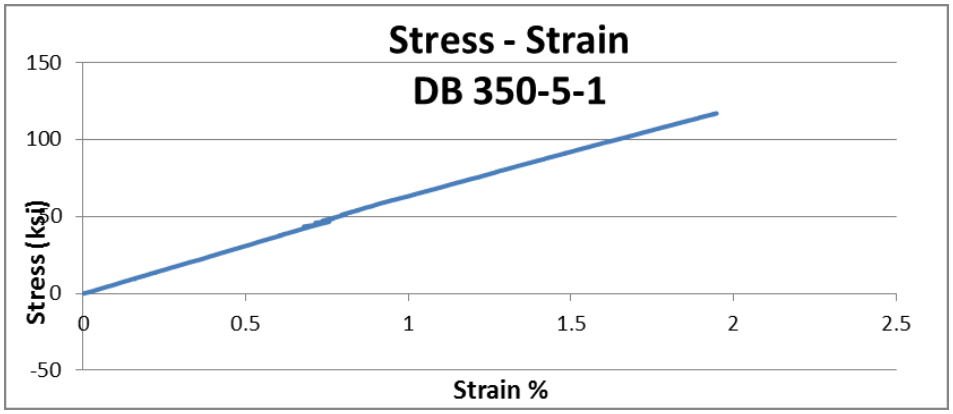

Figure 8-50 Stress – Strain curve for specimen DB 350-5-1

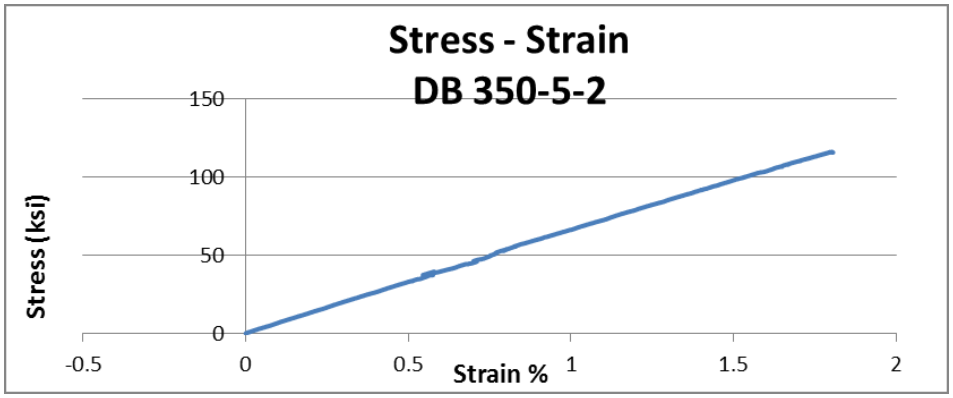

Figure 8-51 Stress – Strain curve for specimen DB 350-5-2

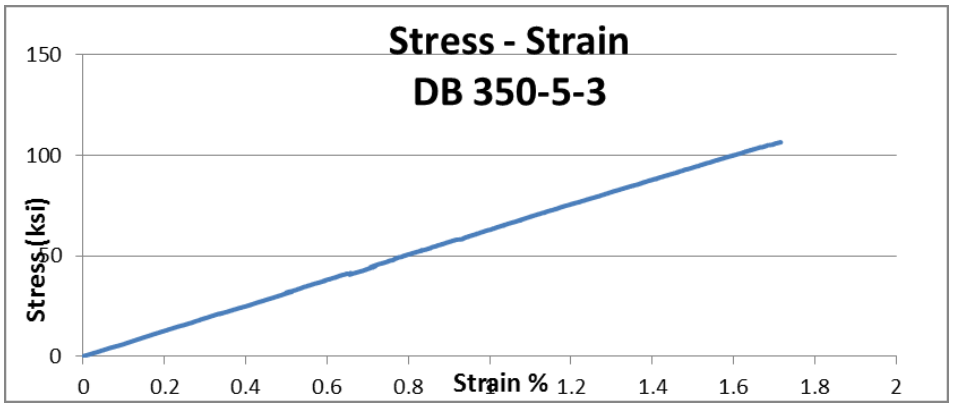

Figure 8-52 Stress – Strain curve for specimen DB 350-5-3

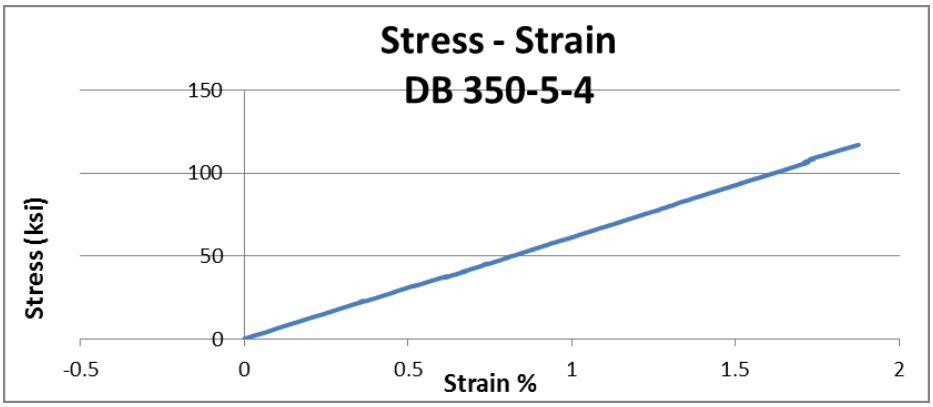

Figure 8-53 Stress – Strain curve for specimen DB 350-5-4

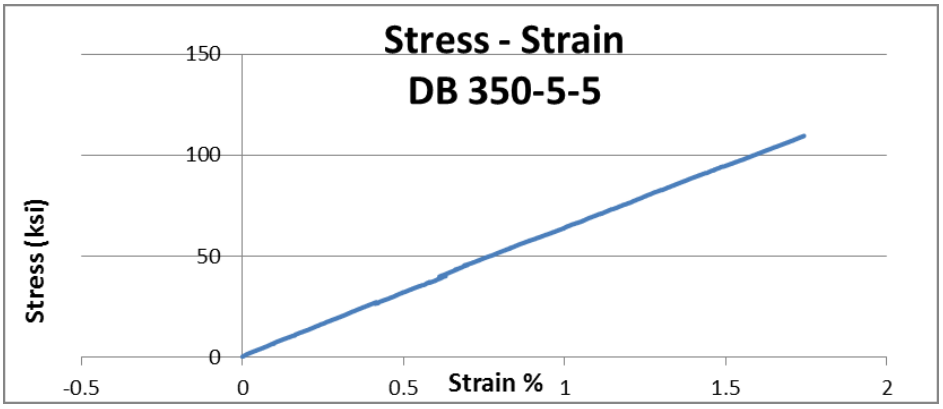

Figure 8-54 Stress – Strain curve for specimen DB 350-5-5

8.12 DB-350-10:

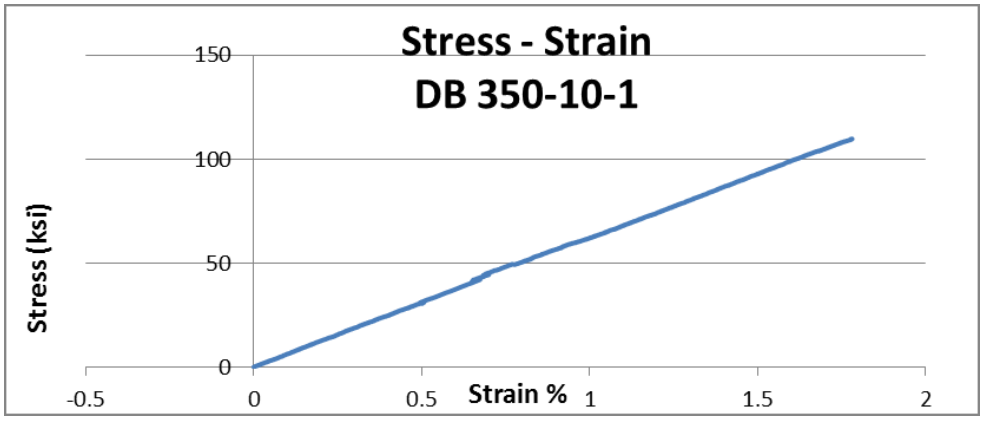

Figure 8-55 Stress – Strain curve for specimen DB 350-10-1

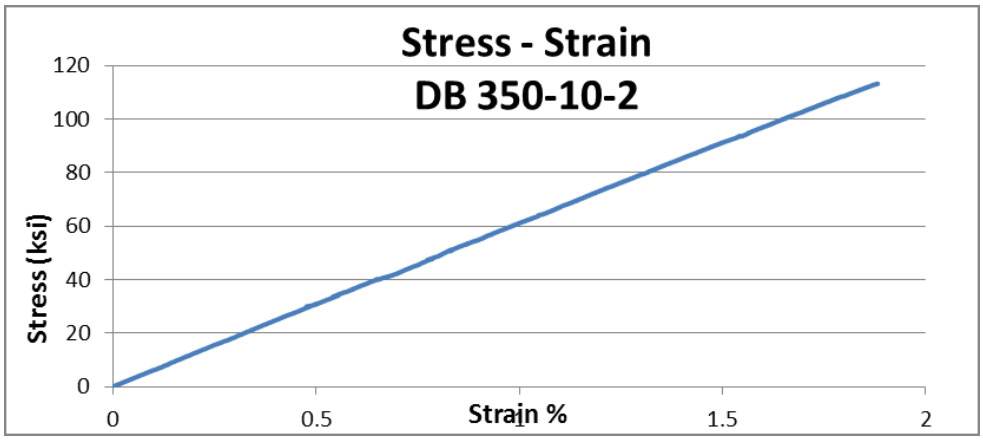

Figure 8-56 Stress – Strain curve for specimen DB 350-10-2

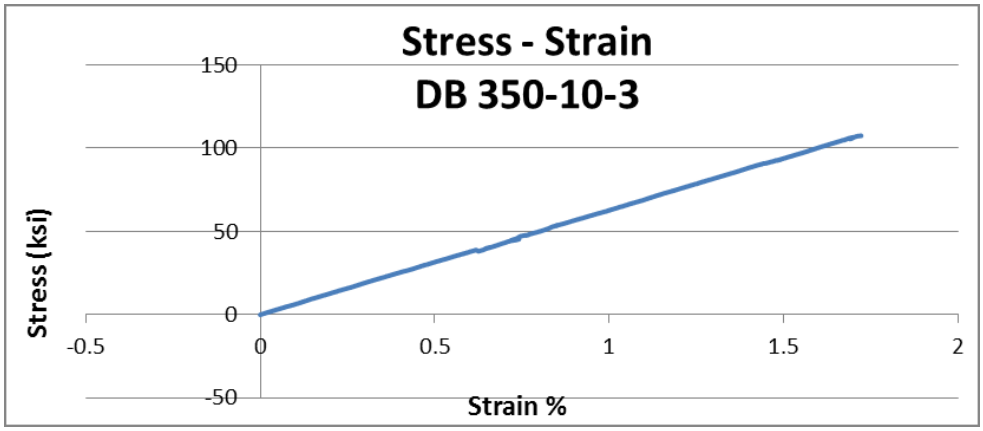

Figure 8-57 Stress – Strain curve for specimen DB 350-10-3

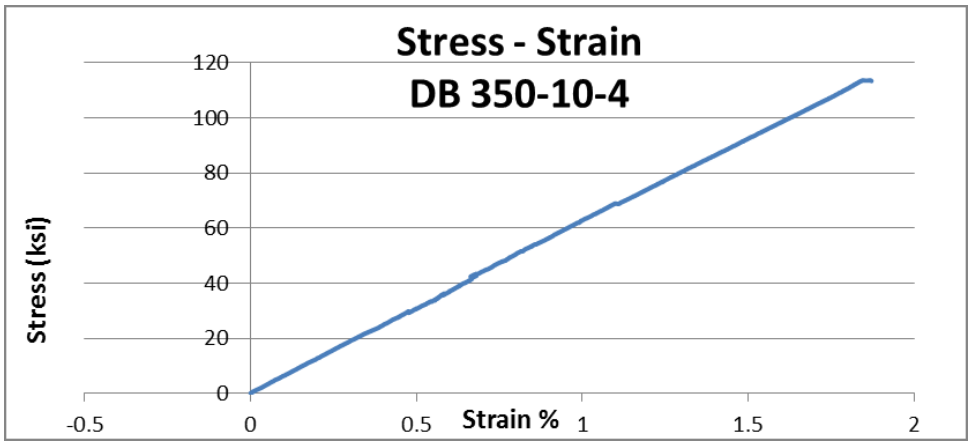

Figure 8-58 Stress – Strain curve for specimen DB 350-10-4

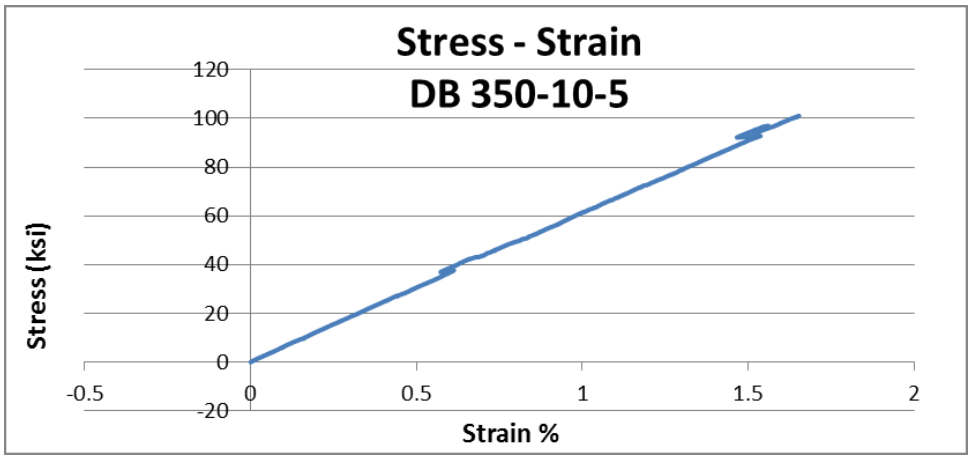

Figure 8-59 Stress – Strain curve for specimen DB 350-10-5

8.13 DB-350-30:

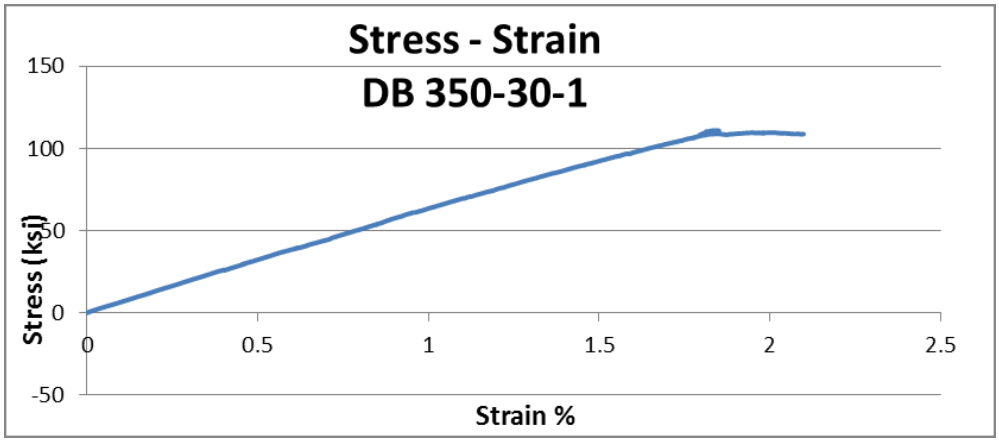

Figure 8-60 Stress – Strain curve for specimen DB 350-30-1

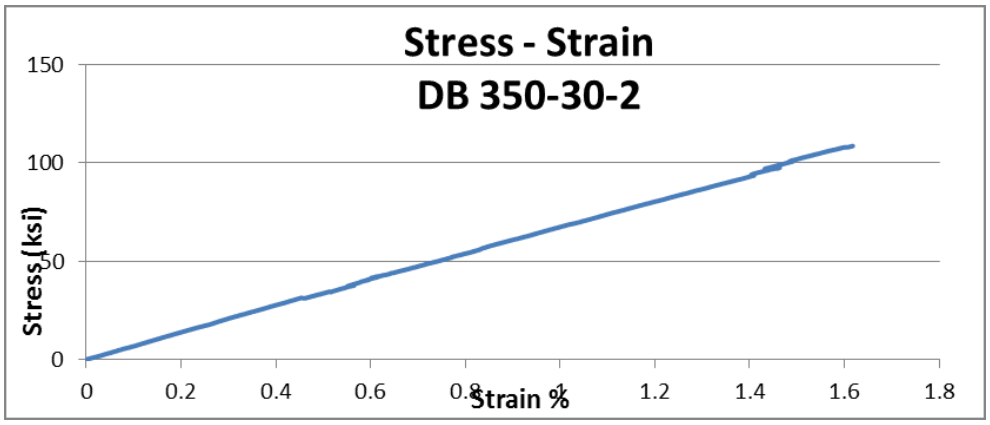

Figure 8-61 Stress – Strain curve for specimen DB 350-30-2

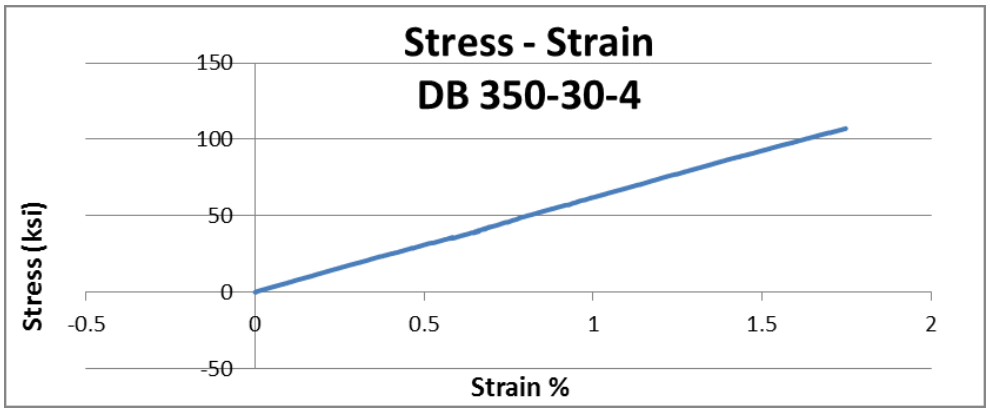

Figure 8-62 Stress – Strain curve for specimen DB 350-30-4

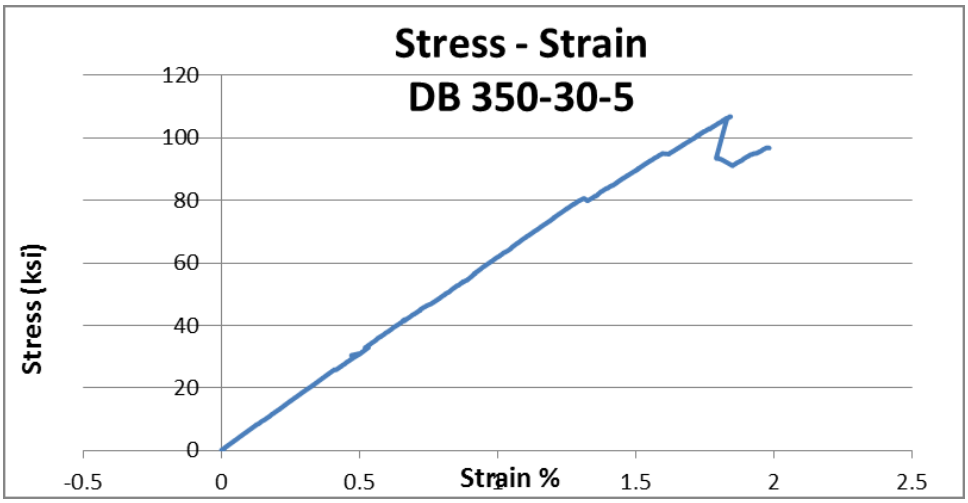

Figure 8-63 Stress – Strain curve for specimen DB 350-30-5

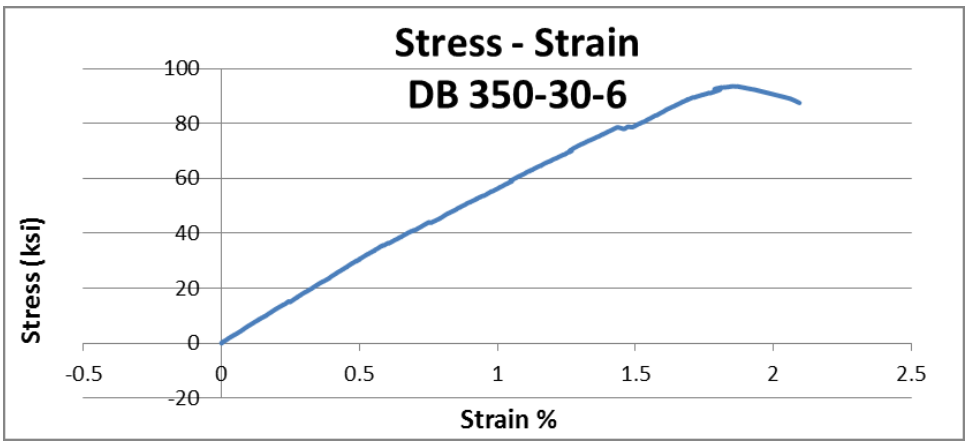

Figure 8-64 Stress – Strain curve for specimen DB 350-30-6

8.14 FS-CONTROL:

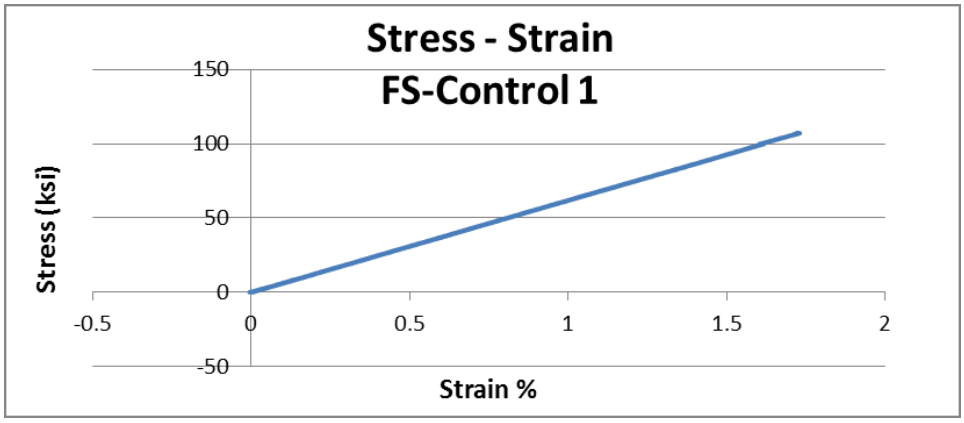

Figure 8-65 Stress – Strain curve for specimen FS-Control 1

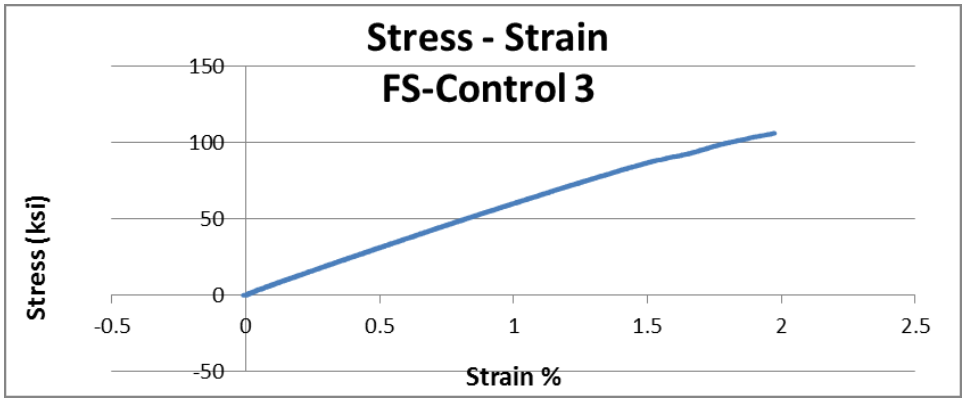

Figure 8-66 Stress – Strain curve for specimen FS-Control 3

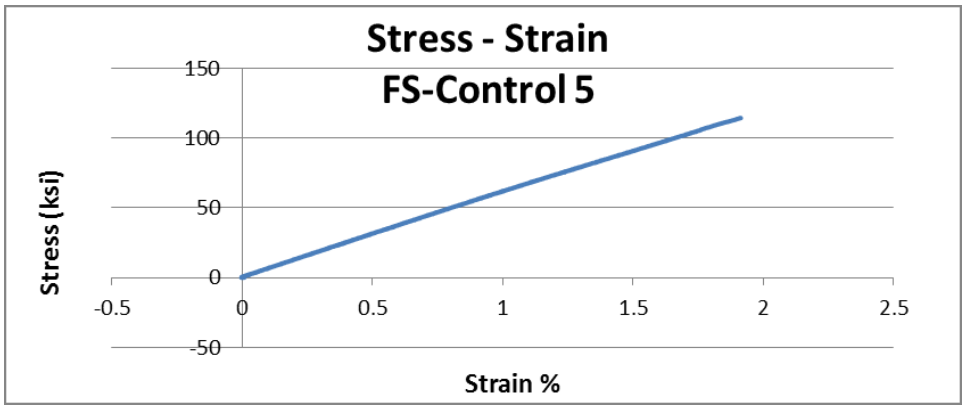

Figure 8-67 Stress – Strain curve for specimen FS-Control 5

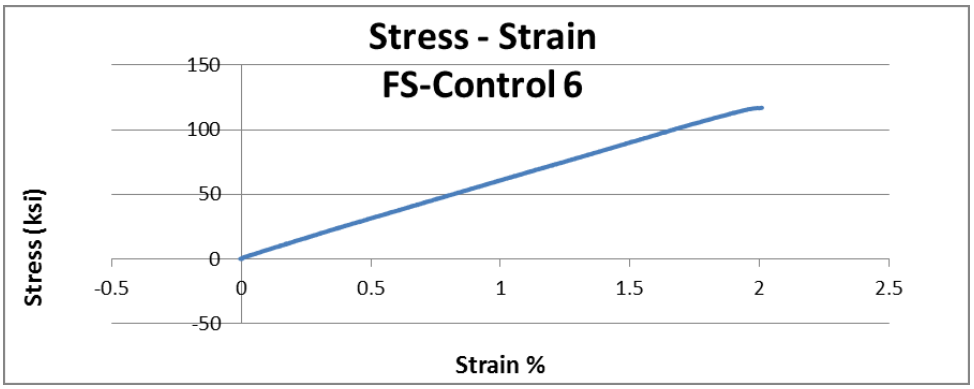

Figure 8-68 Stress – Strain curve for specimen FS-Control 6

8.15 FS-AFR-350:

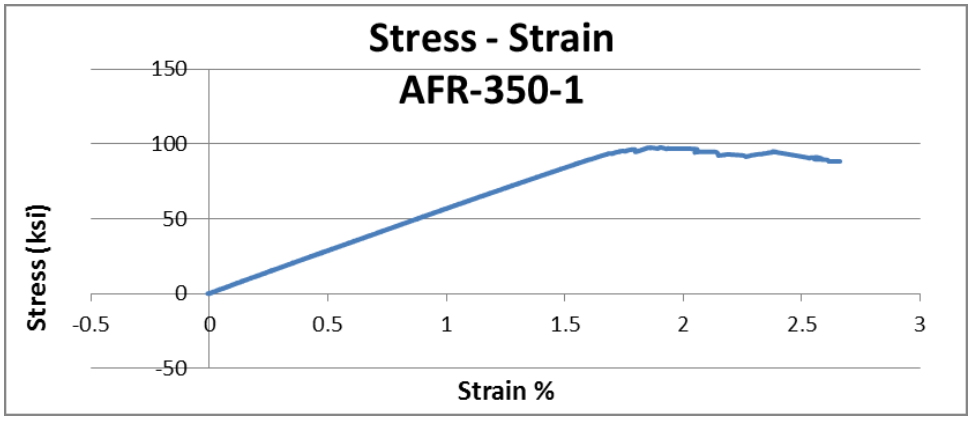

Figure 8-69 Stress – Strain curve for specimen FS-AFR-350-1

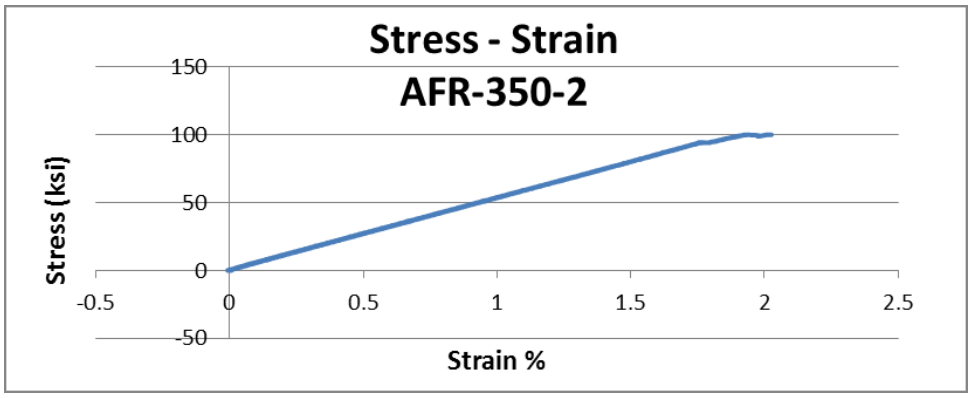

Figure 8-70 Stress – Strain curve for specimen FS-AFR-350-2

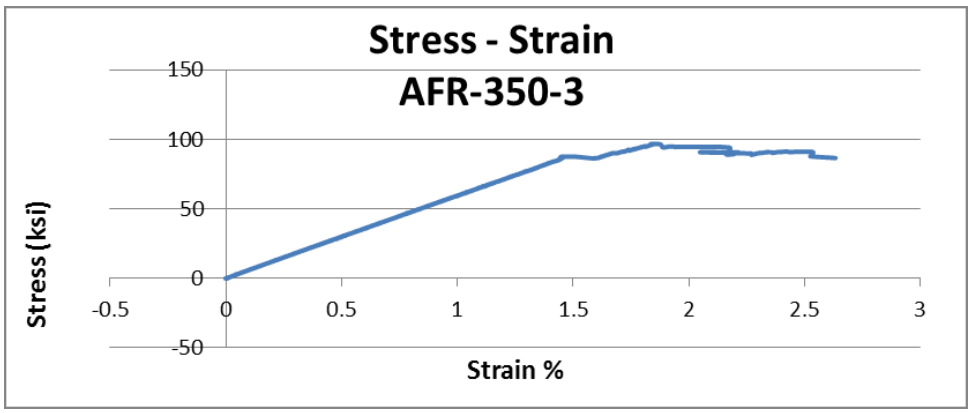

Figure 8-71 Stress – Strain curve for specimen FS-AFR-350-3

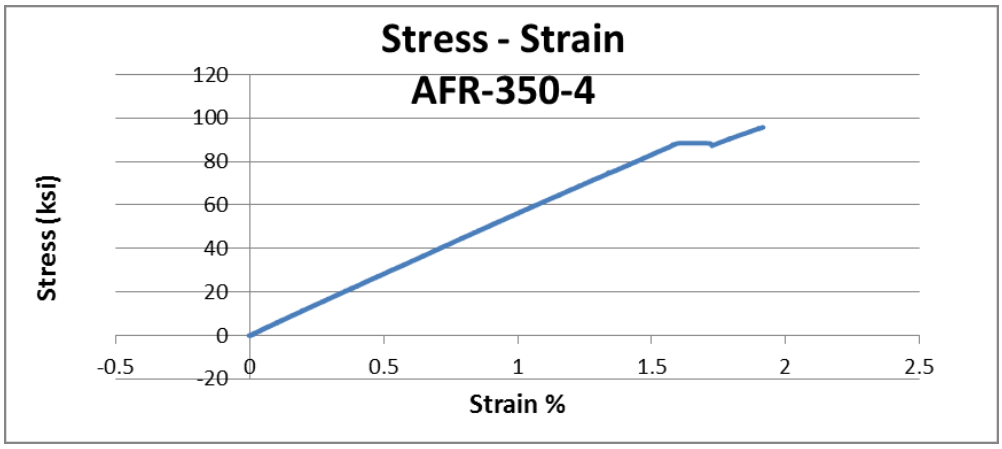

Figure 8-72 Stress – Strain curve for specimen FS-AFR-350-4

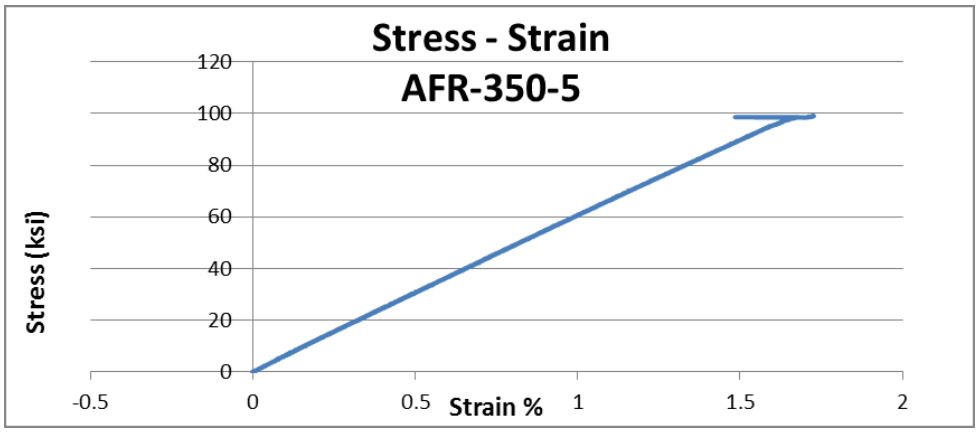

Figure 8-73 Stress – Strain curve for specimen FS-AFR-350-5

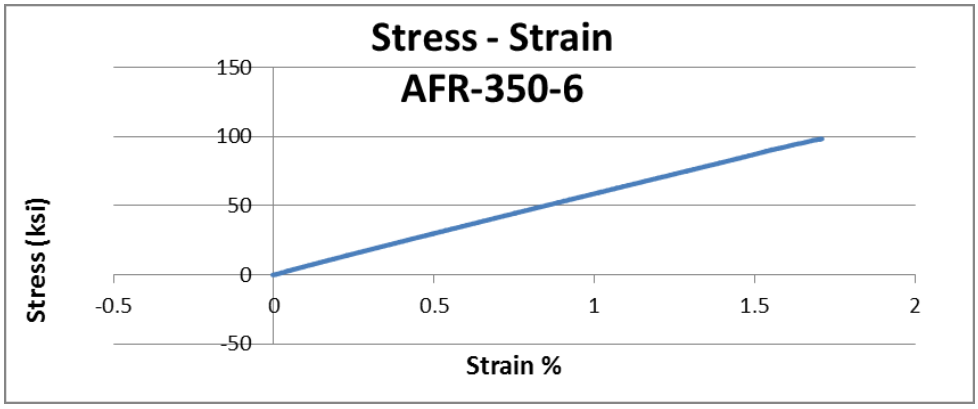

Figure 8-74 Stress – Strain curve for specimen FS-AFR-350-6